

Three-Dimensional Finite Element Analysis of Conventional and Ultrasonic Vibration Assisted Micro-Drilling on PCB

Muddu Allaparthi



Department of Industrial Design

National Institute of Technology Rourkela

Three-Dimensional Finite Element Analysis of Conventional and Ultrasonic Vibration Assisted Micro-Drilling on PCB

Dissertation submitted to the

National Institute of Technology Rourkela

in partial fulfillment of the requirements

of the degree of

Doctor of Philosophy

in

Industrial Design

by

Muddu Allaparthi

(Roll Number: 513ID1003)

Under the supervision of

Prof. Mohammed Rajik Khan



December, 2018

Department of Industrial Design

National Institute of Technology Rourkela



December 04, 2018

Certificate of Examination

Roll Number: *513ID1003*

Name: *Muddu Allaparthi*

Title of Dissertation: *Three-Dimensional Finite Element Analysis of Conventional and Ultrasonic Vibration Assisted Micro-Drilling on PCB*

We the below signed, after checking the dissertation mentioned above and the official record book of the student, hereby state our approval of the dissertation submitted in partial fulfillment of the requirements of the degree of *Doctor of Philosophy in Industrial Design* at *National Institute of Technology Rourkela*. We are satisfied with the volume, quality, correctness, and originality of the work.

Prof. Mohammed Rajik Khan
Principal Supervisor

Prof. K.P. Maithy
Member, DSC

Prof. M. Masanta
Member, DSC

Prof. S.C. Mohanty
Member, DSC

Prof. Meghanshu Vashista
External Examiner

Prof. A. Satapathy
Chairperson, DSC

Prof. BBVL Deepak
Head of the Department



Department of Industrial Design

National Institute of Technology Rourkela

Prof. Mohammed Rajik Khan

Assistant Professor

December 04, 2018

Supervisor Certificate

This is to certify that the work presented in the dissertation entitled *Three-Dimensional Finite Element Analysis of Conventional and Ultrasonic Vibration Assisted Micro-Drilling on PCB* submitted by Muddu Allaparthi, Roll Number 513ID1003, is a record of original research carried out by him under my supervision and guidance in partial fulfillment of the requirements of the degree of *Doctor of Philosophy in Industrial Design*. Neither this dissertation nor any part of it has been submitted earlier for any degree or diploma to any institute or university in India or abroad.

Prof. Mohammed Rajik Khan

Principal Supervisor

*I dedicate my dissertation to my beloved **Parents***

Declaration of Originality

I, *Muddu Allaparthi*, Roll Number *513ID1003* hereby declare that this dissertation entitled “*Three-Dimensional Finite Element Analysis of Conventional and Ultrasonic Vibration Assisted Micro-Drilling on PCB*” presents my originality work carried out as a doctoral student of NIT Rourkela and, to the best of my knowledge, contains no material previously published or written by another person, nor any material presents by me for the award of any degree or diploma of NIT Rourkela or any institution. Any contribution made to this research by others, with whom I have worked at NIT Rourkela or elsewhere, is explicitly acknowledged in the dissertation. Works of other authors cited in this dissertation have been duly acknowledged under the sections “Reference” or “Bibliography”. I have also submitted my original research records to the scrutiny committee for evaluation of my dissertation.

I am fully aware that in case of any non-compliance detected in future, the Senate of NIT Rourkela may withdraw the degree awarded to me on the basis of the present dissertation.

December 04, 2018
NIT Rourkela

Muddu Allaparthi

Acknowledgment

The journey of reaching any milestone is never easy without a determined ambition, sincere dedication and a perfect person who can torch your path of ignorance. I am obliged to my supervisor **Prof. Mohammed Rajik Khan**, Assistant professor, Department of Industrial Design for being an embodiment of the constant source of inspiration and knowledge. Under the guidance, I have learnt the art of doing research and the real value of life.

I sincerely thank **Prof. S.K Sarangi**, former Director, NIT Rourkela for his motivational speeches at regular interval of my tenure. I also sincerely thank **Prof. Amitesh Biswas**, Director, NIT Rourkela for his support in submitting the thesis.

I express my sincere thanks to **Prof. B.B Biswal**, former HOD, Department of Industrial Design, NIT Rourkela for providing me the necessary facilities in the department. I take this opportunity to express my deep sense of gratitude to the members of my Doctoral Scrutiny Committee members, **Prof. A. Satapathy** (Chairman), and **Prof. K.P. Maity**, Department of Mechanical Engineering, and **Prof. S.C. Mohanthy**, Department of Mechanical Engineering, and **Prof. M. Masanta**, Department of Mechanical Engineering, for their constant encouragement and valuable suggestions while carrying out my research.

At the same time, I am thankful to the teaching staffs of the department, whose valuable suggestions at the right time helped me reaching the goal.

I sincerely acknowledge the helping hand of the laboratory staffs and other nonteaching staffs of NIT Rourkela, for their timely help and support. My friends, whose consolation during the bad days and encourage words, helped me maintain the equilibrium during the course of fulfilling my ambition.

Lastly, I must thank the invisible force which we define as the almighty **God** for giving me patience and driving me towards never ending process of learning.

Muddu Allaparthi

Abstract

Recent advancement in society's demands has forced industries to produce more and more precise micro parts. With an advancement in engineering sciences, current manufacturers in various fields such as aerospace, medical, electronics, automobile, biotechnology, etc. have achieved the potential to fabricate miniaturized products, but with numerous technical challenges. Dimensional accuracy and surface integrity of the machined components are the key challenges and at the same time, cost minimization is strongly desired. To meet these challenges and demands, improvements in machining regarding new procedures, tooling, tool materials and modern machine tools are highly essential. Micromachining has shown potential to achieve the fast-growing needs of the present micro manufacturing sector. Additionally, new machining techniques like ultrasonic machining, laser drilling, etc. have been developed as an alternative source to reduce obstructions caused during macro/micro machining.

The present research aims to perform three-dimensional (3D) finite element dynamic analysis for micro-drilling of multi-layer printed circuit boards (PCBs). Both conventional and ultrasonic vibration assisted micro-drilling (UVAMD) FE simulations have been compared to predict and evaluate the effect of process parameters on the output responses like stress generation and reaction forces and burr formation on the workpiece surfaces. The Lagrangian based approach is followed for the FE simulation including the mass and inertial properties of the proposed FE model. The predicted FE results are compared with the past experimental work for thrust force evaluation and burr formation on workpiece surfaces. The present work is supported with modal and harmonic analysis of stepped and conical horns along with micro drill bit. Here, horns made up of Aluminum 6061-T6, Titanium and Mild steel are chosen with micro drill bit of 0.3 mm diameter with varying tool materials (Tungsten carbide and High speed steel). The effects of natural frequencies with different mode shapes within the range of 15-30 kHz are shown. The frequency responses of micro drill with displacement conditions have been presented for longitudinal modes.

The present simulation results will be helpful to conduct proper experimentation in order to achieve efficient machining and surface finish. The results enumerate that the drilling parameters have a strong influence on thrust forces and stresses occurring in micro-drilling. Ultrasonic assisted micro-drilling has a good potential in reduction of forces generated by

selecting proper machining parameters. The FE simulation of UVA micro machining can further be enhanced and extended to various materials like plastics, sheet metal, other PCBs, etc. to predict the performance with varying machining and geometrical parameters.

Key Words: Micro-drilling; FEA; Ultrasonic vibration; Thrust forces; Modal analysis; Harmonic response analysis.

Contents

Certificate of Examination	i
Supervisor Certificate	ii
Dedication	iii
Declaration of Originality	iv
Acknowledgement	v
Abstract	vi
Contents	viii
List of Figures	xi
List of Tables	xiv
Abbreviations	xv
Nomenclature	xvi
1 INTRODUCTION	
1.1 General.....	1
1.2 Micromachining.....	2
1.2.1 Micro-Milling	3
1.2.2 Micro-Drilling.....	4
1.3 Ultrasonic Machining	17
1.3.1 Ultrasonic Vibration Assisted Drilling	19
1.3.2 Ultrasonic Vibration Assisted Micro-Drilling	20
1.4 Burrs.....	20
1.4.1 Milling Burrs.....	21
1.4.2 Drilling Burrs	23
1.5 Organization of Thesis	25
2 LITERATURE REVIEW	
2.1 General.....	26
2.2 Conventional Micromachining	27
2.3 Modeling Approaches.....	28
2.3.1 Analytical Modeling	28
2.3.2 FE Modeling	29
2.3.3 Empirical Modeling	30
2.3.4 Mechanistic Modeling	31
2.3.5 Geometric Modeling	34

2.4 Ultrasonic Assisted Machining	36
2.5 Workpiece and Design Issues	39
2.6 Machining Burrs	42
2.7 Research Gaps Identified	45
2.8 Motivation.....	46
2.9 Objectives and Novelty of the Research work.....	47
2.10 Closure	47
3 FE DYNAMIC ANALYSIS OF CONVENTIONAL MICRO-DRILLING	
3.1 Methods and Materials.....	48
3.1.1 Geometry of Tool and Work Piece	48
3.1.2 Material and Constitutive Model	50
3.1.3 Mesh Generation.....	53
3.1.4 Boundary Conditions	54
3.2 FE Simulation Results	56
3.2.1 Stress Analysis	56
3.2.2 Thrust Force and Torque Analysis.....	59
3.2.3 Burr Formation Analysis	61
3.2.4 Discussion	63
3.3 Conclusion	64
4 FE ANALYSIS OF ULTRASONIC VIBRATION ASSISTED MICRO-DRILLING	
4.1 Methods and Materials.....	65
4.2 FE Simulation Results	66
4.2.1 Stress Analysis	67
4.2.2 Thrust Force Analysis	67
4.3 Conclusion	71
5 FE MODAL AND HARMONIC ANALYSIS OF ULTRASONIC HORN	
5.1 Wave Equation for Horn Profile.....	73
5.1.1 Stepped Horn	74
5.2.2 Conical Horn.....	74
5.2 Geometry of Micro-Drill Bit and Ultrasonic Horn.....	74
5.3 FE Modal Analysis	76
5.3.1 Material Selection	76
5.3.2 Meshing and Boundary Condition	76
5.4 FE Harmonic Analysis.....	82
5.5 Discussion.....	84
5.6 Conclusion	85

6 CONCLUSIONS AND FUTURE DIRECTIONS

6.1 Conclusions.....	86
6.2 Scope for Future Work	88

Bibliography

Dissemination

List of Figures

1.1	Classification of micromachining	4
1.2	Longitudinal cross-section of drilled holes (a) electro jet drilling, (b) laser drilling ...	6
1.3	Cutting mechanism of conventional drilling	7
1.4	Geometrical representation of cutting lip geometry.....	8
1.5	Chisel edge zone.....	11
1.6	Micro drill bits.....	13
1.7	2D geometry of twist drill (a) conventional drill, (b) micro-drill	14
1.8	PCB micro-drills (a) multilayer drill, (b) spade drill, (c) flex drill,(d) standard drill, (e) micro via drill (f) ultra micro drill and (g) slot drill	15
1.9	Solid carbide twist drill (a) SEM image, (b) Material characterisation through EDS analysis.....	16
1.10	Coatings on micro drill bits; (a) solid carbide coated twist drill, (b) diamond abrasives on flute section	16
1.11	Layout of the PCB (a) complete PCB in use, (b) inner view of PCB laminate with vias and through holes	17
1.12	Ultrasonic machine developed by DMG MORI; (a) flexible integration machine, (b) spindle setup.	18
1.13	Concepts of ultrasonic assisted drilling (a) drill vibration, (b) work piece vibration	19
1.14	Burrs observed in face milling (a) knife burr, (b) wave-type burr, (c) curl-type burr, (d) edge breakout and (e) secondary burr	21
1.15	Drilling burrs	22
2.1	Cutting lip model for a conical drill	32
2.2	2D views of cutting lip (a) geometry, (b) forces and cutting speed	32
2.3	Centering model of micro drilling for PCB	42
2.4	Experimental lay out for micro drilling of PCB	46
3.1	Methodology adopted (a flow diagram).....	49
3.2	Pictorial view of micro-drill bit.....	49
3.3	Schematic layout of tool and workpiece model	50
3.4	Meshing on tool and work piece	55
3.5	Boundary conditions applied to tool and work piece	56
3.6	Stress distribution in work piece material (speed 60 krpm and feed rate 0.3 mm/s)	

at time (a) 0.00025 s, (b) 0.00050 s, (c) 0.00075 s and (d) 0.001 s	57
3.7 Damage initiation of top (Cu) layer as per the JC criterion (sectional view).....	58
3.8 Fiber damage initiation in GFRP layer as per the Hashin's damage criterion under (a) fiber compression, (b) fiber tension (sectional view).....	58
3.9 Matrix damage initiation in GFRP material layer as per the Hashin's damage criterion under (a) matrix compression, (b) matrix tension (sectional view)	58
3.10 Thrust forces generated on multilayered PCB at 0.3 mm/s with varying speeds	60
3.11 Thrust force generated for double board PCB drilling at speed 60000 rpm with feed rate 1 mm/s	60
3.12 Variation of thrust forces with respect to varying speeds (a) Simulation result and (b) Experimental results (Zheng et al. 2013)	60
3.13 Variation of thrust forces with respect to varying feed rates (a) Simulation result and (b) Experimental results (Zheng et al. 2013)	61
3.14 Burr formation with varying speed (a) 60 krpm, (b) 70 krpm, (c) 80 krpm and (d) 90 krpm	62
3.15 Burr height predicted as per FE simulation.....	63
4.1 Methodology adopted (a flow diagram).....	66
4.2 Von Mises stress distribution on workpiece material with varying time at speed 60 krpm and feed 0.3 mm/s	67
4.3 Variation of thrust forces with respect to time of step size 0.001 s at constant feed 0.3 mm/s and varying speed for UVAMD	69
4.4 Variation of thrust forces at 60 krpm with feed of 0.3 mm/s with respect to time for CMD and UVAMD.....	69
4.5 Variation of thrust forces for CMD and UVAMD with varying speed (a) at constant feed of 0.3 mm/s (FE results) (b) at 19.1 kHz resonance and constant feed of 0.202 m/min with micro drill bit of size Φ 1 mm (experimental results).....	69
4.6 Comparison of simulation vs. analytical thrust forces for UVAMD at constant speed 60000 rpm with varying feed rate	71
5.1 Micro-drill bit (a) 2D pictorial view (all dimensions in mm), (b) 3D CAD model with expanded view of flute	75
5.2 CAD design of stepped horn assembled with micro-drill bit (a) 3D model (b) 2D orthographic view	75
5.3 CAD design of conical horn assembled with micro-drill bit (a) 3D model (b) 2D orthographic view	75

5.4	Meshing of (a) stepped horn and micro-drill assembly (b) flute portion	77
5.5	Meshing of (a) conical horn and micro-drill assembly (b) flute portion.....	77
5.6	Mode shapes recorded for stepped horn (Al 6061-T6) assembled with micro-drill bit (WC) at various natural frequencies (a) 17308 Hz, (b) 17452 Hz, (c) 20008 Hz, (d) 22087 Hz, (e) 25619 Hz and (f) 28813 Hz	79
5.7	Mode shapes recorded for conical horn (Al 6061-T6) assembled with micro-drill bit (WC) at different natural frequencies (a) 16975 Hz, (b) 16976 Hz, (c) 20298 Hz, (d) 25517 Hz, (e) 28101 Hz and (f) 28102 Hz	81
5.8	Displacement boundary applied on back end (a) stepped horn, (b) conical horn	82
5.9	Frequency response at 20008 Hz for Al 6061-T6 stepped horn and WC micro drill bit assembly (a) equivalent stress, (b) total deformation	83
5.10	Frequency response at 20298 Hz for Al 6061-T6 conical horn and WC micro-drill bit assembly (a) equivalent stress, (b) total deformation	83
5.11	Frequency vs. Amplitude of stepped horn (Al 6061-T6) assembled with micro-drill bit (WC) at 30 μm (a) equivalent stress, (b) total deformation	83
5.12	Frequency vs Amplitude of conical horn (Al 6061-T6) assembled with micro-drill bit (WC) at 30 μm (a) equivalent stress, (b) total deformation	84

List of Tables

2.1	Review on various modelling approaches	44
2.2	Notations for Table 2.1	45
3.1	Layer thickness of the workpiece material.....	50
3.2	Mechanical properties of the tool and work piece	51
3.3	JC model parameters of copper material.....	52
3.4	Hashin damage model parameters of GFRP material	53
3.5	Orthotropic elastic properties of GFRP material	53
3.6	Meshing details of tool and work piece	54
3.7	Machining parameters considered for CMD FE simulation	55
3.8	Process parameters and simulation results of CMD	59
4.1	Machining parameters considered for FE analysis of UVAMD.....	66
4.2	Process parameters and simulation results of UVA micro drilling.....	68
4.3	Comparative result of thrust forces in UVAMD as per analytical and FE simulation approach	71
5.1	Material properties of horn and micro-drill bit	76
5.2	Mesh details of horn and drill bit assembly	77
5.3	Natural frequencies recorded for stepped horn assembled with tungsten carbide micro-drill bit.....	78
5.4	Natural frequencies recorded for stepped horn assembled with high speed steel micro-drill bit.....	78
5.5	Natural frequencies recorded for conical horn assembled with WC micro drill bit ..	80
5.6	Natural frequencies recorded for conical horn assembled with HSS micro-drill bit..	80

Abbreviations

2D	Two-dimensional
3D	Three-dimensional
ALE	Arbitrary lagrangian eulerian
C3D8R	Eight-node brick element
CAD	Computer aided design
CAE	Computer aided engineering
CATIA	Computer aided three-dimensional interactive application
CCL	Copper clad laminate
CFRP	Carbon fiber reinforced plastic
CNC	Computer numerical control
CMD	Conventional micro-drilling
CO ₂	Carbon dioxide
ECM	Electro chemical machining
ECD	Electro chemical discharge machining
EDM	Electrical discharge machining
ESD	Electro static discharge
FE	Finite element
FESEM	Field emission scanning electron microscope
JC	Johnson-cook
GFRP	Glass fiber reinforced plastic
HSS	High speed steel
MEMS	Micro electrical mechanical systems
NURBS	Non-uniform rational basis spline
R3D3	Three node bilinear rigid tetrahedral element
SC8R	Eight node quadrilateral continuum shell element
STEM	Shaped tube electrolyte machining
UM	Ultrasonic machining
UAD	Ultrasonic assisted drilling
UVAMD	Ultrasonic vibration assisted micro-drilling
VAD	Vibration assisted drilling
WC	Tungsten carbide
YAG	Ytterbium-doped

Nomenclature

Δr	Radial element of width
r	Radius
ΔL	Oblique element on the lip
ρ	Semi point angle
ω	Web angle
f_p	Cutting force
f_Q	Thrust force
f_R	Radial force
f_{pc}, f_{qc}, f_{rc}	Cutting force coefficients
f_{pe}, f_{qe}, f_{re}	Edge force coefficients
t_o	Uncut chip thickness at the lip
s	Feed
v	Velocity angle
τ	Shear strength
θ_o	Stagnation angle
w	Half web thickness
η	Chip flow angle
i	Inclination angle
α_n	Rake angle
α_{ref}	Reference rake angle
δ	Helix angle of drill
t_{lim}	Limiting value
r_e	Cutting edge radius
φ_n	Shear angle
C	Merchant's machine constant
$\dot{\epsilon}$	Shear rate on shear plane
V	Cutting velocity (mm/s)
h	Primary shear zone thickness
Thru _{lip} and Torq _{lip}	Thrust force and torque at cutting lips
R_a	Radius of indentation zone
ΔF_p and ΔF_Q	Elemental cutting and thrust forces

$s / 2$	Thickness
α_s	Feed angle
Thru _{chi} and Torq _{chi}	Thrust force and torque at chisel edge
ϕ	Slip line field angle
Thru _{ind} and Torq _{ind}	Thrust force and torque at indentation
Thru and Torq	Total thrust and torque on the drill
A	Amplitude
F	Frequency
n	Spindle rotational speed
f	Feed rate
t	Time
θ	Rotational angle of the drill
dl	Surface for the differential element from the drill axis
h_1	Dynamic uncut chip thickness
B	Intermediate parameter
k_{rd}	Dynamic cutting edge angle
η_d	Dynamic feed angle
r	Radius
$\Delta\theta$	Element rotational angle of the drill
λ_{sd}	Cutting edge inclination angle
γ_{fd}	Dynamic side rake angle
γ_{nd}	Dynamic normal rake angle
p	Half point angle of the drill
ω	Intermediate angle
ϕ_{nd}	Dynamic shear angle
λ_{nd}	Dynamic friction angle
η_{cd}	Dynamic chip flow angle`
r_l	Chip length ratio
ρ	Relative radius
r / R	Ratio of the distance from the drill center segment to the drill radius
F_t	Total thrust force
k	Shear strength
f	Feed rate
κ	Point angle of the drill
λ	Friction angle

α	Tool rake angle
φ	Shear plane angle
R	Drill radius
δ	Ratio of the web thickness to the drill diameter
h	Helix angle
F_t	Thrust force
d	Drill bit diameter
F_n	Dimensionless feed parameter
S	Cutting speed parameter
N	Spindle speed

Chapter 1

INTRODUCTION

1.1 General

Machining has become a backbone to the modern manufacturing industry and is used for manufacturing of the almost all the variety of components or parts being shaped according to the requirement of the present needs. Machining is termed as removal of undesirable material from the workpiece with a cutting tool to obtain the finished product with desired shape, size and surface quality. Machining is characterized by its versatility and ability of achieving accuracy and good surface finish in the most economic way by its cutting techniques (EI-Hofy et al., 2013). The cutting techniques are elaborated as machining by cutting, mechanical abrasion and erosion processes. These processes are divided by its cutting action, abrasion and comes under traditional machining in which chip removal occurs with the contact of the workpiece with the tool. The absence of tool or contact with the work piece are known as non-traditional machining processes. The non-traditional machining processes are introduced to cut more hard to machine materials like carbides, high strength thermal resistant alloys, fiber reinforced composite materials, ceramic materials. alternative machining for machining parts of complex shapes which are harder, stonger and difficult to cut by the traditional machining processes. These methods are arbitrated by the machinability of material with respect to the machining parameters, cutting tool material and workpiece material and its physical properties.

Recent advancement in manufacturing technology has been focused on variety of miniaturized products in industries to produce more and more precise micro parts. With these engineering sciences and innovation, the demand for these micro parts is increased rapidly in various fields such as aerospace, medical, electronics, automobile, biotechnology, etc. with numerous technical challenges. Surface integrity and dimensional precision of the machined work piece and at the same time cost minimization is strongly desired. To meet these challenges and demands, improvements in the machining regarding new procedures, tooling, tool materials and modern machine tools are highly essential. Micromachining has shown potential to explore the fast-growing needs of the present micro manufacturing

sector. Additionally, new machining techniques like ultrasonic micromachining have been developed as an alternative source to reduce obstructions caused during machining. This chapter discusses on present trend in micromachining processes: traditional micro milling, micro-drilling, ultrasonic vibration assisted macro and micro-drilling processes.

1.2 Micromachining

Micromachining has been reported since 1960s and has emerged as an essential machining process in the present-day manufacturing sector (Piljek et al. 2014). Micromachining is the miniaturized shaping of objects by removing excessive material from a new stock. For such a purpose, both conventional and non conventional methods of machining are adopted. Micromachining has lately become an essential technique for the minimization of work piece size and dimensions. It denotes to the technology and practice of making three-dimensional structures, surface profiles, and components with sizes of the order of micrometers. Conventional methods of micromachining utilize fixed and controlled tools that can specify the profile of 3D shapes by a well-designed tool surface and path. These methods remove material in amounts as small as tens of nanometers, which are acceptable for many applications of micromachining. The volume or size of the part removed from the workpiece, in mechanical methods termed as the unit removal., consists of the feed pitch, depth of cut, and the length that corresponds to one chip of material cut. Turning, drilling, and milling have proven to be applicable to the micromachining of shapes in the range of micrometers through the miniaturization of the required tools.

One of the most important goal of the improvement of micromachining is to incorporate microelectronic printed circuit into micromachined structures and to develop fully integrated systems (Hofy et al., 2013). Recently, the need for semiconductor devices, extremely compact electrical circuits, and integrated circuit packages that contain devices having micro dimensions has led to the introduction of micromachining. The circuit board must have micro holes if relays and switches are required to be assembled using microsized parts. Fuel injection nozzels for automobile have become smaller in size and more accurate to solve many environmental problems. In the area of biotechnology that includes biological cells and genes, the tools required to handle them must have microeffectors. Miniaturization of medical tools for inspection and surgery is another candidate for micromachining processess (Masuzawa, 2000).

The micro in micromachining indicates micrometer and represents the range of 1-999 μm , however, micro likewise means very small. In the field of machining by material removal, micro indicates small parts that cannot be easily machined. Actually, the range of micro varies according to person, period, type of product and machining method. In micromachining, there are two main guidelines, the reduction of the unit removal rate and improvement of the equipment precision.

Though the machining techniques are analogous to macro machining (conventional), the process model or scaling of parameters are not applied directly due to chip thickness (Piljek et al., 2014). This approach adopted on reduction of the macro machining process, equipment and tooling with an importance on their scaling down effects. The scope and context of micro-cutting needs to be defined because the term may have several meaning for numerous purposes. Mechanical micromachining has relatively more advantages regarding the choice of materials, accuracy, complexity of geometry for various products as compared with micro-electro-mechanical systems (MEMS) based machining techniques like lithography. Also, it has the capability to bridge the gap between macro, micro and nano fields (Huo, 2013). However, micromachining has reported principal concerns such as geometrical limitations, tooling aspects, tolerance issues, machining control, machinable materials, thermal aspects and chip thickness. The classification of micromachining processes and key aspects influencing the micro domain are shown in Figure 1.1.

1.2.1 Micro-Milling

Micro-milling is an evolving technology and can be regarded as one of the most flexible and versatile micro-cutting process. It has the ability to produce a wide variety of complex micro parts and structures. In the past years, substantial research has been carried out in the domain of micro-milling modeling, simulations and experiments. In order to determine the feature size and the surface roughness, micro-tooling is important to micro-milling. Commercially available micro-milling cutters have tool diameters varying from 25-1000 μm (Huo, 2013). Most of the micro-milling tools having diameter varying from 25-1000 μm have only two flutes because of their inadequate rigidity and due to difficulty in fabrication due to their complexity. Some of the very small diameter tools (<100 μm) have only one flute, especially made of CVD or natural diamond. In terms of milling operations, while micro end milling using either ball-nosed or flat end mills dominates micro-milling applications, peripheral milling utilised in macro-milling is uncommon for micro-milling.

Premature tool chipping and breakage is one of the challenges in the micro-milling. A limited number of choices therefore remain for fabricating the micro tool. While coated micro grain tungsten carbide tools are widely used for micro-milling jobs, natural diamond or CVD micro-milling tools are used in applications demanding accuracy and good surface finish.

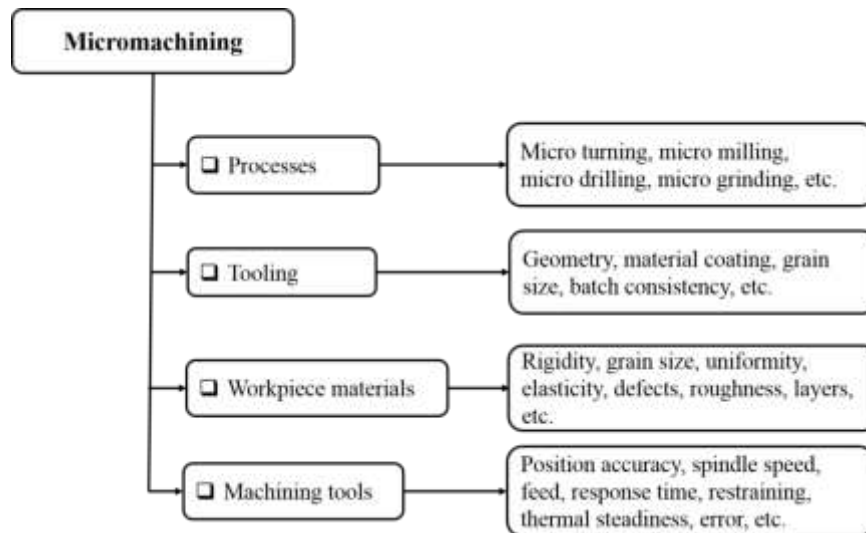


Figure 1.1: Classification of micromachining

Preferably, micro-milling should be performed in a micro machine specially designed for micro-milling purpose or precision milling machine, but it can also be carried out by retrofitting a high speed spindle in a traditional CNC machining centre. Micro-milling tools having small diameter requires high stiffness spindle to retain high precision in the presence of large cutting forces and also extremely high rotational speeds to achieve even normal machining rates. High machining precision also requires low spindle running temperatures to reduce thermal distortion while a fine surface finishing capability can only be attained with a spindle speed having low motion errors. So, precise high speed spindle with operating speeds more than 1,00,000 rpm are normally preferred.

1.2.2 Micro-Drilling

Micro-drilling operation is the backbone for drilling of micro holes and is extensively being used in various microelectronic and mechanical industries. The micro-drill bits usually have a high aspect ratio, i.e. length-to-diameter higher than 10 for drilling deeper holes (Chyan et al., 1998). Micro-drilling process is highly essential in areas of electronic products; such as computers, laptops, watches, camera parts, biomedical devices, PCB manufactures; to allow electrical interconnections among layers of the boards, aerospace, military and rapidly

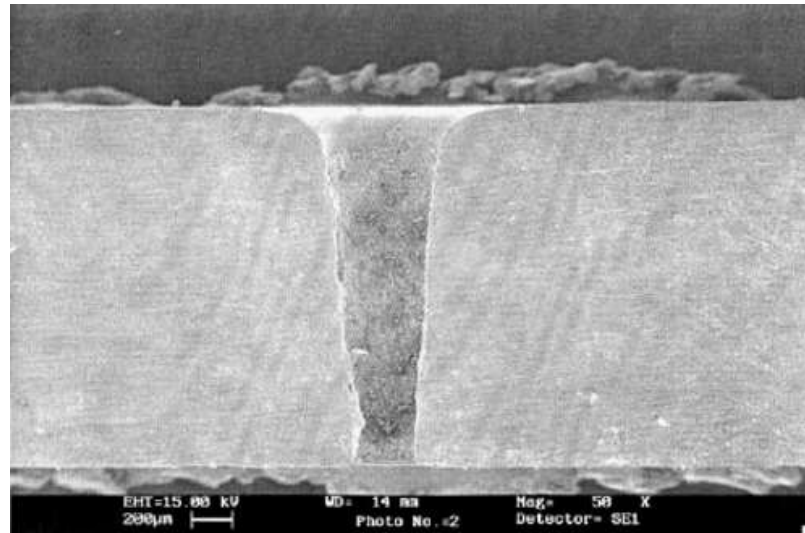
expanding in precision industries. However, there are specific other methods (e.g. laser drilling) for drilling micro holes, but conventional micro drilling is more extensively used in these industries due to its unique mechanical properties independent of workpiece materials (Cheong et al., 1999). Drilling large number of holes is a challenging task and often produces tool wear, drill breakage and reduces the tool life which further leads to average surface hole quality. Therefore, industries are always looking for efficient and precise methods to improve the drilling performance that has a significant influence on quality and processing time which can help to enhance the production and economy. Despite increasing demand in various applications, the quality of holes with accuracy and efficiency depends on the strength of drill bits which are strongly recommended for enhancing micro-drilling productivity. Also, achieving the prerequisite of different proportions, geometries and materials of micro drills are quite challenging to come across the requirements from industry.

Micro-milling when compared to micro-drilling, is a lot more efficient process to generate holes and can machines deep holes too. The machining of flat bottom holes cannot be carried out with micro drilling operation due to drilling point. The high speed spindles are similar for micro-drilling as well as micro-milling, but the speed control in micro-drilling spindle is not desirable when compared to micro-milling. To increase the productivity, air turbine spindles or aerostatic bearings are typically used with maximum speed of more than 1,00,000 rpm.

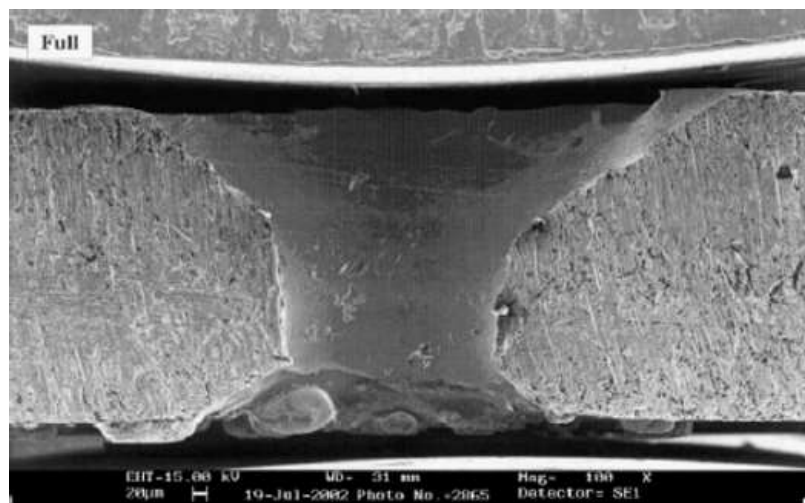
Out of all the micromachining processes, mechanical micro-drilling finds its application in making holes in aviation, medical implants, optics and fiber glass, PCBs, semiconductor devices, etc. Such applications require high accuracy and precision, although there are lot of limitations and issues that need to be addressed in the domain of micro-drilling. One of the most important issue being limited is tool life of the micro drills.

Additional to the mechanical micro-drilling process, innovative hole drilling methods have been developed like laser-drilling, electro chemical machining (ECM), electro chemical discharge machining (ECD), electro static discharge (ESD), shaped tube electrolyte machining (STEM) and electrical discharge machining (EDM). These technique are used to drill holes specifically in high strength materials (Piljek et al., 2014). In lasers, such as ytterbium-doped (YAG), carbon dioxide (CO₂) and excimer, laser beam having different wavelengths are used for drilling holes. In ECM process, acidic solutions are used as electrolyte for fine and small holes (Sen et al., 2005). The major limitations of these

processes are inaccuracy in developing uniform holes, surface finish, etc. Sometimes, clogging also occurs due to failure of tool insulation and stray removal at internal sides of hole walls in through drilling as shown in Figure 1.2. These processes are mainly used for micro-drilling in PCB industries for mass production.



(a)



(b)

Figure 1.2: Longitudinal cross-section of drilled holes (a) electro jet drilling, (b) laser drilling (Sen et al., 2005)

Apart from all these processes, conventional micro-drilling (CMD) is still the most common machining method practiced by present manufacturers in hole processing (Cheong et al., 1999). The main advantages are, drilling of through and blind holes with improved accuracy, independent of work piece material, diameter and hole depth, etc.

Process Mechanics

Micro-drilling merely resembles the conventional generic drill mechanism, yet it is more complicated machining than other machining processes. In typical conventional drilling process, the drilling mechanism is divided into four phases. These phases start from initial drill position before penetrating into the workpiece till it reaches the end of the drill wall. In the through-hole drilling process, the cutting forces generated at the initial penetration of the drill leads to its end. The dynamic cutting forces are one of the essential factors in conventional drilling (Gong et al., 2006). The cutting mechanism of chisel edge and different sectional views of drilling are shown in Figure 1.3.

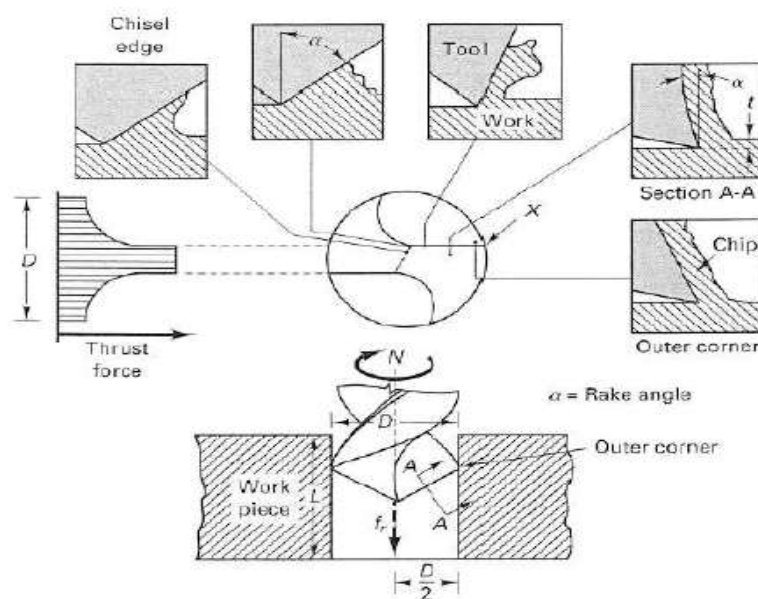


Figure 1.3: Cutting mechanism of conventional drilling (Zhang.Z, 2010)

For micro-drilling, the operating parameters are substantially different due to the reduced size of the cutting tool. In many applications, particularly PCB industries, micro drilling works at higher speed and feed rates for increasing the stability and to decrease the dynamic stresses on micro drills (Yongchen et al., 2006). In micro-drilling process, high-speed rotational spindles are fitted with air bearing technology to reduce the chip load. Another fundamental step used in PCB drilling is pressure foot to wrap the stack and to avoid the drill deviation and breakage at high-speed conditions. In micro drilling, the monitoring of drilling conditions at critical speeds is a complicated and most challenging task. Knowing the conventional drilling process, the types of drills, their geometry and operating conditions are necessary to understand the drilling mechanism. This study will contribute to the better design of drill geometry and also for appropriate usage in better hole making process. In

micro-drilling, mechanistic model for cutting forces is developed using thin zone orthogonal model derived appropriate oblique cutting model (Rahamathullah et al., 2014).

Cutting lip (primary) zone

Figure 1.4 shows the cutting lip geometry of a micro-drill. It is usual to consider a radial element of width Δr at a radius of r from the drill central axis which corresponds to an oblique element ΔL on the lip. The relation between Δr and ΔL is given by $\Delta r = \Delta L \sin \rho \cos \omega$ where, ρ is the semi point angle and ω is the web angle.

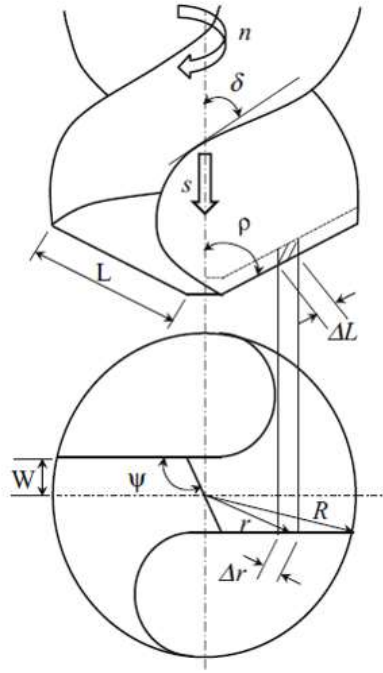


Figure 1.4: Geometrical representation of cutting lip geometry (Rahamathullah et al., 2014)

This element is treated as an oblique cutting edge, and forces acting on it are estimated from the principles of oblique cutting. The cutting edge also introduces ploughing/rubbing effect due to the radius at the edge. Therefore, the forces acting on the chosen element for unit radial width Δr in the cutting (f_p), thrust (f_Q), and radial (f_R) directions are expressed as,

$$f_p = f_{pc} t_o + f_{pe} \quad (1.1)$$

$$f_Q = f_{qc} t_o + f_{qe} \quad (1.2)$$

$$f_R = f_{rc} t_o + f_{re}, \quad (1.3)$$

where, f_{pc} , f_{qc} , f_{rc} are cutting force coefficients; f_{pe} , f_{qe} , f_{re} are the edge force coefficients; and t_o is the uncut chip thickness at the lip region given by,

$$t_o = \frac{s \sin \rho \cos \nu}{2}, \quad (1.4)$$

where, s is the feed and ν is the velocity angle. The cutting coefficients are found from the work of Armarego and Brown, (1969) as,

$$f_{pc} = \frac{\tau \cos \nu \cos i [\cos(\beta_n - \alpha_n) + \tan i \tan \eta \sin \beta_n]}{\sin \phi_n \cos \omega [\cos^2(\phi_n + \beta_n - \alpha_n) + \tan^2 \eta \sin^2 \beta_n]^{1/2}} \quad (1.5)$$

$$f_{qc} = \frac{\tau \cos \nu \sin(\beta_n - \alpha_n)}{\sin \phi_n \cos \omega [\cos^2(\phi_n + \beta_n - \alpha_n) + \tan^2 \eta \sin^2 \beta_n]^{1/2}} \quad (1.6)$$

$$f_{rc} = \frac{\tau \cos \nu \cos i [\cos(\beta_n - \alpha_n) + \tan i - \tan \eta \sin \beta_n]}{\sin \phi_n \cos \omega [\cos^2(\phi_n + \beta_n - \alpha_n) + \tan^2 \eta \sin^2 \beta_n]^{1/2}}, \quad (1.7)$$

where τ is shear strength. The edge coefficients found from the model proposed by Abdelmoneim and Scrutton, (1974) are given as,

$$f_{pe} = \frac{\tau_e}{\sin \rho \cos \omega} \left[\frac{2\theta_o}{\cos \theta_o} + \pi \sin \theta_o \tan \theta_o \right] \quad (1.8)$$

$$f_{pe} = \frac{\tau_e}{\sin \rho \cos \omega} \left[2\sqrt{3} \sin \theta_o \right] \quad (1.9)$$

$$f_{re} = f_{pe} \sin i, \quad (1.10)$$

where the value of the stagnation angle θ_o is taken as 14° . Web angle ω used in the above equation is given by, $\omega = \sin^{-1}(w/r)$, where w is the half web thickness. Based on the Stabler's rule, chip flow angle η is assumed as an inclination angle i which is defined as,

$$i = \sin^{-1} \left(\frac{W \sin \rho}{r} \right). \quad (1.11)$$

The rake angle α_n is given by,

$$\alpha_n = \alpha_{ref} - \nu, \quad (1.12)$$

where, velocity ν is,

$$\nu = \tan^{-1}(\tan \omega \cos \rho) \quad (1.13)$$

and reference rake angle (α_{ref}) is computed for a given helix angle of the drill δ as

$$\alpha_{ref} = \tan^{-1} \left(\frac{\tan \delta \cos \omega}{\sin \rho - \tan \delta \sin \omega \cos \rho} \right). \quad (1.14)$$

When the uncut chip thickness t_o is less than a limiting value t_{lim} , the rake angle α_n gets modified as,

$$\alpha_n = \sin^{-1} \left(\frac{t_o - r_e}{r_e} \right) \text{ for } t_o < t_{\text{lim}}, \quad (1.15)$$

where r_e is cutting edge radius and t_{lim} is the limiting value given by $t_{\text{lim}} = r_e(1 + \sin \alpha_n)$. The modified shear angle relation used to predict shear angle ϕ_n is defined by,

$$\phi_n = \frac{C - \beta_n + \alpha_n}{2}, \quad (1.16)$$

where C is the Merchant's machining constant. The strain rate ($\dot{\epsilon}$) on the shear plane is given by Tounsi et al. (2002) as,

$$(\dot{\epsilon}) = \frac{2V \cos(\alpha_n)}{\sqrt{3}h \cos(\phi_n - \alpha_n)} \quad (1.17)$$

where V is the cutting velocity (mm/s) at radius r and h is primary shear zone thickness ($= t_o/2$). The thrust and tangential forces at j^{th} element on the lip with reference to drill axis can be found from the following equations:

$$\text{Thru}_j = [f_{Q_i}(\cos i \sin \rho) - f_{R_j}(\cos i \cos \rho + \sin i \sin \nu \sin \rho)] \Delta r \quad (1.18)$$

$$\text{Tang}_j = f_{P_j} \Delta r \quad (1.19)$$

Therefore, thrust force (Thru_{lip}) and Torque (Torq_{lip}) on both the lips can be computed by summing over all N elements.

$$\text{Thru}_{\text{lip}} = 2 \sum_{j=1}^{j=N} \text{Thru}_j \quad (1.20)$$

$$\text{Torq}_{\text{lip}} = 2 \sum_{j=1}^{j=N} \text{Tang}_j r_j \quad (1.21)$$

Chisel edge (secondary) zone

The procedure followed for prediction of cutting forces acting on the chisel edge is similar to that described in above section. One portion of the chisel edge represented as C (half chisel edge length minus radius of indentation zone R_a) in Figure 1.5 is divided in to M elements.

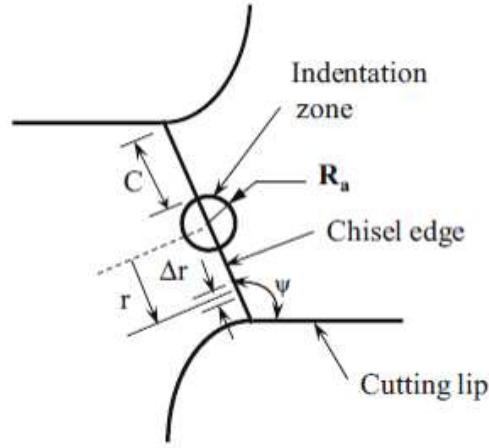


Figure 1.5: Chisel edge zone (Rahamathullah et al., 2014)

Elemental forces ΔF_p and ΔF_Q acting on a given element of width Δr and thickness $s/2$ at a distance of r from the drill central axis in cutting and thrust directions can be represented by Equations (1.1) and (1.2). The relevant cutting force coefficients can be derived from Equation (1.5) and (1.6) using conditions for orthogonal cutting, namely $i = \eta = \omega = \nu = 0$. In the final form, Equations (1.5) and (1.6) appear as,

$$f_{pc} = \frac{\tau \cos[\cos(\beta_n - \alpha_n)]}{\sin \phi_n \cos(\phi_n + \beta_n - \alpha_n)} \quad (1.22)$$

$$f_{qc} = \frac{\tau \sin(\beta_n - \alpha_n)]}{\sin \phi_n \cos(\phi_n + \beta_n - \alpha_n)} \quad (1.23)$$

The edge force coefficients are expressed by Equations (1.5) and (1.6). However, the rake angle at the element on the chisel edge must be taken as,

$$\alpha_n = \alpha_{ref} + \alpha_s, \quad (1.24)$$

where, reference rake angle α_{ref} and feed angle α_s are, respectively, given by

$$\alpha_{ref} = -\tan^{-1}(\tan \rho \cos(\pi - \phi)) \quad (1.25)$$

The limiting condition in Equation (1.15) must be considered while taking into the account the edge radius effect on rake angle in cutting.

Since the feed and cutting velocities are also comparable in the zone, velocity according to the next equation must be taken to compute shear strain $\dot{\epsilon}$ using Equation (1.17)

$$V = \frac{n}{60} \sqrt{s^2 + (2\pi r)^2} \quad (1.26)$$

The thrust and tangential forces at k^{th} element on the chisel edge with reference to drill central axis can be found from the following equations,

$$\text{Thru}_k = [f_{Q_k}] \Delta r \quad (1.27)$$

$$\text{Tang}_k = [f_{P_k}] \Delta r \quad (1.28)$$

The thrust force (Thru_{chi}) and torque (Torq_{chi}) due to chisel edge cutting can be found by summing over all M elements and multiplying by 2 to account for two portions of chisel edge on either side of the indentation zone.

$$\text{Thru}_{\text{chi}} = 2 \sum_{k=1}^{k=M} \text{Thru}_k \quad (1.29)$$

$$\text{Torq}_{\text{chi}} = 2 \sum_{k=1}^{k=M} \text{Tang}_k r_k \quad (1.30)$$

Indentation zone

In the indentation zone, the velocity is near zero, and material in this zone is pushed backward due to compressive stress. This zone cannot be neglected in micro-drilling, as its contribution to the drilling forces is appreciable. The portion of the chisel edge at this zone is considered to be a rigid wedge having a semi-angle of α_n given by Eq. 1.24 in which feed angle α_s is zero. Using slip-line solution provided by normal force acting on the wedge is determined. From the normal force, thrust force and torque at the indentation zone can be found as

$$\text{Thru}_{\text{ind}} = \frac{8\tau(1+\phi)sR_a \sin \alpha_n}{\cos \alpha_n - \sin(\alpha_n - \phi)} \quad (1.31)$$

$$\text{Torq}_{\text{ind}} = \frac{4\tau(1+\phi)sR_a^2 \cos \alpha_n}{\cos \alpha_n - \sin(\alpha_n - \phi)} \quad (1.32)$$

where, angle ϕ is found out iteratively from the relation

$$2\alpha_n = \phi + \cos^{-1} \left\{ \tan \left(\frac{\pi}{4} - \frac{\phi}{2} \right) \right\} \quad (1.33)$$

Radius of the indentation zone is obtained from the relation involving feed s and semi point angle ρ as

$$R_a = \frac{s}{4 \tan \left(\frac{\pi}{2} - \rho \right)} \quad (1.34)$$

Total thrust force acting on a micro drill

Total thrust force (Thru) and torque (Torq) acting on the drill can be found by adding the values at all three zones.

$$\text{Thru} = \text{Thru}_{\text{lip}} + \text{Thru}_{\text{chi}} + \text{Thru}_{\text{ind}}$$

$$\text{Torq} = \text{Torq}_{\text{lip}} + \text{Torq}_{\text{chi}} + \text{Torq}_{\text{ind}}$$

Micro-Drill Geometry

The body structure of micro drill bits are similar to conventional drill bits, but are more slender in flute portion and tends to break easily. The micro-drill bits with different diameters that are most preferred in industry shown in Figure 1.6. Machining factors like high rotational speeds, feed rate, torsional and longitudinal vibration, etc. have direct influence on drill holes and need to be appropriately considered for investigating micro drills (Zhang et al., 2011).



Figure 1.6: Micro drill bits (reproduced from web) [264]

In comparison to macro-drills, there are two fundamental differences in micro-drill bit geometry. First is downsizing the ratio of flute length, the second is the ratio of web thickness over the diameter which are having different characteristics. The 2D orthographic view of twist micro-drill bit geometry is depicted in Figure 1.7. These micro-drills are designed in a particular manner such that the decrease in flute size diameter will reduce the stiffness; the increase in web thickness with low helix angle increases the bending stiffness of the drill bit (Filiz et al., 2010). This indicates that the bending stiffness is more critical for micro drills to resist the vibration. The bending stability is one of the most significant factors that is influenced by the external loading conditions such as feed forces which needs to be considered.

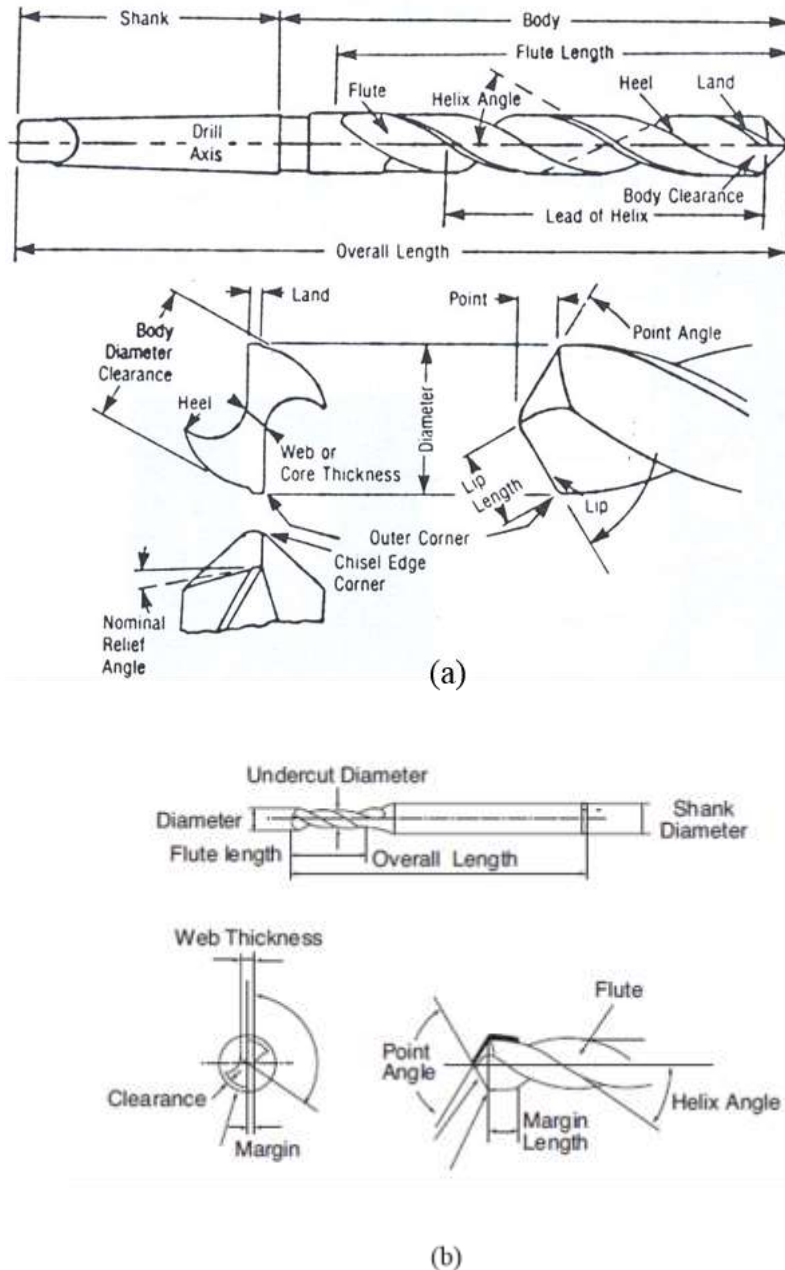


Figure 1.7: 2D geometry of twist drill (a) conventional drill (Lindberg, 1990), (b) micro-drill (Fu et al. 2010)

The drill bit diameter and flute length plays a crucial role in different micro drill applications, thus careful selection is needed for proper functioning (Zhang et al.,2010). Micro-drill bit have 38.1 mm total length and 3.175 mm shank diameter according to international standards. For PCB hole drilling, there are multiple types of micro-drills available such as (a) multilayer drill, (b) spade drill, (c) flex drill,(d) standard drill, (e) micro via drill (f) ultra micro drill, and (g) slot drill (Figure 1.8).

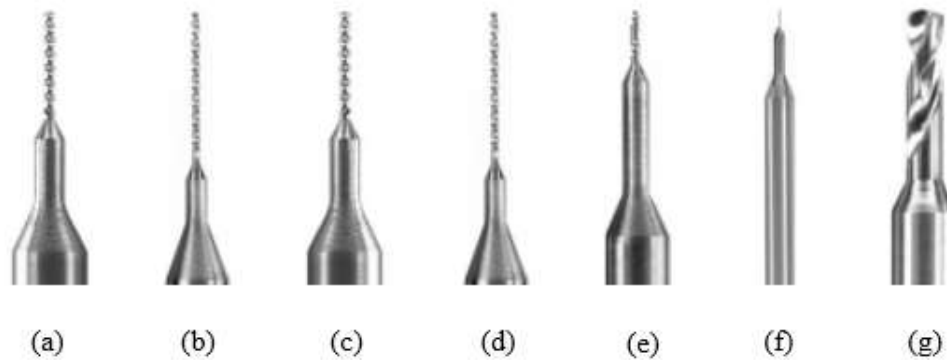


Figure 1.8: PCB micro-drills (a) multilayer drill, (b) spade drill, (c) flex drill, (d) standard drill, (e) micro via drill (f) ultra micro drill and (g) slot drill (Zhang, Z, 2010)

Materials

Mostly, micro-drill bits reflect very small and typical geometrical structure that requires high rigidity, strength, hardness and wear resistance. To cover these attributes, good and strong materials are required to manufacture the micro drills. Usually, tungsten carbide (WC) and high speed steel (HSS) are the most common materials used to make drill bits. HSS is more frequently used in industry because it is comparatively inexpensive and tough, however it has some confines such as poor wear resistance and hot hardness. On the other hand, WC is a bit expensive, but holds less tool wear, having higher hardness and wear resistance. Carbide is a mixture of the binder material cobalt (Co) having 4.75 % wt. and WC (86.22% wt.). These materials bind through powder metallurgical process that belongs to hard and ductile materials. The solid carbide drill bit with EDS (Electron discharge spectrum) spectral analysis showing the combination of different materials weight percentage is shown in Figure 1.9. The new methods were further developed to achieve the drill bit material alloys compressive strength, hardness and Young's modulus to machine numerous work piece materials like ceramic, aluminium, steel, titanium and Inconel. In such cases, coated stub drills are used for improving tool life and productivity. They are covered with carbide, titanium nitrate, Zr-C: H-5 (Zirconium), diamond aggressive coatings, etc. to the flute portion to gain high stiffness as shown in Figure 1.10.

The recent advances in materials have proposed many light weight materials for product manufacture. Materials are classified as metals, polymers, ceramics, composites, etc., which are soft, hard, ductile and brittle. Printed circuit boards belong to the category of the combination of ductile and brittle materials laminated into thin plates.

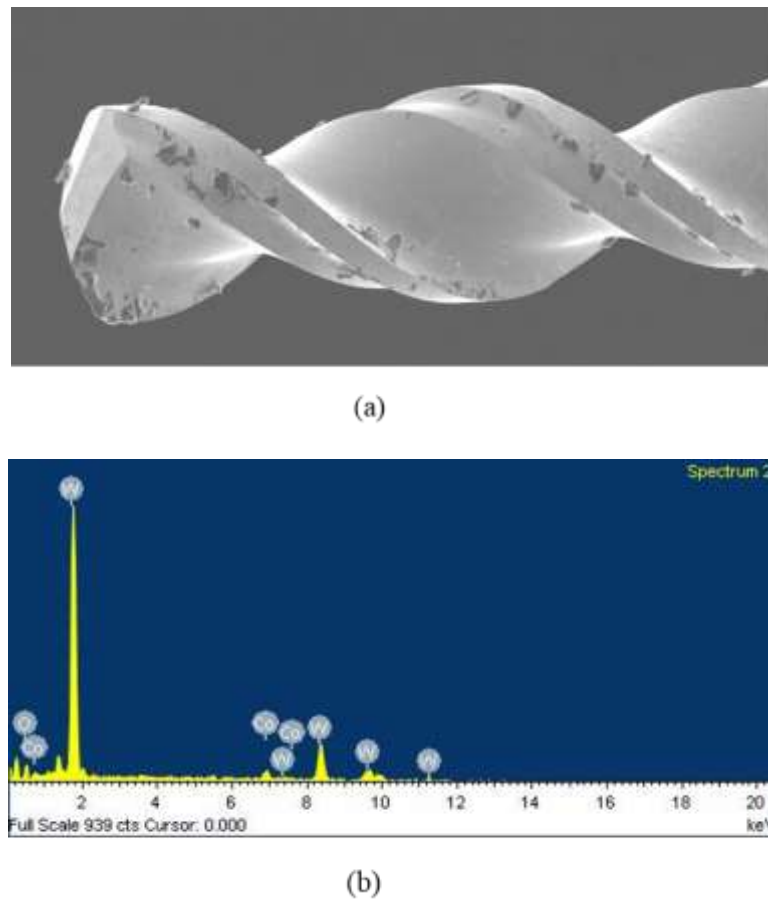


Figure 1.9: Solid carbide twist drill (a) SEM image, (b) material characterisation through EDS analysis

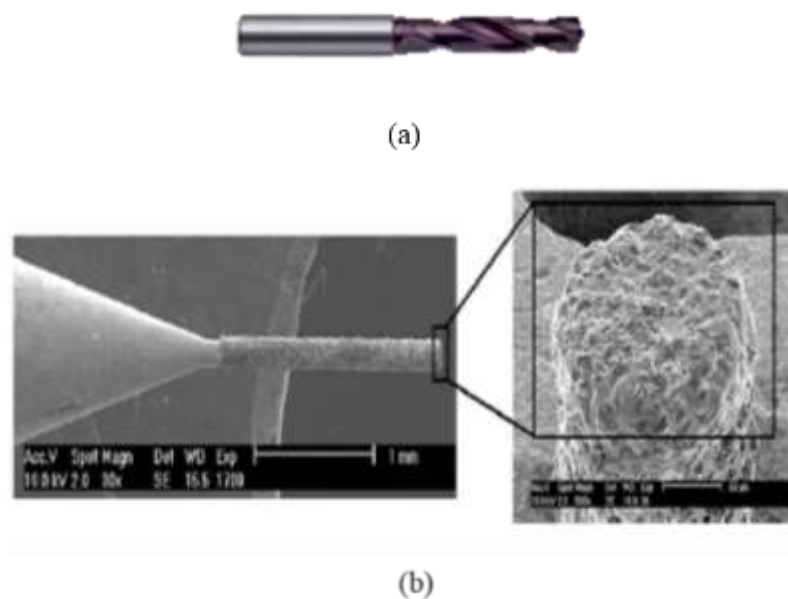


Figure 1.10: Coatings on micro drill bits; (a) solid carbide coated twist drill [265]), (b) diamond abrasives on flute section (Lee et al., 2004)

These thin plates are manufactured with one or more layers laminated in to substrate boards that are used for interlayer connections for electronic components and signalling systems that are found in various applications from toys to radar systems [211]. The most common substrate used for PCBs is made up of glass-fibre-reinforced epoxy (GFRP) with a copper foil bonded to the surface. PCBs are of three types; single layered, double-sided, multi-layered circuit boards that depend on the number of copper foil layers used for insulating. An example of a multilayered board with through-hole plating, the green solder resist and white silk screen printing is depicted in Figure 1.11.

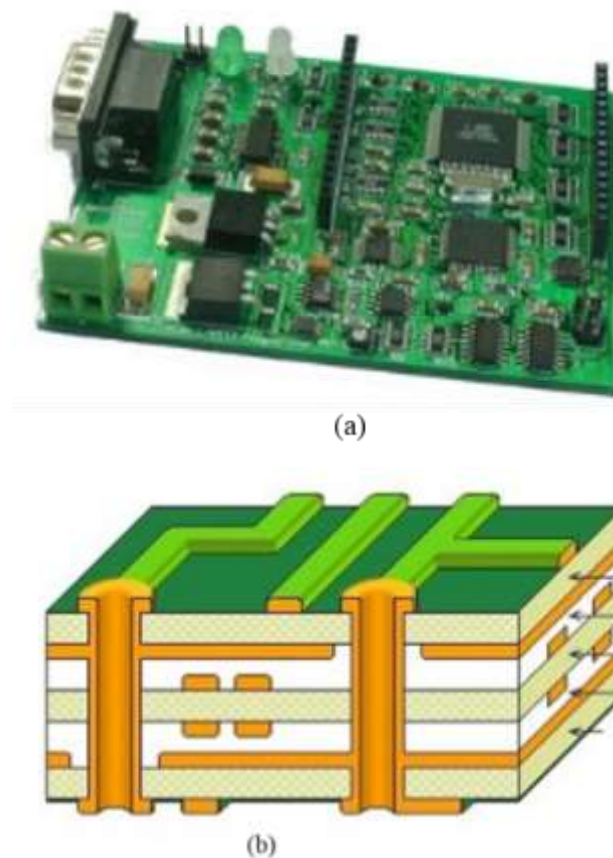


Figure 1.11: Layout of the PCB (a) complete PCB in use, (b) Inner view of PCB laminate with vias and through holes (Reproduced from web) [266]

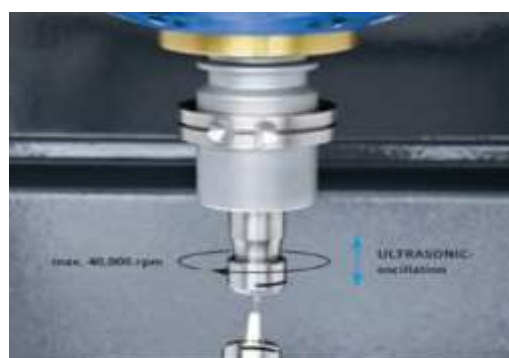
1.3 Ultrasonic Machining

Ultrasonic machining (USM) is a machining technique that incorporates a cutting tool that vibrates at an ultrasonic frequency that drives the abrasive grains to produce a brittle fracture on the workpiece surface. The shape and dimensions of the workpiece are determined by the tool shape and the size of the abrasive grains. Ultrasonic machining is a non-traditional machining technology developed for machining brittle and hard materials, which are

difficult to machine using conventional techniques. In the present competitive market, a lot number of demands have risen for ultrasonic machining technology. The applications of USM has been extended to optical industry, in precision engineering / watch industry, medical technology, high-performance ceramics, composite materials, etc. The ultrasonic machining has covered different conventional machining processes and categorised into ultrasonic cutting/turning, milling, grinding, drilling, etc. In general, the ultrasonic assisted machining system consists of an ultrasonic generator, transducer, waveguide and cutting tool. The required unit removal rate for micro-ultrasonic machining can be realized by using submicron abrasive particles and micro tools that are manufactured by micro-EDM. The major problems are the precision of the setup and the dynamics of the equipment that has greatly reduced by the introduction of on-the-machine tool preparation and vibrations that are applied to the workpiece. So far, DMG Moriseki is one of the present manufacturer and supplier for commercial ultrasonic machines with different diameter ranges as shown in Figure 1.12.



(a)



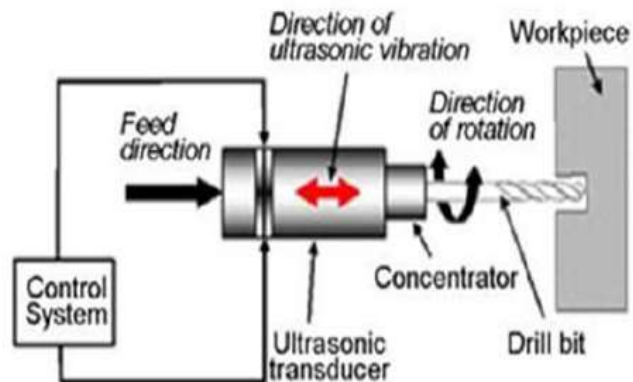
(b)

Figure 1.12: Ultrasonic machine developed by DMG MORI; (a) flexible integration machine, (b) spindle setup. (Adopted from DMG MORI Machine data manual) [267]

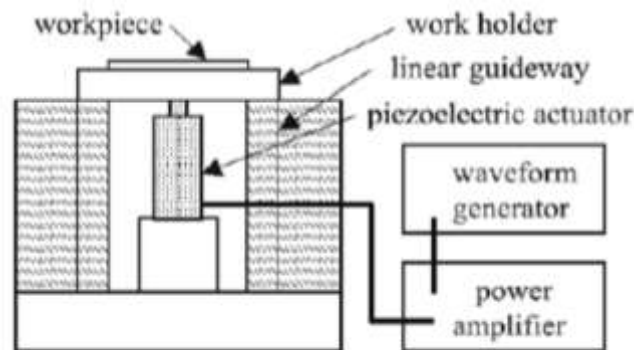
1.3.1 Ultrasonic Vibration Assisted Drilling

Ultrasonic vibration assisted drilling (UAD), is one of the distinctive technique introduced in drilling process to drill the difficult-to-cut and harder materials from the past decade. Vibration-assisted drilling has ability to improve the hole quality, reduction of forces, burr minimization and increase in tool life. Moreover, UAD extended to wide range of applications and gaining prominence in various manufacturing sectors. Investigations have been carried out on micro hole drilling of multi-layered / double layered PCBs.

In recent years UAD technique dragged a lot of attention in academia and in the industries. UAD system consists of ultrasonic transducer, waveguide (horn) and a drill bit tightly clamped with bolts on lower end of the waveguide. The mechanism of UAD works on the principle of converting low-frequency electrical energy into high-frequency mechanical vibration by longitudinal transducer with minimum amplitude and transferred to drill bit via waveguide or vice-versa to workpiece material to enhance the drilling process as demonstrated in Figure 1.13.



(a)



(b)

Figure 1.13: Concepts of ultrasonic assisted drilling (a) drill vibration (Thomas.P, 2008),
(b) work piece vibration (Chern et al., 2006)

Based on the previous experimental studies, numerous advantages are shown in UAD dramatically. Vibro-impact process in UAD has shown reduction of axial forces, chip jams, friction, and unnecessary plastic deformation and increase in surface quality. During the vibroimpact process, a high frequency impulsive force is generated which plays a significant role in enhancing the machining process (Babitsky et al., 2007). Thus, machining is achieved more efficiently by a reduced quasi-static force as compared to a conventional case where the cutting force is continuous and higher. The elimination of burrs and prolonged tool life are possible in UAD to some extent. UAD has previously shown significant potential in its conventional drilling application.

1.3.2 Ultrasonic Vibration Assisted Micro-Drilling

In order to optimize the drilling process and resolve the difficulties as carefully as possible, it is essential to study the drilling process and to examine the possibility of implementing Ultrasonic Vibration Assisted Micro-Drilling (UVAMD) to enhance the performance of micro-drill. UAD technique has shown a major advantage in force reduction which is a potential solution for micro-drill operation that causes instability and drill breakage. Foremost, a lot of research work is reported on UAD technology representing experiments and slight effort of work is reported on UVAMD. Lesser work on micro drilling was done on low frequency vibration drilling at lower speed and feed rates that has shown reduction in burr formation and drill skidding. However, the dynamic issues related to vibration assisted micro-drilling technique are essential to investigate for its advanced application.

1.4 Burrs

Machining operations often leads to edge roughness because of the protruding, ragged material along the edges known as burrs (Hassamontr et al., 1995). In micromachining, fatigue life, surface finish and mating faces of the micro components get severely affected because of such protruding edges known as micro burrs at the work piece edges / surfaces. It is much more difficult to remove micro-size burrs in comparison to macro-size.

In micromachining, burrs can be classified in various ways. Based on their position, burrs can be distinguished as top, bottom, entrance and exit burrs. Based on their shapes and quantity, four different types of burrs can be classified, namely minor burr, primary burr, feathery burr and needle-like burr.

Quantitative prediction of micro burr is impossible because of the unavailability of an accurate analytical model due to its complex mechanism. Also, during the micro-cutting operation, burr removal is generally very difficult and can severely damage the work piece. Due to the very small size of micro burrs, conventional operations of deburring cannot be easily adopted. Micro burr height is strongly affected by cutting parameters, like feed rate and the burr size is related to the amount of tool wear. Also, tool wear and tool life is drastically affected by burr formation.

1.4.1 Milling Burrs

As per Chern et al., 1993, the types of burr produced during milling operation were found to be vastly related to the in-plane exit angle. In milling, five (05) classes of burrs can be observed in Figure 1.14 as (a) the knife-burr, (b) the wave-type burr, (c) the curl-type burr, (d) the edge breakout and (e) the secondary burr.

The types of burr produced during face milling operation are classified based on burr shapes, burr locations and burr formation mechanisms (Hashimura et al., 1999). An exit burr is defined as a burr adhered to the surface machined by the minor edge of the tool. The burr attached to the transition surface machined by the major edge of the tool is named side burr. The one attached to the top surface of the work piece is called top burr.

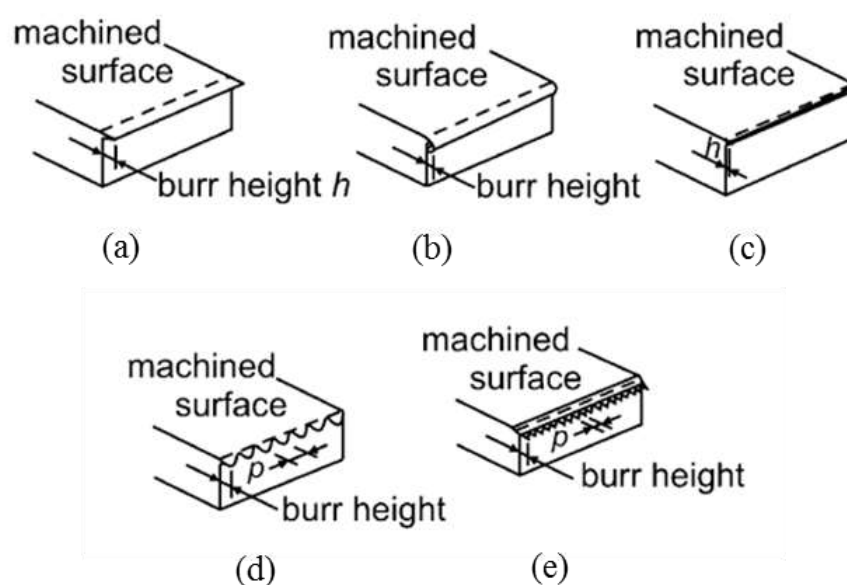


Figure 1.14: Burrs observed in face milling (a) knife burr, (b) wave-type burr, (c) curl-type burr, (d) edge breakout and (e) secondary burr (Chern GL, 1993)

1.4.2 Drilling Burrs

The burrs that arises during drilling operation (Figure 1.15) at the entry of the hole can be a result of tearing, bending action followed by clean shearing, or lateral extrusion. A Poisson burr is the burr formed when a sharp drill comes out of the work piece because of the rubbing at the drill's margins. A rollover burr is formed when a worn out or normal drill comes out of the uncut chip rolls (Kim et al., 2001).

Drilling burrs can be classified as uniform burr with or without drill cap, petal burr or crown burr based on their formation mechanism and shapes. For stainless steel, two categories of burrs namely uniform burr (type I: small uniform burr, type II: large uniform burr) and crown burr were found, whereas for low alloyed steel three categories of burrs namely uniform burr (type I & II), crown burr and transient burr were found (Figure 1.15).

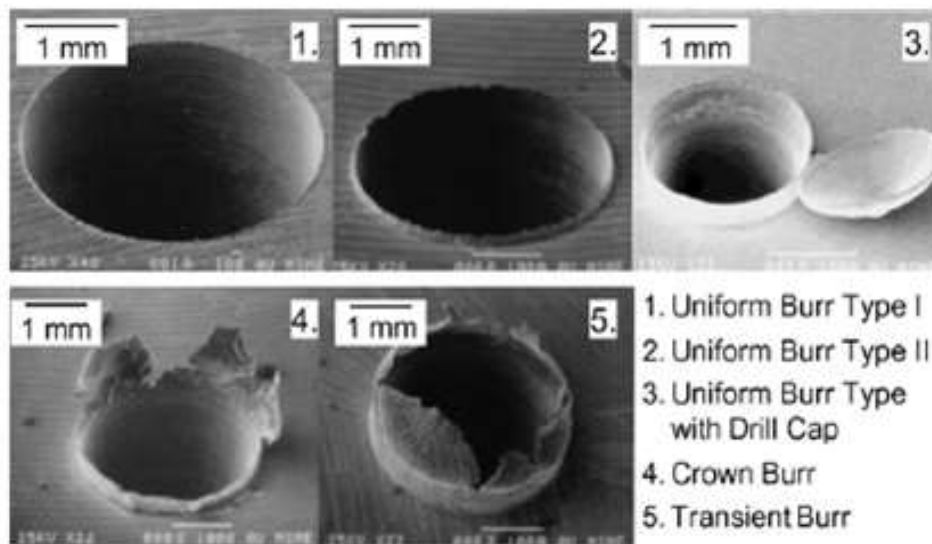


Figure 1.15: Drilling burrs (Kim et al., 2001)

The mechanisms of burr formation cannot be controlled and predicted due to the unavailability of a commonly accepted analytical model. The main reason for this is the complex phenomenon of the drilling mechanism.

In drilling process, the acting thrust force is greatly affected by the ratio of the speed/feed to the diameter of the drill bit. Simultaneously, burr formation is also influenced by the plastic deformation of the exit surface, caused by the governing thrust forces. Increase in feed during drilling process increases the thrust forces. The orthogonal cutting force model is used to correlate the feed and the thrust force with varying drill diameter and expressed as (Bhandari et al., 2014),

$$\Delta F_t = \frac{kf \sin \kappa \sin(\lambda - \alpha)}{2 \sin \varphi \cos(\varphi + \lambda - \alpha)} \Delta W \quad (1.35)$$

$$\Delta W = \frac{(\rho_{i+1} - \rho_i)R}{\sin \kappa}, \quad \text{for } i=1,2,3,\dots,n \quad (1.36)$$

and ρ is the relative radius r/R , which is the ratio of the distance, from the drill centre to the segment, to the drill radius. For the chisel edge of a split point twist drill, a constant rake angle is assumed and the total thrust force F_t is defined as,

$$F_t = \sum_{i=1}^n (\Delta F_{t, \text{chiseledge}} + \Delta F_{t, \text{cuttingedge}}) \quad (1.37)$$

$$F_t = \sum_{i=1}^n (k \cdot f \cdot R \cdot f_n(\varphi \cdot \lambda \cdot \delta \cdot h \cdot \kappa)), \quad (1.38)$$

where k is the shear strength of the workpiece material, f_n is a function of $(\varphi \cdot \lambda \cdot \delta \cdot h \cdot \kappa)$ f is the feed (mm/rev), 2κ is the point angle of the drill, λ is the friction angle, α is the tool rake angle, φ is the shear plane angle, R is the drill radius, δ is the ratio of the web thickness to the drill diameter, and h is the helix angle. The mechanism of burr formation is highly influenced by stress and resultant strain. The effective stress can be expressed as,

$$\tilde{\sigma} = \frac{F_t}{A} \alpha \frac{F_t}{d^2}, \quad (1.39)$$

where, F_t is the thrust force, which is a function of the feed rate (f), diameter (d), drill bit, and work piece material.

$$\tilde{\sigma} = \frac{f}{d} \cdot f_n(\text{Material}(k, \lambda), \text{Geometry}(\varphi, \delta, h, \kappa)) \quad (1.40)$$

For a given drill geometry and workpiece material, burr formation is determined solely by f/d , which is the dimensionless feed parameter (Fn) in the micro drill burr control chart (M-DBCC). Also, the cutting speed parameter (S) is expressed as the product of the drill diameter (μm) and spindle speed (N).

$$F_n = \frac{f}{d} \quad (1.41)$$

$$S = K \times d \times N, \quad (1.42)$$

where, N = spindle speed (min⁻¹), d = drill bit diameter (μm), f = feed (mm/rev), and K is a constant that makes the orders of the two equations equal. N, d, and f are the parameters of the M-DBCC.

1.5 Organization of Thesis

The work carried out in the thesis is briefly outlined and its organization is summarized as below.

Chapter 1 begins with the general overview on micromachining. Here, brief information is given for the micro-drilling process, micro-drill bit geometry and materials, burr formation mechanism and vibration assisted macro/micro-drilling process. (short this chapter)

In chapter 2, a comprehensive state-of-the-art review in the direction of mechanical micro-drilling process and various modeling aspects are presented. Work on ultrasonic machining approaches, experimental setups and machining parameters, etc. considered by past researchers have been discussed. Research need was identified and the objectives of the present work with brief methodology is explained.

In chapter 3, geometric design of micro drill and multilayer PCB is developed to perform finite element dynamic analysis of conventional micro-drilling on multilayered PCB material. Graphical results depicting stresses, forces and burrs generated on workpiece have been discussed and compared with the past experiments.

FE simulation for ultrasonic vibration (UV) assisted micro-drilling on multilayered PCB was performed on CAE (Abaqus/Explicit) environment is presented in chapter 4. Graphical comparison of conventional micro-drilling and UV assisted micro-drilling is shown and burr formation charts are presented. This chapter also provides the correlation between finite element simulations based approach and analytical approach for ultrasonic assisted micro-drilling.

Chapter 5 deals with design of ultrasonic horn for micro-drill. Here, finite element (FE) modal analysis is performed to examine the influence of natural frequency and varying modes shapes of stepped and conical horn considering various combinations of horn and drill bit materials. Further, FE harmonic analysis is also presented to predict the displacement loads on both the horn profiles along with micro drill bit at varying amplitudes.

Chapter 6 presents a summary of the substantial findings of the work done, the current limitations raised by the proposed methodology and few recommendations for future work. These would further enhance the UV assisted micro-drilling process specifically in PCB industries. The final work is enclosed with the list of references acknowledged for the work done.

Chapter 2

LITERATURE REVIEW

The purpose of this chapter is to provide groundwork information on the issues that are addressed and to be considered carefully in the contemporary work and highlight the importance of the present study. It comprehensively covers the preliminary research work that has been done in the area of machining processes and the state-of-art, especially in the domain of conventional micromachining, micro-drilling, materials and design issues, machining burrs, ultrasonic vibration assisted (UVA) drilling and UVA micro-drilling.

2.1 General

Conventional machining techniques still occupy a dominant role of all manufacturing processes. Various advances in machining technologies and new materials developed today, aim to improve productivity, efficiency, product quality and cost minimization. Such advancements require proper industry-driven predictive models for machining processes. Various process parameters, which include choice of optimal cutting conditions, coolant type, cutting tools, etc. must satisfy functional design requirements integrated with optimized process planning. Researchers have shown paths to various aspects of cutting mechanisms, tool geometry, dynamic thrust forces, tool wear, chip formation, burr formation and condition monitoring. Reviews on different processes and documentation of multiple mechanisms in drilling with new materials give insight into the upcoming developments. The drilling operation is a fundamental and most extensively utilised process for machining of holes in the manufacturing sector. For this purpose, high precision and high-speed applications are essential for various productivity enhancement methods in hole drilling process. Various modeling methods for micro-drilling and micro-drilling processes, including strengths and weaknesses of these methods are put into perspective in this chapter. A thorough research report on recent advances in modeling and experimental exploration of burr formation in micro-drilling and micro-milling mainly targeting industrial uses is introduced. Furthermore, a roadmap is proposed for future directions aiming burr minimization in micro-machining. Additionally, literature survey on recent developments

in ultrasonic vibration assisted drilling and other recent methods in micro drilling operation has been discussed.

2.2 Conventional Micromachining

Micromachining is a generally used industrial method to manufacture micro components. The reduction in the size of the cutting tools offers massive scope of research to improve various micromachining processes and finished micro parts. Micromachining methods are similar to those of traditional machining methods. However, simply scaling the parameters or models cannot be applied directly in micromachining. Various issues like size effect of cutting tool edge/radius, tool angles, chip thickness, cutting speed, plastic deformation, etc. need to be considered (Cheng et al., 2013). The scaling down effects of tooling and equipment is done from macro to micro models while considering these size effects. Besides, the effects and properties related to work piece material, such as grain size, hardness, elasticity, etc. are to be considered in micromachining. Such aspects and issues greatly influence the surface quality of the work piece.

Researchers like Shatla et al. (2000), Wang et al. (2001), Zhang et al. (2005), Vijayaraghavan et al. (2007), Isbilira et al. (2011), Karaca et al. (2011), Kyratsis et al. (2011), Heisela et al. (2012), Wang et al. (2012), Matsumura et al. (2013), etc. have worked on different modeling approaches in drilling. Engin et al. (2001), Mativenga et al. (2005), Wan et al. (2007), Chua et al. (2008), Wan et al. (2010), Tapoglou et al. (2012), Kulkarni et al. (2013), etc. have proposed various approaches in milling process. In line of micro cutting tools, some works in the direction of modeling and analysis of micro-drilling has been discussed by researchers like Hinds et al. (2000), Kudla et al. (2001), Nakagawa et al. (2007), Kim et al. (2008), Fu et al. (2010), Zhang et al. (2011), Aziz et al. (2012), Sambhav et al. (2013), etc. Also, some work in the field of micro milling cutters is significantly explored by Bao et al. (2000), Vogler et al. (2004), Jun et al. (2006), Chen et al. (2007), Liu et al. (2007), etc. Investigations related to dynamic cutting forces in micro end milling have been presented by Kang et al. (2007), Li et al. (2007), Filiz et al. (2011) and Li et al. (2011). Jun et al. (2012), Wu et al. (2012), Rao et al. (2012), Mustapha et al. (2013), etc. have worked in the direction of cutting force modeling and finite element simulation of micro-milling. Burr mechanism and control of burr formation in macro- and micro-machining methods also find a lot of significance. Satish et al. (2003), Alrabii et al. (2009), etc. have discussed the formation of burr and its reduction at macro level. Also, Kim et al.

(2004), Lee et al. (2005), Liang et al. (2009), Saptaji et al. (2012), Chen et al. (2012), Aziz et al. (2012), etc. have discussed modeling, analysis and minimization of micro burr in micro milling and drilling. A novel approach for burr minimization in mechanical micro-drilling has been proposed by Okasha et al. (2012) and Zheng et al. (2012). Bhandari et al. (2014) have suggested burr control chart in micro-drilling of PCBs.

2.3 Modeling Approaches

Modeling is a useful tool for engineering design and analysis. Despite of significant advances, knowing several processes using modeling approaches is much more essential. Extensive reviews of these modeling approaches will pave the way towards the understanding of these machining processes.

2.3.1 Analytical Modeling

Analytical modeling techniques abstract the features of parameters or parameterized functions in order to make the modeling task tractable. This technique has been widely used to study and predict cutting forces in metal cutting processes. Bao et al. (2000) have presented analytical cutting force model of micro end mill processes and the tool run out. Vogler et al. (2004), Jun et al. (2006) and Liu et al. (2007) have worked on the dynamic modeling and analysis of machining performance in micro-end milling for surface generation and cutting force prediction. A three-dimensional (3D) cutting force model (analytical) for micro end milling operation has been proposed by Zaman et al. (2006). The proposed model determines the theoretical chip area at any specific angular position of the cutting edge while considering the tool path geometry and the tangential cutting force. Kang et al. (2008) introduced a cutting force model to predict the cutting forces in micro-end milling operation. Modeling of 3D cutting forces in micro end milling with respect to uncut chip thickness has been discussed by Li et al. (2007). Lekkala et al. (2012) investigated various characteristics of burr formation process in micro-end milling. They observed that the tool diameter and depth of cut are the main parameters which influences the burr thickness and height significantly. Ali et al. (2013) proposed a cutting force model which calculates the instantaneous chip thickness in micromachining. Here, they assumed that the ploughing force component is related to elastic recovery between the tool and the work piece. Mijuskovic et al. (2013) investigated the tool deflection analysis in micro milling while taking into account various cutting parameters (width of cut, depth of cut and feed per

tooth). Zhang et al. (2013) discussed about the impact of size on burr formation in micro-cutting. They suggested that due to the size effect of uncut chip thickness and specific cutting energy, the exit burr height increases. Also, it was observed that curl radius plays an important role in increasing the height of exit burrs.

2.3.2 FE Modeling

The finite element (FE) method features exact prediction on a user friendly graphical interface and is extensively used for modeling cutting processes, its simulation and optimization. Thus, FE modeling potentially allow engineers and designers to minimize the need for physical trials and improve cutting tool design, minimizes the lead time and optimizes the process conditions.

The occurrences of stresses in micro-drills using the finite element method was discussed by Hinds et al. (2000). Here, the correlation between the stresses and the life of a drill bit was discussed. Park et al. (2000) have applied finite element model on orthogonal metal cutting, including burr formation in 304L stainless steel. The characteristics of the thick and thin burrs are clarified along with the details of the negative deformation zone. Min et al. (2001) have worked on thrust force analysis and the drilling burr formation, using finite element approach. The FE model and analytical model of micro milling considering size effect, micro cutter edge radius and minimum chip thickness was discussed by Lai et al. (2008). Liang et al. (2009) developed a three-dimensional FE model to analyze micro burr formation in micro end-milling process. Here, the model predicts the influence of various tool edge radius and tool-tip breakage on burr formation in aluminum alloy (Al2024-T6). Afazov et al. (2010) have predicted micro-milling cutting forces through finite element modeling based approach. FE modeling of a micro-drill and proper experimentations on high speed ultrasonically assisted micro-drilling were shown by Zhang et al. (2011). A strong correlation has been shown between the thrust force measurements and the predicted nonlinear force model.

FE analysis follows two numerical formulation methods, either of the Lagrangian and Eulerian methods and sometimes both. Most of the FE analysis for machining was solved by using Lagrangian solver due to numerous advantages over the other. There are several commercial software packages available to compute the modeling process such as ABAQUS, ANSYS, Hyper Mesh, Deform 3D and AdvantEdge for solving different types of problems. Most of the researchers availed these softwares for solving and simplifying various machining difficulties in turning, milling, drilling, grinding and boring, etc. Racz

et al. (2004) have performed a Eulerian FE model of the metal cutting process. Johnson-Cook, hydrodynamic constitutive models are used to investigate the cutting forces, stress and strain distributions on copper. Some of the researchers worked on drilling of harder materials like Aluminum, Brass, Copper, Inconel and Titanium etc. Many industrial sectors are using composite and laminated materials due to their light-weight and high strength. Investigation on fiber damage, bonding, thrust forces, stress-strain relationship, etc. in the area of composite materials like CFRP and GFRP has been done by Dandekar et al. (2008), Isbilir et al. (2012), Isbilir et al. (2014), Phadnis et al. (2012), Phadnis et al. (2013) and Lee et al. (2015).

2.3.3 Empirical Modeling

Empirical models are those that are based entirely on experimental data. These models can be used to develop design of experiments for varying process parameters (e.g., cutting conditions, tool geometry, etc.) and determining process performance such as cutting forces, surface roughness, tool-life, etc. and correlating them to the input conditions. For this reason, this method depends heavily on proper experiments conducted at different cutting conditions, cutting tools, and coolant/lubrication applications.

Lee et al. (2005) have investigated on micro-burr formation in micromachining. Here, they conducted experiments on tool life and various cutting conditions influencing change of burr height. As per their experimentation, they concluded that stresses induced on the tool and work piece directly influences the burr formation and tool wear. Newby et al. (2007) have shown an empirical model for cutting force analysis in micro-end milling operations. Higher feed tooth per radius of cutter ratios and the true trochoidal nature of the tool edge path has been considered. Empirical modeling of vibration in micro end milling of poly methacrylate (PMMA) work piece, considering different parameters like spindle speed, feed rate and depth of cut was represented by Mamedov et al. (2013). Their analysis shows that on comparing with spindle speed, the feed rate and depth of cut has highest influence on vibration during machining process. Zheng et al. (2013) and Bhandari et al. (2014) have conducted experimental studies on burr types and formation zones of multi-layer material sheets (PCB's). In micro drilling, Taguchi's ANOVA technique was used to optimize the drilling parameters for reducing burr height and thrust force.

2.3.4 Mechanistic Modeling

A mechanistic model is one where the basic elements of the model have a direct correspondence to the underlying mechanisms in the system being modeled. A model is derived which relates a comprehensive characterization of the cutter and the cut geometries and the process inputs to outputs while performing few experiments. Amy et al. (2000) have proposed a model by prediction of drilling forces utilizing a minimum cutting energy model for chip flow angle. Gong et al. (2005) have established a mechanistic model considering dynamic forces in micro-drilling process. A mechanistic model of predicting cutting forces in micro-end milling operation considering on cutting tool edge radius effect was presented by Kang et al. (2007). Here, the characteristics of the cutting forces are used for evaluating the tool condition, damaged layer, and surface roughness in micromachining. Park et al. (2009) developed a mechanistic model of shearing and ploughing domain to predict micro-milling forces. Investigation on the effect of elastic recovery based on the interference volume between the tool and the work piece has been presented by Malekian et al. (2009). Jun et al. (2012) presented a new mechanistic approach for micro-end milling. A new methodology for predicting the cutting coefficients in considering the tool edge radius and material strengthening effects have been discussed by Srinivasa et al. (2013). Further, a mechanistic model was proposed to predict the cutting forces in micro-end milling operation taking into account overlapping tooth engagements. Flachs et al. (2014) devised a mechanistic model of thrust force and torque in step-drilling.

To improve the stability of any machining process, the prediction of cutting forces in machining along with mechanics and dynamics of cutting tools, various modelling methods need to be considered. Chandrasekharan et al. (1998) devised a mechanistic model to predict the cutting forces using arbitrary drill point geometry. The cutting lip model is developed to measure the cutting angles and chip thickness as depicted in Figure 2.1. An analytical model to predict the torque and thrust forces generated in high-speed drilling was discussed by Elhachimi et al. (1999). The evolution of cutting forces regarding various parameters, such as feed, speed and the effect of drill geometry have been discussed. The cutting forces and geometry of drill lip presented by Elhachimi et al. (1999) are shown in Figure 2.2. To reduce the efforts for minimising thrust forces in drilling, Bergstrom et al. (2000) proposed a mechanistic model to predict the cutting forces by chip flow angle with minimum cutting energy. Flachs et al. (2014) investigated the step-drilling process. A mechanistic model for

step-drilling of Aluminum (Al7075-T651) was presented and validated with experiments. The predicted forces and burr formation got reduced by using step-drilling method.

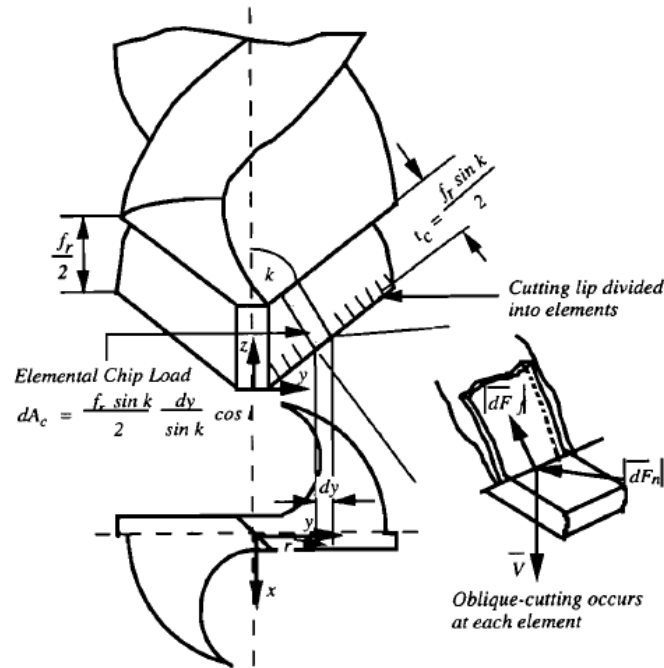


Figure 2.1: Cutting lip model for a conical drill (Chandrashekar et al., 1997)

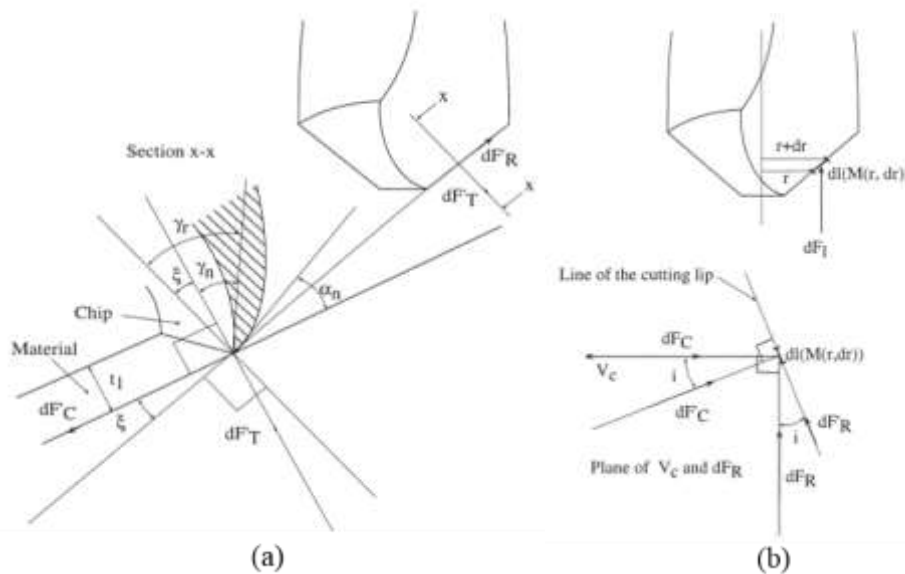


Figure 2.2: 2D views of cutting lip (a) geometry, (b) forces and cutting speed (Elhachimi et al., 1999)

Minukhin et al. (2013), performed geometrical/mathematical analysis of a drill design developed by Chyan et al. (1998), to calculate the thrust forces and torque generated in high speed drilling. The study proved that primary cutting edge is the leading factor that affect the dynamic rake angle and uncut chip thickness. A mathematical model to estimate the

cutting forces and to predict the radial displacement of cutting tool under low frequency conditions considering structural dynamics of the spindle system and tool for measuring the hole quality was performed by Pirtini et al. (2005). During drilling of micro holes, the characteristics of drill bits and work piece materials are essential factors. The increasing aspect ratio of micro drill with reducing the diameter leads to instability and deformation; and increasing in web thickness leads to increase in torsional rigidity of the microdrill. To observe the issues concerning micro drilling operation, Gong et al. (2003) investigated the dynamic characteristics of micro drills. Mathematical model has been developed for pre-twisted and rotating beam subjected to a compressive axial and radial forces at the drill point. The effect of rotary inertia, gyroscopic moments and transverse shear are considered for determining the critical speeds and buckling loads. The simulation results demonstrates that increasing in geometrical cross-sectional area and helix angle will improve critical speeds. Buckling loads will decrease with increase in rotational speeds of the drill. The decrease in flute length also shows impact on restraining boundary conditions. To inspect the precision of the drilling system, a dynamic spindle system model for high speed micro-drilling was developed by Yongchen et al. (2006). The effect of the clamping length, damping and bearing stiffness, spindle speed, the eccentricity of the drill system and the axial drilling forces and dynamic stresses were analysed. The influence of rotational speeds on buckling loads and the thrust forces on critical speeds subjected to varying geometrical parameters and machining conditions was presented by Chen (2007).

Filiz et al. (2010) proposed unified one-dimensional and three-dimensional finite element models to investigate the dynamics of macro and micro drills. A numerical convergence study for bending, axial and torsional vibration were carried out using geometrical parameters. The models were validated with experimental modal analysis to compare the natural frequencies and mode shapes. Micro drills can be easily fractured due to their long and slender structure. To achieve a more efficient micro-drilling process, Kim et al. (2008) proposed step-feed micro-drilling approach for thrust force and burr minimization. Due to an increase in mechanical deep hole drilling applications, the chip formation and heat generation is becoming new challenges in several industries. To reduce the chip formation effect, the shearing zone of the materials needs to be considered. Researchers like Sambhav et al. (2013) studied the ploughing effects at the shearing zone in micro drilling. Rahamathullah et al. (2014) presented the mechanistic model to predict thrust forces on plain and glass-reinforced epoxy sheets and validated the model against micro-drilling experiments. Patra et al. (2015) carried out experimental analysis of cutting forces in

austenitic stainless steel (X5CrNi18-10) generated during micro-drilling. A review of the above literature shows the calibration technique of cutting forces during macro and micro-drilling are developed based on the tool geometry and the cutting parameters. They have shown that the thrust forces and torque leads to average surface finish and leads to burr formation on work piece materials. Also, it is essential to improve methods of prediction of cutting forces on different work piece materials to control the burr formation.

2.3.5 Geometric Modeling

Geometric models are generally distinguished from object-oriented and procedural models, which define the shape/profile directly by a mathematical expression (algorithm) that generates its form/appearance. The shapes/profiles considered in geometric modeling are mostly 2D or 3D based on computer applications in design and manufacturing. These geometric shapes are defined by parametric/implicit mathematical equations.

Fleischer et al. (2008) has defined a geometrical design of micro-milling tools. 3D modeling and FE simulation of a generic end-mill was proposed by Tandon et al. (2009). Here, the generic flat end mill cutter is directly rendered in OpenGL environment in terms of three-dimensional parameters. An interface was developed here that directly pulls the proposed three-dimensional model defined with the help of parametric equations into a commercial CAD modeling environment. Panagiotis et al. (2011) has shown thrust force prediction model of twist drills in a 3D CAD environment using application programming interface (API). Sambhav et al. (2012) has discussed a methodology to model the twist drills with generic point geometry using NURBS. Yan et al. (2013) has presented a visualization design and optimization of helical drill point. Here, numerical modeling and simulation based on mathematical models of helical drill has been done. By considering drill geometric parameters such as lip clearance angle along cutting lip, heel clearance angle along flank surface, cutting edge inclination angle, rake angle, etc. are modified according to different drilling requirements by the aid of the developed CAD simulation system. Minukhin (2013) developed a methodology to predict cutting forces occurring on the primary cutting edges of twist drills. A fundamental geometrical analysis was carried out on the primary cutting edge of a twist drill to understand the correlation between the geometrical features of the drill and the distribution of cutting forces. The suggested methodology presents the proper definitions of the dynamic rake angle and the uncut chip thickness.

Recent improvements in the field of geometric modelling provide designers with an sophisticated and accurate methodology of specifying the geometry of complex designed

objects. The performance of the drilling is considerably affected by the geometry of the twist drill bit and requires accurate measurement. Flank wear and crater wear influences the residual stresses, surface finish and other geometrical tolerances. The twist drill bit consists of parameters like point angle, chisel edge, indentation zone along with cutting lips which are relatively complex and requires precise design. Significant work has been done by the researchers to study the geometry of the conventional twist drills Rincon et al. (1995). They proposed mathematical and analytical models for different drill cross-sections such as planar, conical, helical, Racon® and arbitrary shaped drills and the effect of grinding parameters on drill point angles. They also highlighted the importance of understanding the geometry and specifications of the drill design and their use in developing predictive forces models. Modeling and simulation of machining process is a method to understand high quality machined parts. The shape of the drill tool is one of the fundamental features to affect the dynamic stability and machining accuracy. Generic design of drill bit using CAD approaches for customised applications are essential. It is difficult to represent the exact three-dimensional (3D) profile of a particular drill bit because the geometry is very complicated. The ease of simulation lies with the actual 3D geometric specification of modified cutting tools that would benefit to the manufacturing sector before actual machining, as well as numerous direct applications.

Many aspects of micro-drilling and conventional drilling have primarily similar features, but reducing of the drilling dimensions lead to an array of problems which produce a profound influence on the micro-drilling process Bannan et al. (2006). The dimensional size of the microdrill is less than one-tenth or one-hundredth of the actual size of the conventional drill. Researchers like Lin et al. (1992), Chyan et al. (1998), and Ehmann et al. (1993) developed a mathematical model for micro drill cross-sectional geometries of planar and helical drill bits for controlling the effect of grinding parameters. The importance of cutting angles like clearance angle, helix angle distribution along the chisel edge and cutting lip have been discussed. The literature reveals that the geometry of a cutting tool has a substantial effect on the inputs as well as outputs responses of the machining process. The drill point geometry of the twist drill is the major section in determining the drilling forces namely torque and thrust. Minimization of torque and thrust forces leads to improvement in performance of drill bit, reducing deflection and improving the tool life.

2.4 Ultrasonic Assisted Machining

Ultrasonic vibration assisted micromachining is combination of precision micromachining with small amplitude tool, workpiece. This approach has been applied to a number of processes from micro milling to electro discharge machining. During ultrasonic vibration assisted machining, the cutting tool loses contact with the chips on specified amplitude and frequency, resulting in decreasing of machining forces and improving tool life with accurate surface finish. Any hard and difficult-to-cut materials can be machined using ultrasonic micromachining. A number of research works have been done covering micro ultrasonic machining and vibration assisted conventional drilling by various researchers. Some have been reported in the present section.

Bertsche et al. (2013) proposed a new force model to determine the relationship between the input parameters like cutting speed and feed with process output parameters for rotary ultrasonic milling process (RUSM). Li et al. (2014) studied the cutting performance with micro tools in ultrasonic vibration assisted micro milling. The effect of tool wear on the surface quality, burr formation and tool life were investigated. The study proves that vibration assisted milling (VAM) shows better cutting performance in terms of tool life and surface quality. The study also recommends that the cutting speed should be less than 25% of the maximum speed of the vibration for obtaining longer tool life in dry VAM. The reduction of down milling burrs were found 18% as compared to conventional milling.

Shen et al. (2012), investigated the influence of ultrasonic vibration assistance on surface roughness in micro-end milling. The experiments proved that the forced feed has negative effect on the surface roughness of slot bottom end of the workpiece material. Also, they observed uniform surface on workpiece material in UVAM than conventional milling. Chern et al. (2006) explored the effect of vibration cutting on micro-milling of aluminum 6061-T6. A two-dimensional worktable has been developed to create vibration on workpiece. The results shown that employing vibration to workpiece with proper amplitude and frequency will increase the no of slots with in the tolerance. Also, suggested that high frequencies has negative effect on the tool life. Kuo et al. (2008) proposed to design a rotary ultrasonic milling tool using finite element method. The results revealed that increase in tool length and mass has significant influence on tool node position and lowers the resonance frequency. Kuo et al. (2012) performed experiments on rotary ultrasonic milling to observe the impact of feed rate and depth of cut on surface roughness. Results proved that, the increase in depth of cut and feed rate greatly effects the surface roughness in conventional

milling. The requirement of tool design to increase ultrasonic kinetic energy for material removal has been discussed. Lian et al. (2013) developed experimental setup for ultrasonic vibration assisted micro milling with longitudinal vibration of workpiece. Tool trajectory model using numerical method for ultrasonic amplitude and frequency is performed. Tao et al. (2016) performed experiments on squamous surface with ultrasonic vibration assisted micro milling. The influence of ultrasonic frequency, amplitude, tool diameter, feed, speed on tool tip path were analyzed. The significant influence of feed with ratio of ultrasonic frequency and spindle speed were observed on texture surface of the workpiece material. Vibration drilling revealed a path to perform high machining efficiency and productivity regarding various aspects like reduction of forces, burr minimisation, increasing in tool life, etc. Many researchers showed interest to investigate on vibration assisted drilling process. Effect on hole quality and thrust forces in composite materials with vibration drilling have been studied by Lee et al. (2015). The results indicated that axial vibration on cutting tool reduces the effect of thrust forces compared to conventional drilling. Ramkumar et al. (2004) proposed the vibration assistance to the workpiece for drilling of GFRP composite drilling. An analytical approach for prediction of thrust forces and torque using geometrical parameters of the drill, cutting conditions and vibration parameters and shear flow stress for fibre-reinforced composite materials has been performed by Zhang et al. (2001). Characterization and optimization of vibration-assisted drilling of fibre reinforced epoxy laminates by Sadek et al. (2013). Analytical and experimental investigation of transverse drill vibrations and its effect on cutting forces and torque has been presented by Rincon et al. (1994). The basic understanding of the effect of multifaceted geometry, rotary inertia and gyroscopic moment of drill bit is necessary. Modelling and study on vibratory drilling dynamics, productivity enhancement with micro-drill tool life was performed by Zhaojun et al. (1998).

The characteristics of chatter vibration of the drill bit, analysis of torsional chatter of twist drills considering as untwisted beam was studied by researchers like Bayly et al. (2001) and Ema et al. (2003). Experiments proved that the torsional chatter decreased with stability of the drill bit and burr suppression on work piece. Arvajeh et al. (2006) and Roukema et al. (2007) accomplished the modeling of drilling vibrations and stability in bending of high-speed drilling. Time-dependent kinematic and dynamics analysis on hole formation was investigated. The surface roughness of the work piece material with vibration assisted boring and drilling was performed by Chern et al. (2007). A brief review on the application of vibration-assisted machining in turning operations of brittle, hard and ductile materials

was conducted by Brehl et al. (2008). Chang et al. (2005), Chang et al. (2009) and Chang et al. (2010) investigated the effect of thrust forces and burr formation using ultrasonic assisted drilling. Experiments have been conducted on aluminum alloys and the burr height was compared with conventional drilling process. Results proved that UVD has ability to reduce the thrust forces. Prediction of vibration analysis using artificial neural network was proposed by Eski et al. (2012). Vibration characteristics of piezoelectric torsional transducers were shown by Kim et al. (2003). Numerical simulation of the drill bit with transducer to obtain the longitudinal mode shapes for preferred ultrasonic frequency conditions was performed by Thomas et al. (2007). Ultrasonic test rig was developed to conduct the drilling experiments. Babitsky et al. (2007) conducted the experimental analysis on ultrasonic energy transfer to the drill bit during drilling process. Vibro impact on the drill bit and analytical solution for the drill workpiece model was developed for ultrasonically assisted drilling. Nath et al. (2008) performed an experimental study on difficult-to-cut materials using ultrasonic vibration cutting. Inconel and Titanium are the hardest materials as compared to the other lightweight metallic materials. Investigation on drilling Inconel 738-LC and Ti6Al4V using ultrasonic-assisted drilling was performed by Azarhoushang et al. (2007), Liao et al. (2007) and Baglani et al. (2013). Ultrasonic drilling of composite materials also shown similar advantages over conventional drilling. Researchers like Phadnis et al. (2013), Makhdum et al. (2012), and Mehbudi et al. (2013) investigated the effects of cutting forces and delamination factors on CFRP and GFRP materials using ultrasonic vibration drilling. Numerical analysis has been performed and compared with the experimental results. Experimental investigation of thrust forces while drilling cortical bone was done by Alam et al. (2011, 2015). The research on ultrasonic assisted drilling identified a technique for reducing the forces and burr formation in several materials. The modeling techniques for UV machining further need to be critically reviewed and must be beneficial for micro machining operations.

Ultrasonic vibration assisted micro drilling has nevertheless followed the UAD process. Due to geometrical complexity of micro drills, change in machining conditions often tends to break it easily. Investigation of skidding motion in ultrasonic vibration micro-drilling was performed by Zhang et al. (1994). Chern et al. (2006) performed experiments using workpiece vibration during the micro-drilling process. Tests on high speed ultrasonically assisted micro-drilling and FE modelling of microdrill was done by Zhang et al. (2011). The effect of speed, feed and thrust forces with varying frequency and amplitude were shown.

A novel micro deep-drilling assisted with ultrasonic vibration using a micro long flat-drill was conducted by Aziz et al. (2012).

2.5 Workpiece and Design Issues

Weule et al. (2001) have discussed about prerequisites for the micro-cutting of steel using tungsten carbide tools and the interaction between the properties of the materials and the process parameters on the manufacturing. Uhlmann et al. (2005) has presented a dynamic load and strain analysis for the optimization of micro end-mills. They conducted experimental analysis on cemented carbide micro end mills by high frequency tool loads and in feeds. A parametric tool design was proposed based on the FE simulation analysis. Wang et al. (2005) has presented new tool material binder less cubic boron nitride (BCBN), which is used for high-speed milling of a widely used titanium alloy (Ti-6Al-4V). Li et al. (2008) has discussed modeling and experimental analysis of micro-end milling and explored the influence of tool wear, minimum chip thickness and micro tool geometry on the work piece surface roughness. Kim et al. (2008) applied design of experiment method for thrust force minimization in step-feed micro drilling. An attempt was made to minimize the thrust forces in the step-feed micro-drilling process by taking into account thrust forces, three cutting parameters, feed rate, step-feed, and cutting speed. Jaromir Audy (2008) presented an optimization of drill point geometry through computer assisted modeling. The purpose of his study points that the modification of drill point geometry reduces the influence of negative rake cutting, which results in lowering the cutting forces (thrust, torque and drilling power) respectively. Aramcharoen et al. (2009) have been discussed on Size effect and tool geometry in micro-milling of tool steel. They explored on deriving the ratios of specific cutting force, surface finish and burr formation in micro-scale machining. Biermann et al. (2010) has carried out the improvement of work piece quality in face milling of aluminum alloys. To avoid deburring, in this study, the influence of process cooling on work piece quality is investigated. Using a process cooling with carbon dioxide, the surface quality was improved and the burr formation was minimized.

There are wide varieties of materials available for day-to-day applications and classified as alloys, composites and ceramics. Further improvement in technology helped to develop a new range of materials to strengthen the physical structure of the final product. They are metal matrix and composite sandwich materials that plays a crucial role in modern aviation industries. Metal matrix materials are the laminated materials mixed with composites and

epoxies and possess different material properties at each stage. Drilling of holes for these materials is always a challenging task as they are in large number to hold the joints. During drilling various damages occur in holes. Among them fibre-breakage matrix cracking, fibre pull-out and delamination are more significant. Delamination happens in a laminate when its layers begin to separate in the entrance and exit of the hole and causes major damage. Several investigations have been done to reduce the damage cause factors in these materials. Researchers like Khoran et al. (2015), Monaghan et al. (1992), Vijayaraghavan (2005) and Doomra et al. (2015) performed the analytical, numerical and experimental analysis of drilling thrust force and torque to control the delamination. Analytical cutting force models for drilling fibre-reinforced materials, analysis of fracture mechanism with surface quality and delamination free drilling of composite materials has been investigated by Hocheng et al. (2005), Sedlacek et al. (2008) and Lazar (2012). Carbon fibre reinforced plastics (CFRP) and Glass fibre reinforced plastic (GFRP) materials belong to the composite group. Due to lightweight and having the compatible strength used in aircraft industries. So many researchers have shown their interest to investigate the drilling process on these materials. Chakladar et al. (2012) performed experimental and finite element study on drilling woven glass fibre material. Improvements in tool geometry to reduce the tool wear and minimising the delamination to reduce the tool wear of the drill bit has been discussed. Rawat et al. (2009) developed a machinability map approach algorithm on dry high-speed drilling process for woven glass fibre material. Some of the researchers like Chen (1997), Mohan et al. (2005), Zitoune et al. (2007), Lopez -Puente (2008), Rahme et al. (2011), Feito et al. (2014) and Nie (2014) proposed the analytical, numerical and experimental models to predict drilling thrust forces with numerous variables on machining conditions for CFRP. Some researchers focused on the issues like progressive damage, failure in unidirectional, fracture energies, loading conditions and time-dependent factors that affect the composite materials by Hashin (1981), Brown (2004), Gopinath (2011), Amaya (2012) and Isbilir (2013). Delamination, fracture toughness, geometrical parameters, failure criteria under high strain conditions for GFRP materials were investigated by Okutan (2002), Majzoobi et al. (2011), Vijayaraghavan (2005), Karim (2005) and Mishra (2009). Experiments on drilling of thick composite material with a small-diameter twist drill have been conducted by Rahme et al. (2015).

PCBs are thin plated structures made of one or more layers. The base material of PCBs consists of copper foils bonded to the surface with glass fibre reinforced epoxy resin. PCBs are categorised into three types depending on their construction such as single-sided, double-

sided, and multi-layered. They are extensively found in almost every kind of electronic devices, aviation, precision machinery and in medical equipment. Drilling of microholes is one of the key steps in PCB industries, requires with precision and hole accuracy. Most of the researchers accomplished various experiments and analysis on micro drills and their effects on PCB holes. The stiffness of micro drill bit is also one of the key factors that influences the hole accuracy. The low stiffness of micro drill causes wandering motion and leads to deviation of the initial drill position and enlargement of holes as shown in Figure 2.3. Even the small variation in the hole may change the accuracy and forms tight tolerances in PCB materials. Influence of radial run out on hole quality in PCBs subjected to high speeds is presented by Watanabe et al. (2008). For PCB drilling, the static and dynamic runout must be less than 0.0254 mm and recent developments in air spindle technology has achieved the accuracy less than 10 μm to reduce the radial runout (Zhang, 2008). The micro drill bits are manufactured with minor diameters and high aspect ratio. Due to the precise geometry of micro drill, it is unable to pass the chips continuously. This leads to increasing friction between the flute and the workpiece. The friction causes more heat generation between hole walls and forms smear, consequently causing tool wear on the drill bit. Zheng et al. (2012) performed experiments on multi-layered PCB and shown the characteristics of chip formation on high-speed micro drilling. The factors affecting the chip formation at different stages on multilayered PCBs has been shown. Due to the continuous production of micro-holes on PCBs, the performance of the drill reduces up to some extent and can lead to damage of the hole or breakage of the drill bit. Investigation of wear mechanism and performance of micro drills on high-speed drilling of PCB hole were conducted by Chen et al. (1994) and Zheng et al. (2012). Interaction of carbide micro drills and drilling wandering motion of micro drills on hole wall surface was shown by Zheng et al. (2015). Experiments were performed to study the hole accuracy, hole quality and burr formation on PCBs at high speed conditions by Wang et al. (2014) and Zheng et al. (2013).

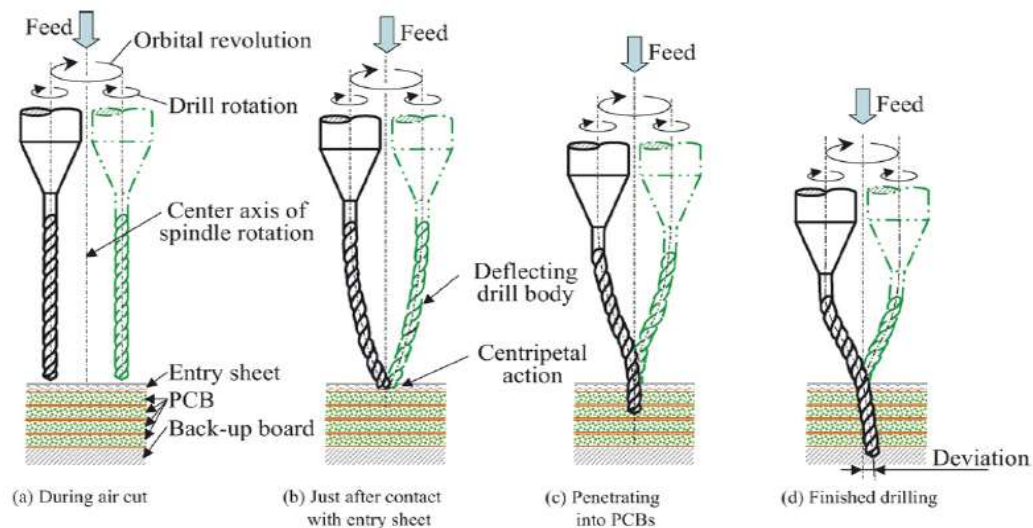


Figure 2.3: Centering model of micro-drilling for PCB (Watanabe et al., 2008)

Several studies on drilling operation replacing the traditional method with a non-traditional process like electrochemical drilling and laser-based drilling have been done. Researchers like Okasha et al. (2012) and Sen et al. (2005) showed interest to perform experiments for drilling holes on hard and difficult to cut materials. Lee et al. (2003), Lee et al. (2004) and Egashira et al. (2002) studied the effect of hole quality with diamond abrasive coated micro drill bits on ceramic bodies. Tool life improvement and hole quality in deep hole drilling of brass and steel have been examined by Kim et al. (2009) and Rahman et al. (2009). Experiments to prevent burrs on metal foils by using adhesives have been done by Kim et al. (2006). Kao et al. (2012) studied on high-speed drilling and performance of coated micro drills. Condition monitoring of drilling process with fluid lubricants on tools has been shown by Jantunun (2002), Kim et al. (2006) and Nan et al. (2011). Machining performance using wear map approach on micro-drilling process has been done by Imran et al. (2012).

2.6 Machining Burrs

Every conventional machining operation produces some burrs. The size of the burr depends on the cutting tool geometry, machining conditions and workpiece material properties, etc. Since, burrs can lead to bad surface finish, tool wear, etc., there is a need to identify factors which causes burr formation. The influence of drill diameter, helix angle, point geometry, speed and workpiece material on burr formation were investigated by Gillespie et al. (1976). Experiments were conducted to observe burr height, thickness and radius for 303Se stainless steel, 1018 steel and aluminium 6061-T6 materials. A considerable amount of work has been done to present the burr formation on different micromachining processes representing

different workpiece materials by Lee et al. (2005), Lekkala et al. (2011), Lin et al. (2000) and Stein et al. (1997). The Investigation of interlayer burr formation on stacked aluminium sheets was conducted by Hellstern (2009). Analytical and experimental approaches are used to find the burr size. Researchers like Alrabii (2009), Lekkala et al. (2011) and Segonds et al. (2013) performed analytical studies on burr formation mechanism and its characteristics formed by drilling, slot end milling, and micro end milling processes. Experiments on high-speed micro drilling and formation of different types of burrs were shown by Sugawara et al. (1982), Lee et al. (2005) and Ali et al. (2013). Mathematical modelling for predicting burr height using multi-gene genetic programming was presented by Garg et al. (2014). Ko et al. (2003) have discussed on drill geometry parameters that reduce the burr. Kim et al. (2006) conducted experiments on step feed micro drilling and shown the effect of thrust forces on burrs. Burrs are propagated when the chisel edge of the drill bit contacted to the workpiece Sugawara et al. (1982). In micro drilling, such raised edges called as micro burrs at the workpiece edges/surfaces severely affect the surface finish, mating faces and fatigue life of the micro-components. Removal of such micro-size burrs is much more challenging than its macro counterpart. Burr formation affects the quality, functionality, assembly and reduces its life or causes failure of the product Stirn et al. (2001). Deburring of micro-parts is not possible due to bad accessibility and tight tolerances in microcomponents which lead to increase in manufacturing cost by Dornfeld et al. (1999). Monitoring the burr formation is also a critical need to control the factors. Researchers like Kondo et al. (2012), investigated on tool breakage and burr formation caused by tool wear in the micro-drilling process. Chang et al. (2005) have been conducted experiments on burr size reduction by ultrasonic assistance.

Improvement of hole wall quality in printing wiring boards was studied by Nakagawa et al. (2007). The influence of workload was measured based on the torque and drill temperature. The experiments reveals that the reduction of workload on drill will reduce the friction and will help to obtain effective high hole quality. The thrust force of the drilling process is affected by the ratio of the feed to the drill diameter. To overcome the issue of burr formation at favorable machining conditions, burr control charts was presented by Bhandari et al. (2014). Experiments are carried at high speed micro drilling on double layered PCB to classify the burr formation. Burr formation mechanism, burr geometry characteristics, burr height and drill bit breakage are discussed at different machining conditions.

In all these approaches, analytical or experimental models were utilised for predicting burr formation based on the input data of work piece material properties, tool geometry and cutting conditions. From the above literature, the author has presented the profound work done on burr formation in micromachining processes exploiting modelling approaches for a quick view as shown in Table 2.1.

Table 2.1: Review on various modelling approaches

List of Authors	Machining operation	Modeling approach	Workpiece / Cutter combination (dia. in mm)	Burr Analysis
Bhandari et al., 2014	M4	Empirical	W5 & W6 / C1 tip, C4 shank, dia. 0.4,0.6,0.8	B [#] , B ⁺
Sambhav et al., 2013	M4	Analytical	W3 / C1 dia. 0.508	-
Zheng et al. (2013)	M4	Empirical	W9,W1 & W9 / C 3 dia. 0.4	B [*]
Zhang et al. (2013)	M5	Analytical	W3 / C6	B [#] , B [*]
Chen et al. (2012)	M2	FE model	W2 / C7 (1 flute), C8 (2 flutes).	B [*]
Aziz et al. (2012)	M6	Empirical	W3 / Micro drill dia.0.09 & grinding dia. 0.1	B [*]
Saptaji et al. (2012)	M1	Empirical	W1 / C1 of dia. 0.5	B [*]
Okasha et al. (2012)	M4	Empirical	W8 / laser micro drilling	B ⁺
Zheng et al. (2012)	M4	Empirical	W7, W1 & W10 / C3dia. 0.1	B [*]
Wu et al. (2012)	M1	FE model	W3 / C1 of dia. 0.3	-
Rao et al. (2012)	M1	Analytical	W3 / C4 (2 flutes), dia. 0.5	-
Jun et al. (2012)	M1	Analytical	W1 / C1 of dia. 0.1	-
Ozel et al.2011	M1	FE model	W2 / C2 of dia. 0.1-0.3	B [*]
Tang et al.2011	M1, M7	Empirical	W11 / C4 of dia. of 40	B [*]
Lekkala et al.(2011)	M1	Empirical	W1 & W3 / C2 of dia.0.3, 0.4	B ⁺
Li et al. (2011)	M1	FE model	W3 / C1 (2 flutes), dia. 0.5	-
Zhang et al. (2011)	M5	FE model	W6, W9 & W10 / C1 dia. 0.1	-
Chang et al. (2010)	D	Analytical	W1 / C1 dia. 4 , 3.35	B ⁺
Liang et al. (2009),	M1	FE model	W1 / C1 dia. 0.5	B [*]
Fu et al.(2009)	M4	FE model	W4 / C2 dia. 0.1	-
Alrabii et al. (2009)	M & D	Empirical	W3 / C4 dia. 10 (M), C4 dia. 5-12.5 (D)	B [*]
Kim et al.(2008)	M4	Empirical	W3 / dia. 0.1, 0.2	-
Nakagawa et al.(2007)	M4	Empirical	W7 / C3 dia. 0.6	-
Kang et al. (2007)	M1	Mechanistic	W1 / C2 (2 flutes), dia. 0.2	-
Li et al. (2007)	M1	Analytical	W9 / 2 flutes, dia. 0.1-1	-
Liu et al. (2007)	M1	FE, Empi.	W1 / C2 (2 flutes), dia. 0.508	-
Zaman et al. (2006)	M1	Analytical	W3 / C1(2 flutes), dia. 1	-
Lee et al. (2005)	M1, M4	Empirical	W3 / C1 (2 flutes), dia. 0.254	B ⁺
Kim et al. (2004)	M1	Analytical	W11 / C1(2 flutes), dia. 2.38 & 0.635	-
Vogler et al. (2004)	M1	Analy., FE.	W12 / dia. 0.508	-
Satish et al. (2003)	M	Geometric	W1 / dia. 80	B [*]
Chu et al. (2000)	M	Geometric	W1 / C4(2 flutes), dia. 6.35	B [*]
Bao et al. (2000)	M1	Analytical	W1, W3 & W9 / C1(2 flute), C4(4 flutes), dia. 0.127- 3.175	-

Table 2.2: Notations for Table 2.1

Machining operation	Workpiece material (W)	Cutting Tool Material (C)	Burr Details (B)
Macro-milling (M)	Aluminum alloy (W1)	Tungsten carbide (C1)	Type of burr- B [#] (Uniform, Transient, flake, curl and poison)
Macro-drilling (D)	Titanium alloy (W2)	solid carbide (C2)	
Micro-milling (M1)	Steel alloy (W3)	Cemented carbide (C3)	
Micro-ball end milling (M2)	Printed Circuit Board (W4)	High-speed Steel (C4)	Formation zone- B [*] (Entrance, Exit, Top, Side and Slot base)
Micro-face milling (M3)	PCB (W5)	Titanium coated insert (C6)	
Micro-drilling (M4)	Fiber reinforced plastic (W6)	Cubic boron nitrite (C7)	
Micro-cutting (M5)	PCB-(FR-4) (W7)	Mugen coating (C8)	Geometry - B ⁺ (Height, Thickness and Size)
Micro slot cutter (M6)	Inconel alloy (W8),		
	Copper (W9)		
	Glass (W10)		
	Brass (W11)		
	Iron alloy (W12)		

2.7 Research Gaps Identified

Based on the literature review, the knowledge gap in the earlier investigations are presented.

- Most of the micro-drilling operations on PCBs is reported well but limited to experimental investigations, having a high risk of repeated experiments that consumes time, money and energy.
- A number of research efforts have been devoted to the experimental investigations on drill breakage, tool wear, hole accuracy and chip formation on PCBs. However, the stresses generated on work piece material that effect the surface integrity and burr formation are found in few literatures.
- Though, some experimental and analytical models are developed to estimate the burr formation, no three-dimensional (3D) model exists for multi-layered PCBs for showing the micro burr formation at variable machining parameters.
- Very few papers have been reported on ultrasonic vibration assisted micro-drilling (UVAMD). The parameters like ultrasonic frequency, amplitude influencing on the work piece material in terms of reduction of forces and burr formation has not been addressed so far.

2.8 Motivation

Micro-drilling process is the bottleneck condition that provides micro holes for electronic interconnections to be placed on PCB surfaces in a large number. High spindle speed and high in-feed are recommended in such PCB drilling operations. Nail heading, smear and burr formation are the major problems that regularly persist in hole making process of PCBs. In metal drilling operations, coolants are used to control the heat generation, but in PCB drilling process, coolants are not used due to difficulty in cleaning the burrs. However, deburring is proposed to remove the burrs protuted on the PCB surfaces which is an additional step that might be always cost-ineffective and time consuming. In PCBs, due to its versatile nature having a combination of materials with different mechanical properties, it is challenging to acquire micro holes with high accuracy and better surface finish. A high speed air bearing spindle is generally used for micro drilling to minimize the problems like wandering and radial runout. Another limitation is the formation of chip balls in flexible boards due to heat development and limited space for chip transportation (Zhang et al., 2012). An experimental layout of micro-drilling in PCB manufacturing is presented in Figure 2.4. To increase the productivity, multiple boards are placed together with entry and backup materials. They are helpful in eliminating entry and exit burrs and to hold the drill bit position with accuracy. This requires high stiffness for micro drills that creates more challenges for micro-drilling.

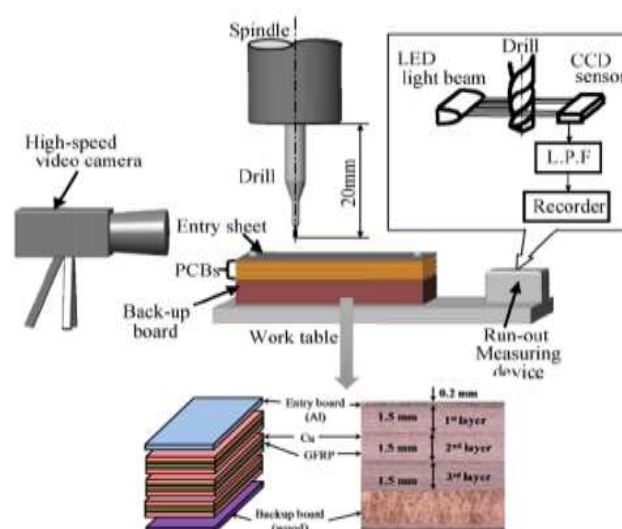


Figure 2.4: Experimental lay out for micro drilling of PCB (Watanabe et al., 2008)

As a result of the persisting problems and huge demand towards product miniaturisation, there is a requirement for advances in micro manufacturing technologies and their

consolidation in new production platforms. These platforms must enable both function integration and length-scale integration with the existing machining process. The trends in micro manufacturing and ultra-precision accuracy fields requires a fresh look at new process techniques and machine technologies that must allow developing machining systems to support this growth.

2.9 Objectives of the research work

Through this work an attempt is made to set the objectives and scope of this research work which are outlined as follows:

- To perform 3D FE dynamic analyses for micro-drilling of multi-layer PCB material. The influences of thrust forces on micro drill bit and stress distribution in work piece material need to be analysed.
- To predict the burr formation during conventional micro-drilling of multi-layer PCB material.
- To present 3D FE simulation of UVAMD of multi-layer PCB materials and to examine the influence of process parameters on the output responses like stress generation and reaction forces.
- To conduct modal and harmonic analysis of stepped and conical horns assembled with micro drill bit with multiple material combinations in CAE environment.

2.10 Closure

A frame work has been shown to highlight the latest evolutions in micro manufacturing. A brief review on various modeling approaches in macro / micro machining processes has been elaborately discussed. The key issues related to minimization of micro burr formation in micro milling / drilling has been addressed. A significant change has been realized in developing more advanced modeling techniques from traditional 2D to 3D methods. This helps to explore various micro-manufacturing processes in a more precise manner with control over burr formation. Besides, efforts among various researchers from academia and industrial experts are essential to move ahead in this regard. Implementation of recent development on machining technologies like ultrasonic vibration assisted micro-drilling have been presented. Further, research gaps were identified and the objectives of the present research have been stated.

Chapter 3

FE DYNAMIC ANALYSIS OF CONVENTIONAL MICRO-DRILLING

In the present chapter, three dimensional (3D) finite element (FE) dynamic simulation of micro-drilling process on multi-layered printed circuit board material has been performed. The influence of thrust forces on micro drill bit and stress distribution on work piece material have been analyzed. Variation of thrust forces with respect to speed and feed are depicted graphically for the simulating machining conditions. The data generated through FE simulations is helpful to plan and conduct experiments and further research.

3.1 Methods and Materials

In the present work, a FE analysis based on Lagrangian formulation is performed to simulate the conventional micro-drilling process. For this purpose, commercial FE software Abaqus/Explicit is used. Due to the dynamic characteristics of the micro-drilling process, the mass and inertia effects are incorporated in the model. Also, the dynamic explicit FE element integration has been proposed for this study. Here, the simulation performs the crack initiation and growth in the workpiece material and predicts the cutting forces, torque and stresses generated in the work piece. The contact constraints and other kinematic conditions between the tool and the work piece surfaces have been properly established in the model. This is essential to run the simulation smoothly and to predict the results accurately. The details of the methodology and the flow diagram is depicted in Figure 3.1.

3.1.1 Geometry of Tool and Work Piece

To predict the influence of various operating parameters in micro-drilling of PCB material, a drill work piece model should include the actual geometry, the material properties and the kinematic conditions of the contact regions. For this purpose, an accurate three-dimensional (3D) micro-drill is generated and FE simulation is performed for micro-drilling. A 3D solid model of 0.3 mm diameter twist drill with a point angle of 118° and helix angle of 35° is

developed in CAD environment of CATIA V6. For our convenience in FE simulation, flute length of 2.5 mm is considered for model generation as depicted in Figure 3.2.

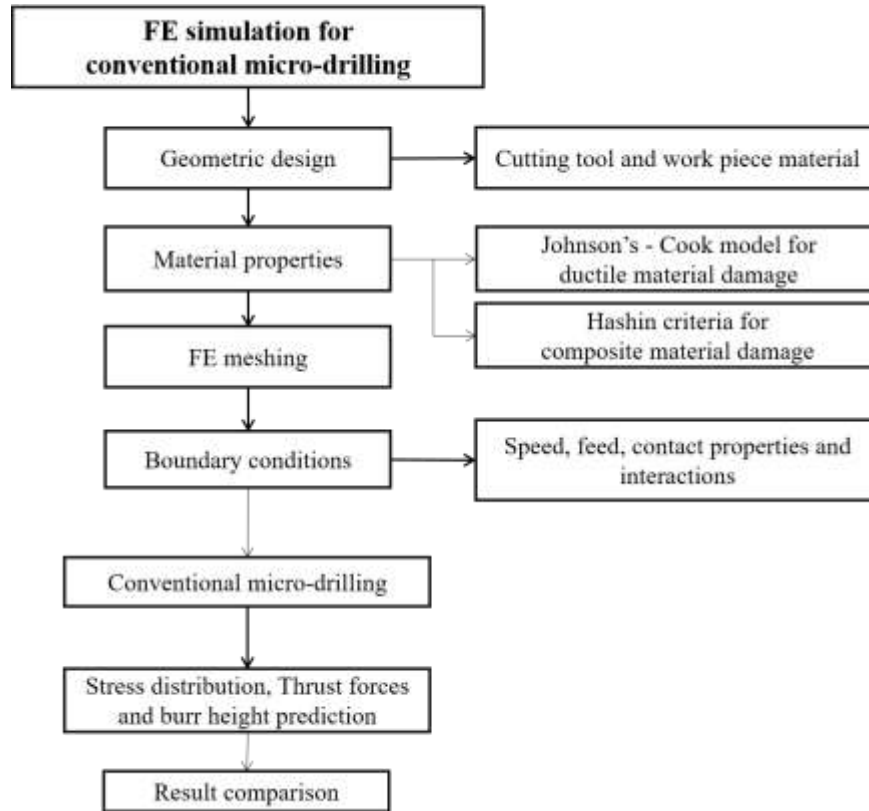


Figure 3.1: Methodology adopted (a flow diagram)

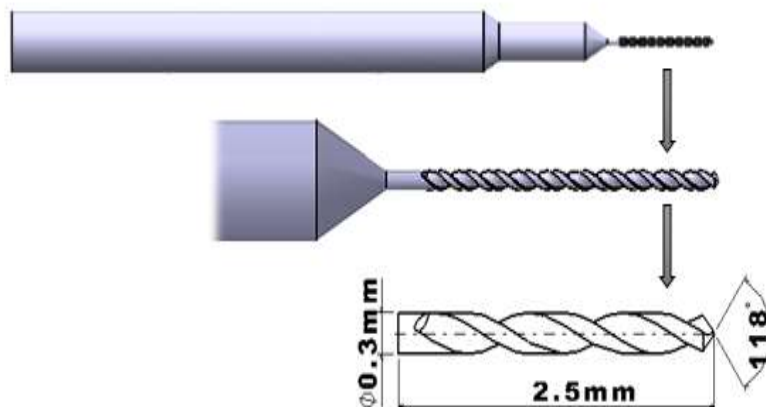


Figure 3.2: Pictorial view of micro-drill bit

The work piece geometry comprises of a four layered PCB, designed and developed in CAD module available in Abaqus/ Explicit 6.14. The laminated stack consists of copper (Cu) foil and glass fiber reinforced plastic (GFRP) having the dimensions of $2 \text{ mm} \times 2 \text{ mm} \times 0.372$

mm thickness. Each layer thickness of Cu and GFRP is listed in Table 3.1. A unidirectional GFRP material with fiber orientation of $0^\circ/90^\circ/0^\circ/90^\circ$ is pursued as fiber tension / compression and matrix tension / compression (Isbilir et al., 2012). Prepreg is glued in between copper foil and GFRP, and is not considered for the simulation because the core material and prepreg are primarily made from same materials. The schematic layout of the work piece and drill model with detail specification is shown in Figure. 3.3.

Table 3.1: Layer thickness of the workpiece material

Layer orientation	Cu foil 1	GFRP 1	Cu foil 2	Cu foil 3	GFRP 2	Cu foil 4	Total thickness
Thickness (mm)	0.018	0.15	0.018	0.018	0.15	0.018	0.372

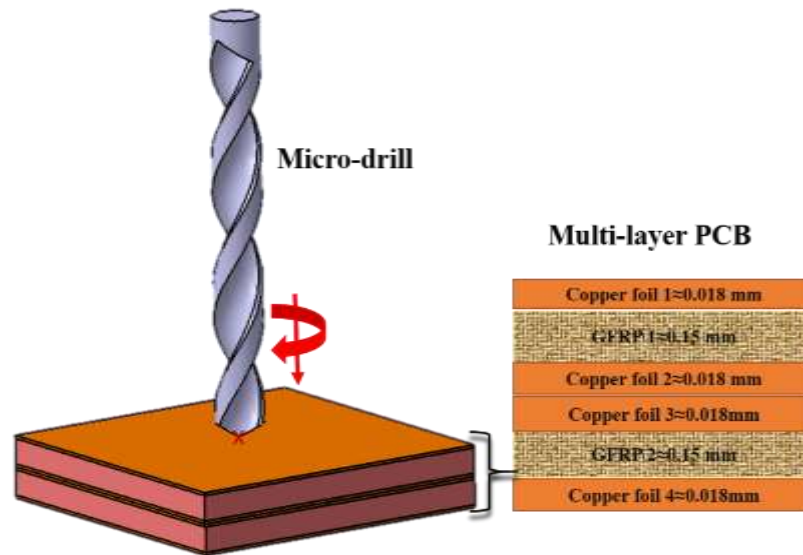


Figure 3.3: Schematic layout of tool and workpiece model

3.1.2 Material and Constitutive Model

The micro-drill is modeled as a rigid body and the mass and inertia are included to the reference point located at the cutting edge to simulate corresponding kinematics of the process. Tungsten carbide (WC) has been assigned for the micro-drill tool. The mechanical behavior of copper foil exhibits greater tensile strength and has better elastic elongation before reaching permanent deformation. Hence, copper foil can be modeled as isotropic, linear elastic and temperature dependent material. On the other side, the GFRP is a composite material composed of fiber glass with an epoxy resin bounded together. The GFRP material significantly exhibits different mechanical properties that are determined by the type of matrix and the fibers used, their ratio and orientation with the composite structure

to withstand loads subjected to fiber tension, compression, shear and flexure. Hence, GFRP is termed as anisotropic material in the sense of the properties like stiffness, toughness, strength, etc. that differs in different directions. The mechanical properties of materials assigned in this study are listed in the Table 3.2.

Table 3.2: Mechanical properties of the tool and work piece

Mechanical properties	WC	Cu	GFRP
Density (ρ) (kg/m ³)	15,700	8940	1900
Poisson ratio (ν)	0.34	0.3	0.3
Young's modulus (E) (GPa)	700	110	-

The constitutive library provided in Abaqus/Explicit contains a range of linear and nonlinear material models of various categories to describe the material's behavior. Constitutive models are the mathematical simplification of the complex physical behavior of various engineering materials. The material properties defined by the microstructure of the material for metals, alloys, polymers, fiber composites (with polymer or metal matrix), concrete and wood is to a greater extent. The fundamental approach to constitutive modeling is based on a thorough understanding of microstructural processes that causes deformation, stress, strain, strain rate, temperature and failure in the material. In the present analysis, Johnson-Cook's (JC) material constitutive model has been used for copper and Hashin damage criteria model for the GFRP material.

Johnson-Cook Material Model

Johnson and Cook proposed a constitutive model (Ghahremaninezhad et al. 2011) for metals and alloys subjected to large strains and high temperatures. Hence, it is termed as most popular and simple empirical model that fits the material data and well suitable for computational codes. Here, the JC damage initiation criterion is considered for predicting the onset of damage in the Cu layers of the work piece. In this model, the flow stress depends on the strain, strain rate, and temperature effects. Abaqus-Explicit software provides a dynamic failure model specially for the JC plasticity model, which is considered only for high strain rate deformation of metals. The JC dynamic failure model is dependent on the value of the equivalent plastic strain at elemental integration points. when the damage parameter exceeds the value 1, it is assumed to cause failure. According to JC constitutive material model, Von-mises tensile flow stress of the work piece is described as follows (Ghahremaninezhad et al., 2011)

$$\sigma = \left(A + B\varepsilon^n \right) \left[1 + C \ln \left(\frac{\dot{\varepsilon}}{\dot{\varepsilon}_0} \right) \right] \left[1 - \left(\frac{T - T_{room}}{T_{melt} - T_{room}} \right)^m \right], \quad (3.1)$$

where, σ is the equivalent stress, A is the initial yield stress, B is the hardening modulus, n is the work-hardening exponent, C is the strain rate dependency coefficient, m is the thermal softening coefficient, ε is the equivalent plastic strain, $\dot{\varepsilon}$ is the plastic strain rate, $\dot{\varepsilon}_0$ is the reference strain rate (1.0 s^{-1}), T_{room} is the room temperature, T_{melt} is the melting temperature. The JC criterion failure strain ε_f is written in the following form,

$$\varepsilon_f = \left[D_1 + D_2 \exp \left(D_3 \frac{\sigma_m}{\sigma_e} \right) \right] \left[1 + D_4 \ln \left(\frac{\dot{\varepsilon}}{\dot{\varepsilon}_0} \right) \right], \quad (3.2)$$

where, σ_m is the mean stress, σ_e is the Von-mises effective stress and D_1 to D_4 are the material constants. The material constants for copper are: $D_1=0.54$, $D_2=4.89$, $D_3=-3.03$ and $D_4=0.014$. The JC model parameters used for copper material are listed in Table 3.3.

Table 3.3: JC model parameters of copper material (Ghahremaninezhad et al., (2011))

A (MPa)	B (MPa)	C	n	m	ε_0	T_{room} (k)	T_{melt} (k)
90	292	0.025	0.31	1.09	1	294	1356

Hashin Damage Criteria

Generally, the laminated materials exhibit different phases such as soft matrix and brittle fiber on altered plies at each level. Hence, they are considered as linear elastic with orthotropic behavior. Hashin damage initiation criteria is considered for the GFRP material, as the model can predict orthotropic damage in elastic brittle materials. The damage model considers the failure modes namely, fiber tension/compression and matrix tension/compression. The relationship between the principle stress σ_{ij} and the various failure modes are mathematically represented as (Isibilir et al., 2012),

$$\text{Fiber tension } (\hat{\sigma}_{11} \geq 0): F_f^t = \left(\frac{\hat{\sigma}_{11}}{X_T} \right)^2 + \alpha \left(\frac{\hat{\tau}_{12}}{S_L} \right)^2 \quad (3.4)$$

$$\text{Matrix tension } (\hat{\sigma}_{22} \geq 0): F_m^t = \left(\frac{\hat{\sigma}_{22}}{Y_T} \right)^2 + \left(\frac{\hat{\tau}_{12}}{S_L} \right)^2 \quad (3.5)$$

$$\text{Fiber compression } (\hat{\sigma}_{11} < 0): F_f^c = \left(\frac{\hat{\sigma}_{11}}{X_c} \right) \quad (3.6)$$

$$\text{Matrix compression } (\hat{\sigma}_{22} < 0): F_m^c = \left(\frac{\hat{\sigma}_{22}}{2S_T} \right)^2 + \left(\frac{\hat{\tau}_{12}}{S_L} \right)^2 + \left[\left(\frac{Y_c}{2S_T} \right)^2 - 1 \right] \frac{\hat{\sigma}_{22}}{Y_c} \quad (3.7)$$

where, X_T is longitudinal tensile stress, Y_T is transverse tensile strength, X_c is longitudinal compressive strength, Y_c transverse compressive strength, S_T longitudinal shear strength and S_L is transverse shear strength respectively. α is a factor that provides the value of shear stress contribution to the fiber tensile initiation criterion. $\hat{\sigma}_{11}$, $\hat{\sigma}_{22}$ and $\hat{\tau}_{12}$ are the components of the effective stress tensor, which is used to evaluate the initiation criteria. The damage / crack initiation values and the mechanical properties as per the Hashin criteria assigned to GFRP material by Chakladar et al. (2012) are shown in Table 3.4 and 3.5 respectively.

Table 3.4. Hashin damage model parameters of GFRP material

X_T (MPa)	X_c (MPa)	Y_T (MPa)	Y_c (MPa)	S_c (MPa)	S_T (MPa)	α
686	620	39	128	89	140.5	1

Table 3.5. Orthotropic elastic properties of GFRP material (Chakladar et al., (2012))

Elastic modulus, E (GPa)	Poisson's ratio, (ν)	Shear modulus, G (GPa)
$E_X=3.042$	$\nu_{xy}=\nu_{yz}=0.29$	$G_{XY}=G_{YZ}=2.081$
$E_Y=E_Z=4.023$	$\nu_{zx}=0.39$	$G_{XZ}=1.440$

3.1.3 Mesh Generation

The elements are characterized by its family, degrees of freedom, number of elements and nodes, formulation and integration (Abaqus user manual (6.14)). There are wide range of elements available in element library for solving various problems. Commonly used element families are continuum solid / shell elements, beam elements, rigid, membrane, truss, infinite, springs and dashpot elements. Optimization of mesh used for the present simulation is considered based on the balancing of computational resources available, and requirement of high accuracy results. Reasonable element size should be preferred for the need of complicated geometries. A refined mesh size of 0.02 mm, three node 3D bilinear rigid

tetrahedral element (R3D3) has been assigned to drill bit. In Abaqus-Explicit, rigid bodies are particularly effective for modeling relatively stiff parts of a structure for which tracking stress waves and distributions are not important. An eight node linear brick element (C3D8R) with reduced integration is applied on copper foils with approximate global size 0.01 mm. A fine mesh of eight noded quadrilateral in-plane continuum shell element (SC8R) with reduced integration and hour glass control finite membrane strains is assigned to GFRP material. Continuum shell elements capture more accurately the through response for composite laminate structures. The generated mesh on flute part of the drill bit comprises of 14,588 elements, mesh generated on each copper foil is 80,000 elements and 6,00,000 elements on each GFRP material as listed in Table 3.6. The generated mesh on complete assembly model is shown in Figure 3.4.

Table 3.6: Meshing details of tool and work piece

Material	Micro-drill	Copper foil	GFRP
Element size (μm)	0.02	0.01	0.01
Type of element	Linear quadratic tetrahedron (R3D3)	Linear 8 noded brick element (C3D8R)	8 noded quadrilateral in plane general continuum shell (SC8R)
No of elements	14,588	80,000	6,00,000

3.1.4 Boundary Conditions

The motion of the drill bit is controlled by a reference point (RP) as shown in Figure 3.5. Here, it is assigned with a single noded mass and rotary inertia element, where boundary conditions of axial velocity and rotations are applied ($u_x=u_y=u_{rx}=u_{ry}=0$). The work piece is constrained in all directions in a fixed position ($u_x=u_y=u_z=0$). To investigate the influence of process parameters on micro-drilling like cutting speed and feed, FE analysis has been implemented while combining 4 cutting speeds with 4 feed rates at a step time of 0.001 sec to utilize the computational efficiently. The machining parameters considered for FE simulation for the present study are listed in Table 3.7.

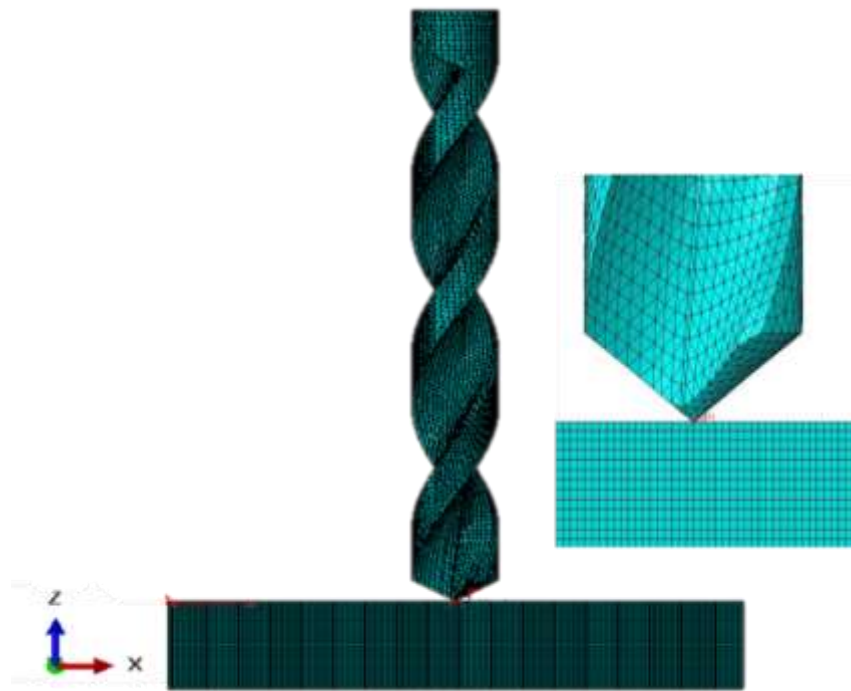


Figure 3.4: Meshing on tool and work piece

Table 3.7: Machining parameters considered for CMD FE simulation

Machining parameters	Conventional micro-drilling
Cutting speed (krpm)	60, 70, 80, 90
Feed rate (mm/s)	0.3, 0.4, 0.6, 0.8

The contact constraints and other kinematic conditions required to control the interaction between the surfaces of the tool and the workpiece material, namely friction and master-slave relationship are to be established in the model by Isbilir et al. (2014). This is essential to run the simulation smoothly and to predict the results accurately. In the present study, the pure surface-to-surface contact has been assigned to work piece material with no friction. The surface of the cutting tool is set to be a master object and the surface of the workpiece is a slave object. This means the surface of the work piece will deform according to the motion of the drill and the elements of the work piece cannot penetrate in to the tool. The coefficient of friction is taken as 0.3.

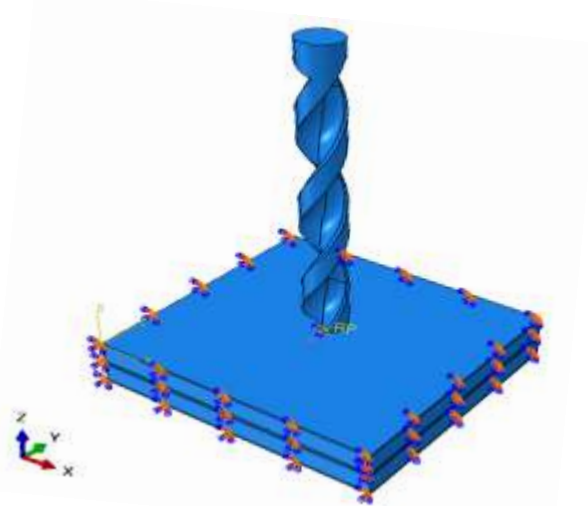


Figure 3.5: Boundary conditions applied to tool and workpiece

3.2 FE Simulation Results

In the present FE analysis, drilling of the finished hole completed in three stages. The drill touches the workpiece top layer in the initial phase. In the second phase, the drill cutting edges penetrates and contacts with the workpiece where the stresses, thrust and torque are attained. And in final stage, the drill point exits the work piece from the bottom layer where the burrs can be seen. As per the simulation results, the von-mises stresses, thrust forces and torque values obtained for the conventional micro-drilling process at varying speed and feed are listed in Table 3.8.

3.2.1 Stress Analysis

The progressive damage and stress distributions on the multi-layered PCB work piece during conventional micro-drilling process were analyzed. The stress distribution on the work piece material are depicted in the Figure 3.6. From the images, it can be seen that the stresses is persuaded in the workpiece as the micro-drill touches different workpiece layers. The Von Mises stress increased progressively at the entry of the hole and then continued steadily until the hole was drilled through. As the drill penetrates in to the copper layer, the material undergoes linear elastic behavior depending on the elastic limit and thus fails according to the damage model. When the elements fail, they are removed from the model. Figure 3.7 shows the damage initiation as per the J-C criterion at entry of the drill bit over the top layer (Cu) of the PCB material. Figures 3.8 and 3.9 shows the damage initiation as per the Hashin's criteria in GFRP material both under fiber tension and matrix tension while

drilling. Figures 3.7, 3.8 and 3.9 reveals that the damage initiation meets the value 1 as per both the damage criterion which is necessary to evaluate the tendency of the material to go through damage without modeling the damage process. Figure 3.8 (a) and (b) show the contour plots of the F_f^t and F_f^c respectively at the time of 0.0025s of drilling process. Figures 3.9 (a) and (b) show the contour plots of the F_m^t and F_m^c respectively at the time of 0.0025s of micro-drilling process. These parameters are defined in Equations 3.4 to 3.7 in Section 3.1.2. The areas of the workpiece for which the values of F_f^t , F_f^c , F_m^t and F_m^c reaches value 1, failure in the mode occurs. Comparison of Figures 3.8 (a) and (b) indicates that the dominant mode of failure in fibre is compression. This result is expected since the compressive failure strength of any ply in fiber direction is significantly lower comparing to the tensile failure strength. Similarly, comparison of Figures 3.9 (a) and (b) indicates that the dominant mode of failure in matrix is tension. The reason is that the tensile failure strength of a ply in the transverse direction is lower comparing to the compressive failure strength.

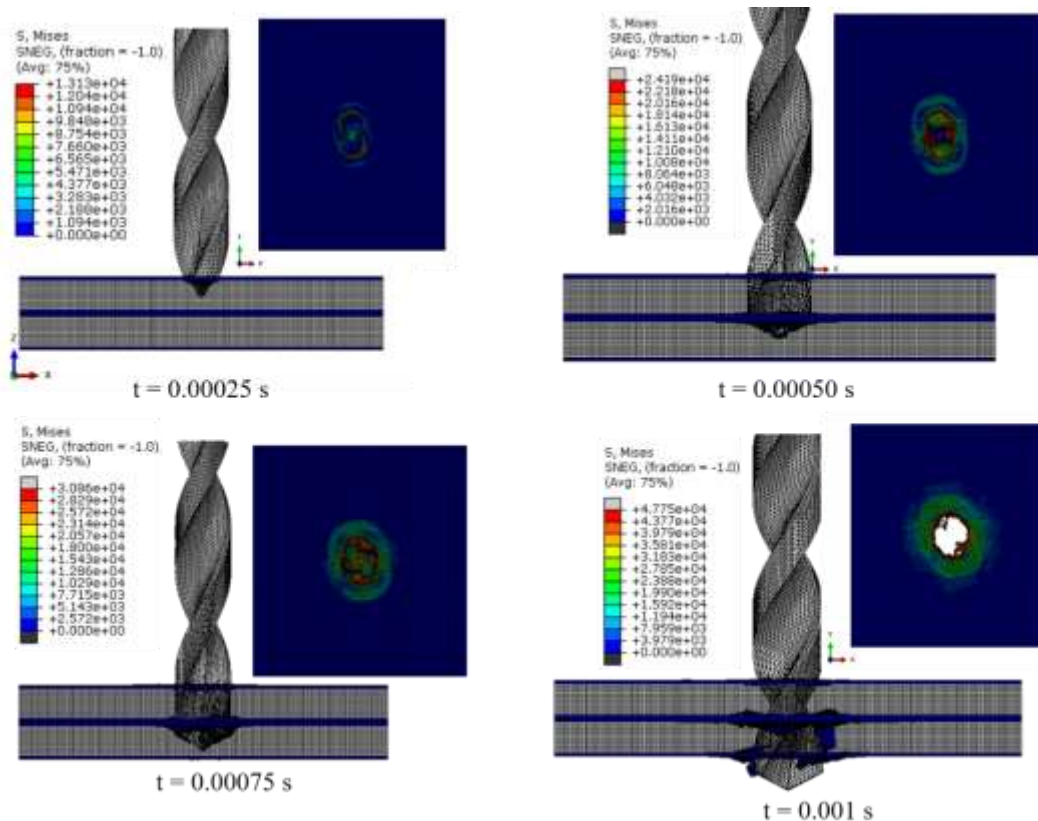


Figure 3.6: Stress distribution in work piece material (speed 60 krpm and feed rate 0.3 mm/s) at time (a) 0.00025 s, (b) 0.00050 s, (c) 0.00075 s and (d) 0.001 s

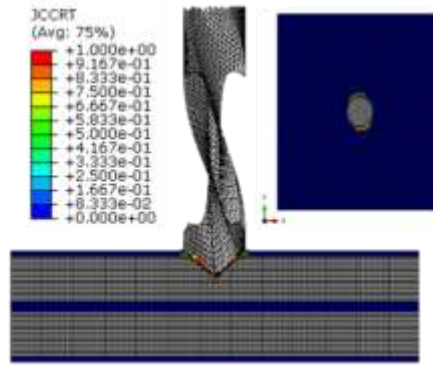


Figure 3.7: Damage initiation of top (Cu) layer as per the JC criterion (sectional view)

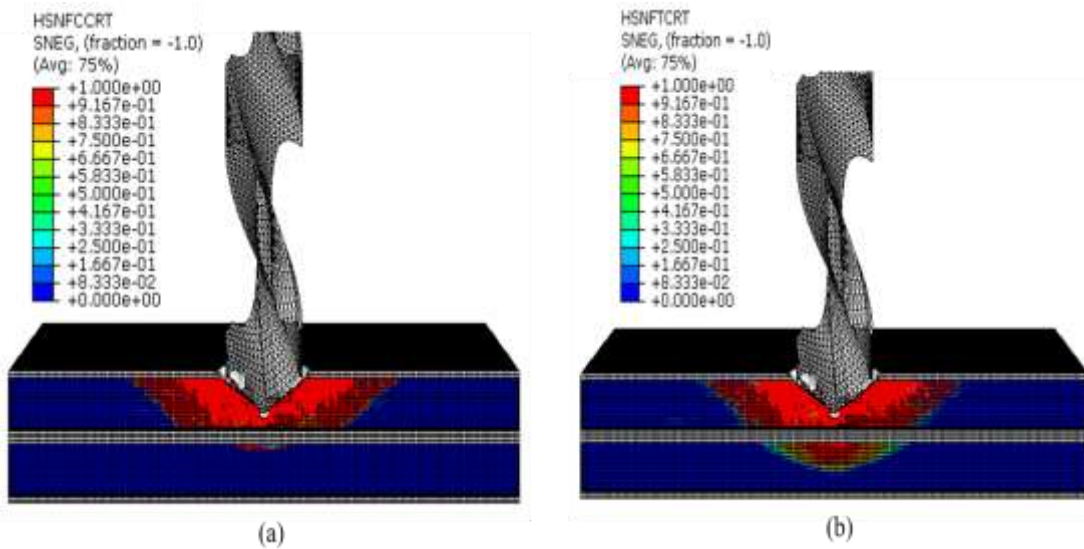


Figure 3.8: Fiber damage initiation in GFRP layer as per the Hashin's damage criterion under (a) fiber compression, (b) fiber tension (sectional view)

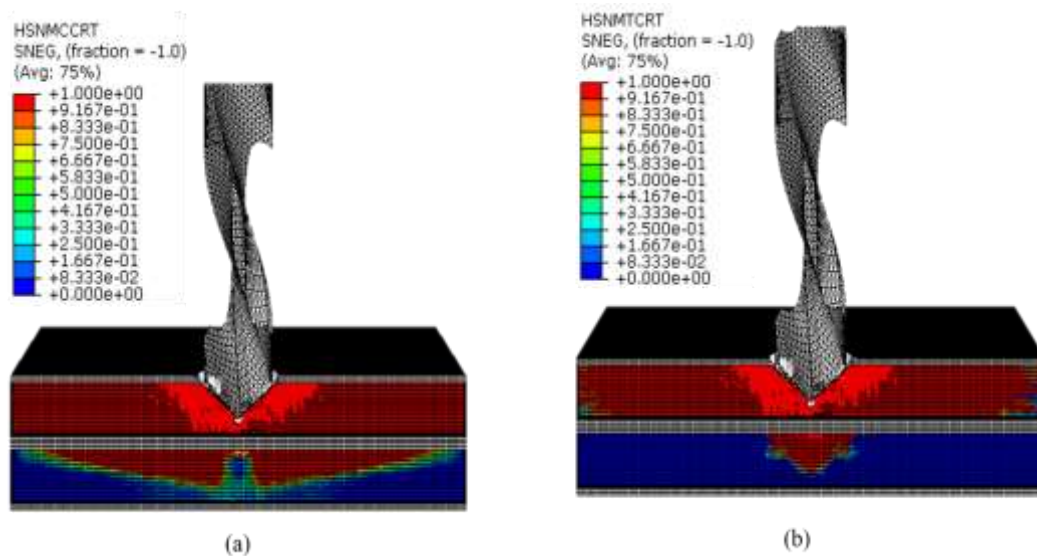


Figure 3.9: Matrix damage initiation in GFRP material layer as per the Hashin's damage criterion under (a) matrix compression, (b) matrix tension (sectional view)

3.2.2 Thrust Force and Torque Analysis

The influence of cutting parameters on the thrust forces was observed in the FE analysis. The FE model projected the thrust forces ranging from -10N to 60N in conventional micro drilling (CMD). The variation of thrust forces with respect to time with varying speed at constant feed of 0.3 mm/s are graphically shown in Figure 3.10. The first peak force is observed when the drill is penetrating in to the top copper layer at stage I. Smooth forces were generated when the drill starts drilling first glass fiber and a rapid increase of cutting force was observed at stage II with the middle copper layers. The cutting force again slightly decreases in drilling of second GFRP layer and a slight increase observed at bottom copper layer and dropped as the drilling cycle ends. An experimental work done on double layered PCB drilling by Zheng et al. (2013) is shown in Figure 3.11. After comparing Figures 3.10 and 3.11, it has been observed that the thrust forces increases when cutting edges touches the copper layer and slightly reduces during GFRP material in experimental and in simulation result. The graphs are plotted for varying thrust forces with respect to speed in Figure 3.12 and with feed in Figure 3.13 and compared the results with Zheng et al. (2013).

Table 3.8: Process parameters and simulation results of CMD

Speed (rpm)	Feed (mm/sec)	Thrust forces (N)	Von-mises stress (Pa)	Torque (Nmm)	Burr height (mm)
60,000	0.3	4.2	2.48e5	0.097	0.05
	0.4	6.8	8.07e4	0.099	0.07
	0.6	26	1.19e5	0.114	0.06
	0.8	32	1.31e5	0.225	0.10
70,000	0.3	5.3	7.78e4	0.135	0.07
	0.4	6.1	1.31e5	0.157	0.10
	0.6	25	1.61e5	0.135	0.10
	0.8	34	9.62e4	0.27	0.11
80,000	0.3	8.3	1.10e5	0.168	0.06
	0.4	9.8	5.69e4	0.247	0.12
	0.6	14	1.15e5	0.236	0.11
	0.8	41	1.55e5	0.297	0.09
90,000	0.3	13	1.50e5	0.219	0.06
	0.4	9.3	7.46e4	0.27	0.13
	0.6	1.2	9.73e4	0.391	0.11
	0.8	35	1.27e5	0.36	0.15

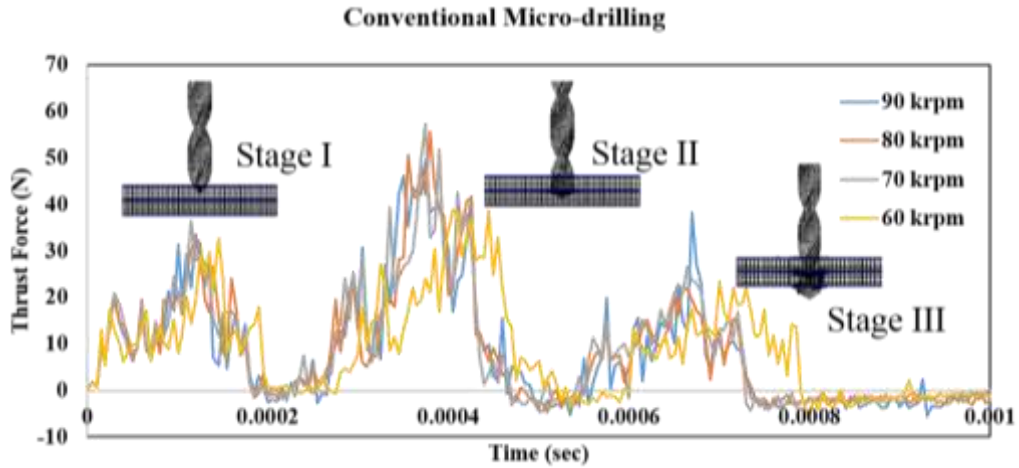


Figure 3.10: Thrust forces generated on multilayered PCB at 0.3 mm/s with varying speeds

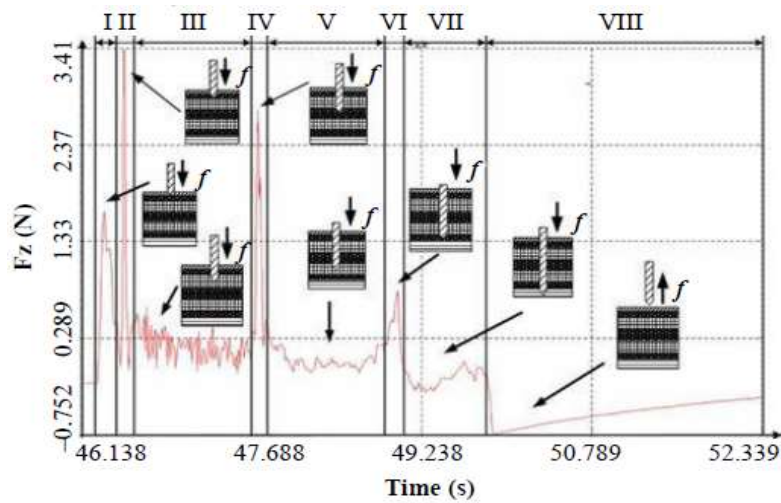


Figure 3.11: Thrust force generated for double board PCB drilling at speed 60,000 rpm with feed rate 1 mm/s (Zheng et al., 2013)

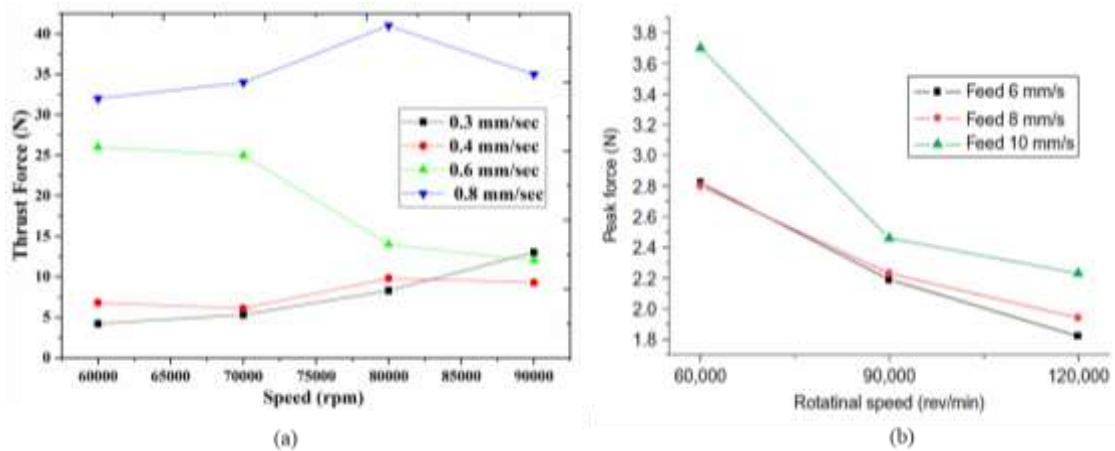


Figure 3.12: Variation of thrust forces with respect to varying speeds (a) Simulation result and (b) Experimental results (Zheng et al. 2013)

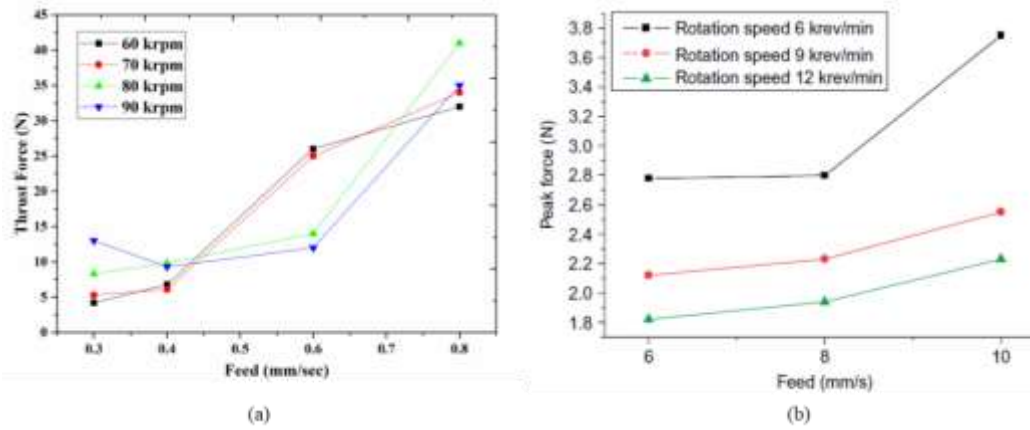
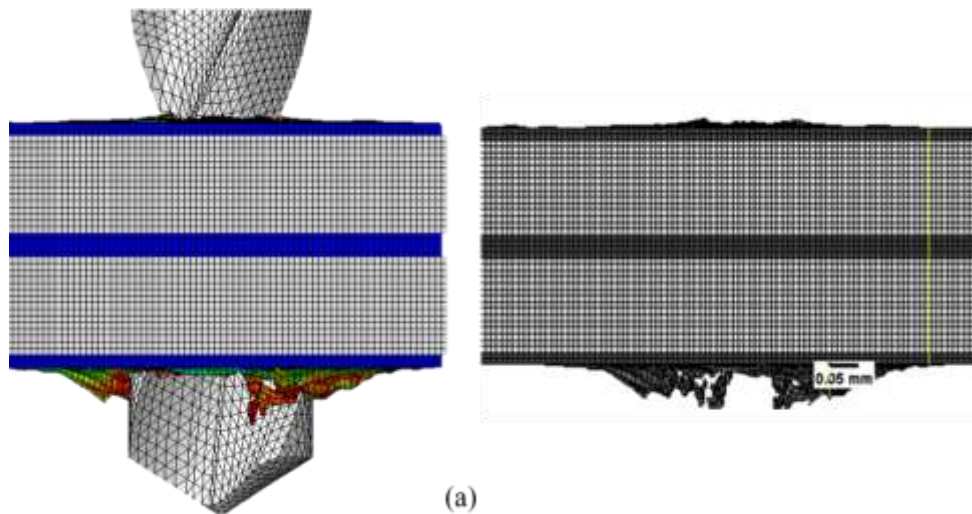


Figure 3.13: Variation of thrust forces with respect to varying feed rate (a) Simulation result and (b) Experimental results (Zheng et al. 2013)

3.2.3 Burr Formation Analysis

In present analysis, the burr formation at exit hole of the work piece material was analyzed for multi-layered PCB material. Figure 3.14 shows the burr formation on multi-layered PCB material at various speeds with constant feed rate of 0.3 mm/s from the FE simulation result. The entrance burr was observed slightly on the top layer of the work piece material due to the lower thrust generated in the initial stage. Burr height generated on work piece material was measured by using Imagej analysis software developed by National Institutes of Health (NIH). The burr height can be calculated by pixels generated on the known distance to be measured. The burr height calculated for the present FE simulation was compared with the experimental work conducted by Zheng et al. (2013) with similar data as shown in Figure 3.15. The exit burr was generated on the bottom layer due to the continuous generation of forces and the drill bit movement through the remaining copper foil at the exit of the hole.



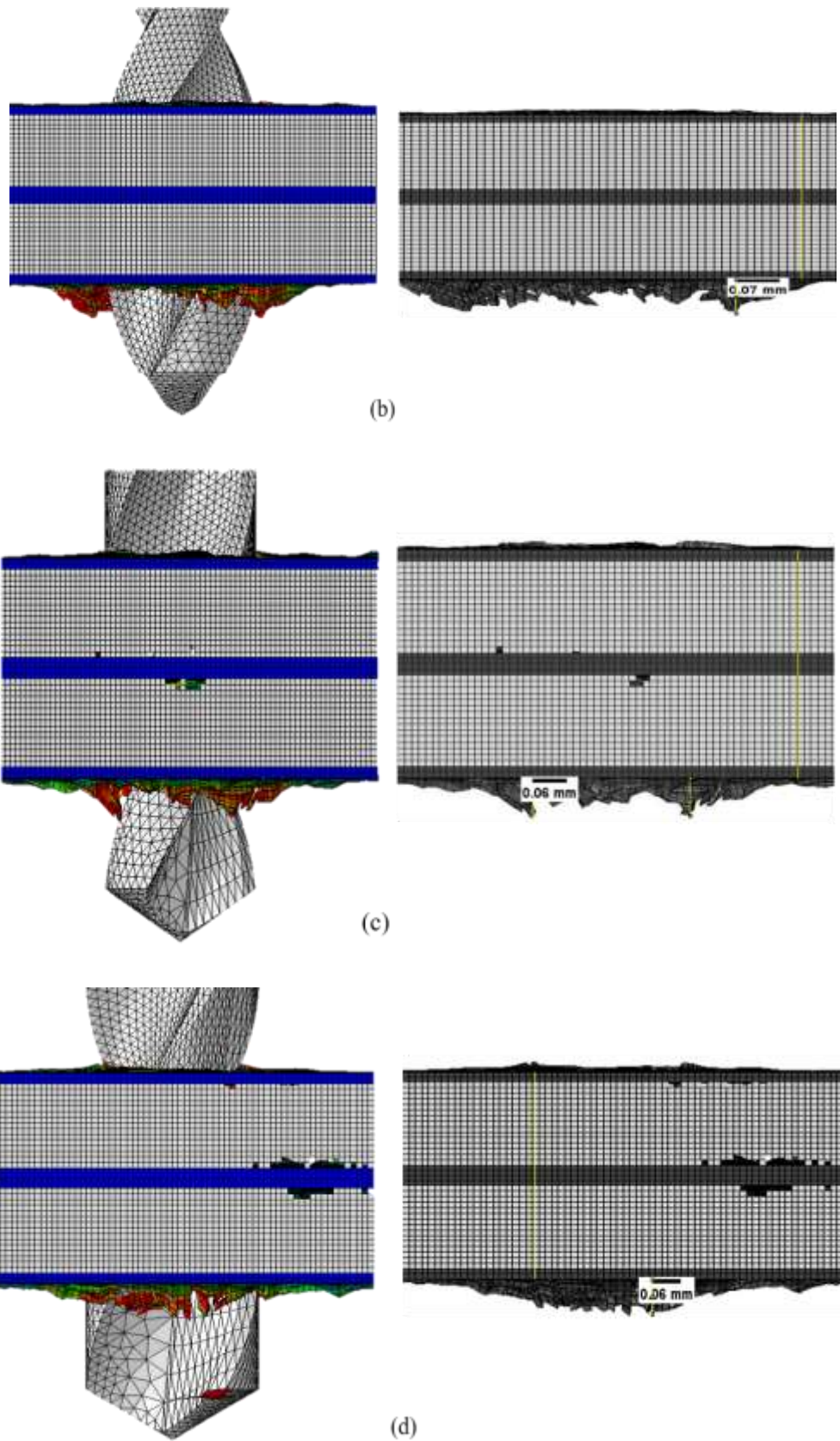


Figure 3.14: Burr formation with varying speed (a) 60 krpm, (b) 70 krpm, (c) 80 krpm and (d) 90 krpm

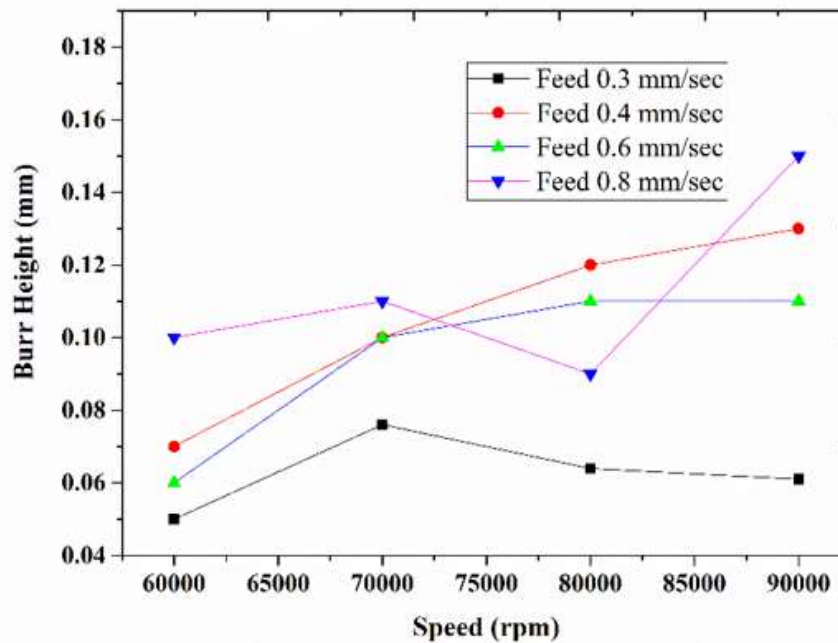


Figure 3.15: Burr height predicted as per FE simulation

3.2.4 Discussion

As per the FE simulation results shown in Table 3.8, at spindle speed of 60,000 rpm, the increase in feed rate (0.3-0.8 mm/s) shows the gradual increment of thrust forces (4-32 N) and change of Von-mises stress from $2.48e5$ - $1.31e5$ Pa. Again, the torque is increasing with increasing feed rate. Similarly, for the speed above 60,000 rpm till 90,000 rpm, the feed rates showed the same phenomenon. Also, from Figure 3.12 (a), it was observed that the maximum thrust force was generated at 80,000 rpm at a feed rate of 0.8 mm/s and the minimum thrust force was observed at 60,000 rpm at 0.3 mm/s feed rate. Hence, thrust forces rises at high speed and feed rates. From Figure 3.10, it can be seen that the peak value of the thrust force produced by copper foil is higher as compared with the glass fiber reinforced epoxy (GFRP) when feed rate is low. Though, the difference between them decreases as the feed rate increases. The results are compared with the experimental work done by Zhang et al. (2013) with 0.4 mm micro drill bit operated at a cutting speed of 60-120 krpm at feed rate 6-10 mm/s (Figures 3.12 (b) and 3.13 (b)). Also, it was evident that the maximum Von-mises stress ($2.48e5$ Pa) was generated at 60,000 rpm at a feed rate of 0.3 mm/s and the minimum stress ($5.69e4$ Pa) was observed at 80,000 rpm at 0.4 mm/s feed rate. Therefore, Von-mises stress rises at low speed and feed rates but it reduces at higher speed and feed rate.

Exit burr formation as predicted in FE simulation are presented in Figure 3.14. The minimum burr height was 0.05 mm observed at 60,000 rpm at feed 0.3 mm/s and the maximum burr height was 0.15 mm observed at 90,000 rpm at feed rate 0.8 mm/s (Figure 3.15). The height of the burr increases with increase in feed rates. In PCB drilling, the exit burrs are formed due to heat softened copper foil that no longer resists to the thrust force (Zheng et al. 2012). In Figure 3.15, a sharp fall in burr height from 0.11 to 0.09 mm corresponding to feed rate of 0.6 to 0.8 mm/s respectively can be seen. For rest of the plots, burr height increases as the feed rate and corresponding thrust force increases. This drop in burr height may be due to rolling up of the chip material at some instances which is obvious. As the thrust force was maximum, it can be assumed that at the exit burr, width of burr might be larger than its height. Finally the simulation results concluded that the speed and feed has significant influence on generated thrust force. The optimum parameters recommended for PCB micro-drilling at low speed is 60,000 rpm with 0.3 mm/s feed and at high speed is 90,000 rpm with 0.4 mm/s.

3.3 Conclusion

In the above chapter, an attempt was made to show the FE simulation for conventional micro drilling on multi-layered PCB work piece material using Lagrangian finite element formulation. A 0.3 mm diameter drill bit was utilized to perform the analysis while considering four different cutting speeds in combination with four different feed rates. Results show that the cutting parameters have a significant influence on thrust forces and stresses generated in micro-drilling. The thrust forces decreases with high speed and lower feed rates. Also, the exit burr formation was observed at higher feed rates due to increase in thrust forces. The results were compared with the existing experimental work on PCB. Study justifies that the finite element simulation technique is viable, accurate for various methods in drilling process. Having better models for prediction of interface with the tool and the work piece would have better results with less errors.

Chapter 4

FE ANALYSIS OF ULTRASONIC VIBRATION ASSISTED MICRO- DRILLING

This chapter presents the finite element analysis of an ultrasonic vibration assisted micro drilling process on multi-layer PCB. The influence of input parameters like ultrasonic frequency and amplitude with the effect of speed and feed is formulated to predict the output responses. Aiming at the machining factors, material performance and outputs, the model validation was carried out by selecting suitable boundary conditions in FE simulation. Further, the stress distribution and reaction forces developed on work piece material were discussed. The obtained results are compared with FE conventional micro-drilling presented in earlier chapter and also with past experimental work of researchers.

4.1 Methods and Materials

In the present work, FE analysis is performed based on Lagrangian formulation developed to simulate the UVAMD process in Abaqus/Explicit. The details of the methodology and the flow diagram is depicted in Figure 4.1. Due to the dynamic characteristics of the drilling process, the mass and inertia effects are incorporated in the model. To reduce the computational efforts and to discretize the complexity of simulation, a predefined field approach for UVAMD is followed in Abaqus-Explicit. The kinematic boundary conditions and machining parameters of the drill bit and work piece material are considered same as mentioned in the last chapter. The specification of the geometric design are shown in Figures 3.2 and 3.3. The material properties assigned are as listed in Tables 3.2, 3.3, 3.4 and 3.5. The mesh generation and boundary conditions are shown in Figures 3.4 and 3.5. The ultrasonic vibration circular frequency of 20 kHz have been additionally imposed on the drill bit with a time dependent boundary condition of 0.001s. The initial amplitude of the drill bit vibration is taken as 20 μm . The machining parameters imposed on drill bit are shown in Table 4.1.

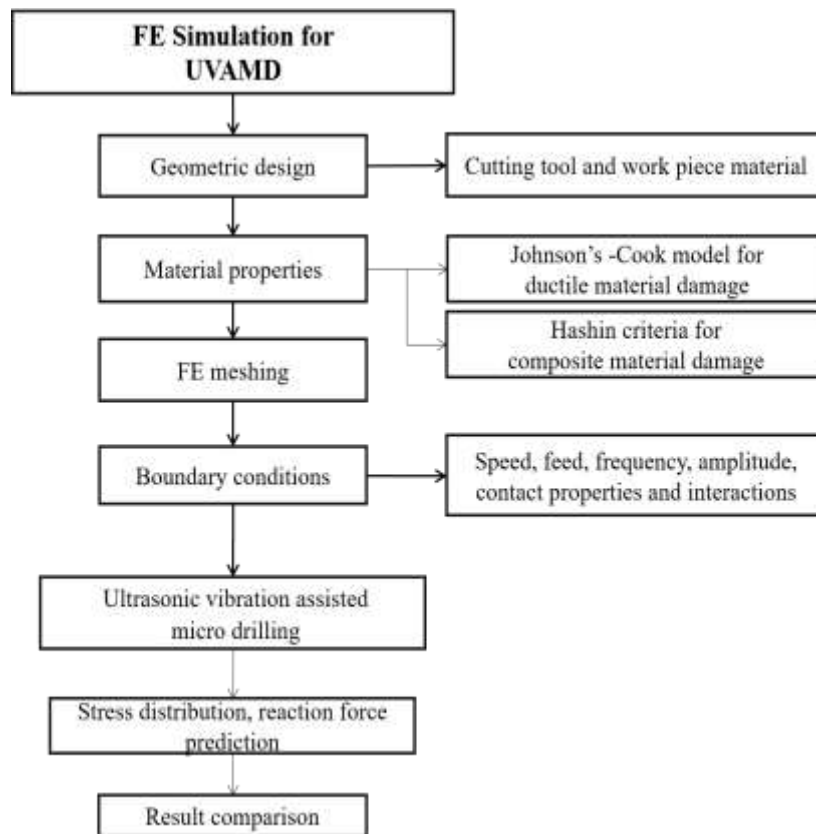


Figure 4.1: Methodology adopted (a flow diagram)

Table 4.1: Machining parameters considered for FE analysis of UVAMD

Machining Parameters	UAMD
Cutting speed (krpm)	60,70,80,90
Feed rate (mm/s)	0.3
Ultrasonic frequency (kHz)	20
Amplitude (μm)	20
Time period (s)	0.001

4.2 FE Simulation Results

In the present FE analysis, the stress distribution and the influence of cutting parameters on the thrust forces obtained from the simulation results for the ultrasonic vibration assisted micro-drilling on multi-layered PCB is analyzed and depicted. For the simulation of UVAMD, following assumptions are considered,

- The cutting tool vibrates and the work piece remains static.
- The vibration acting on the drill bit is considered purely in axial direction and the deformation will take place in work piece only.

4.2.1 Stress Analysis

The stress distributions on the Cu and GFRP layer of the work piece material at a speed of 60,000 rpm and feed of 0.3 mm/s at an instantaneous time is shown in Figure 4.2. The Von Mises stress increased progressively from the entrance of the hole to exit surface of the workpiece material. As compared with the conventional micro-drilling, there was a slight increase in stresses on work piece material. It can be assumed that the vibration frequency and amplitude has impact on the heat generation and temperature distribution during the intermittent action between tool and work piece.

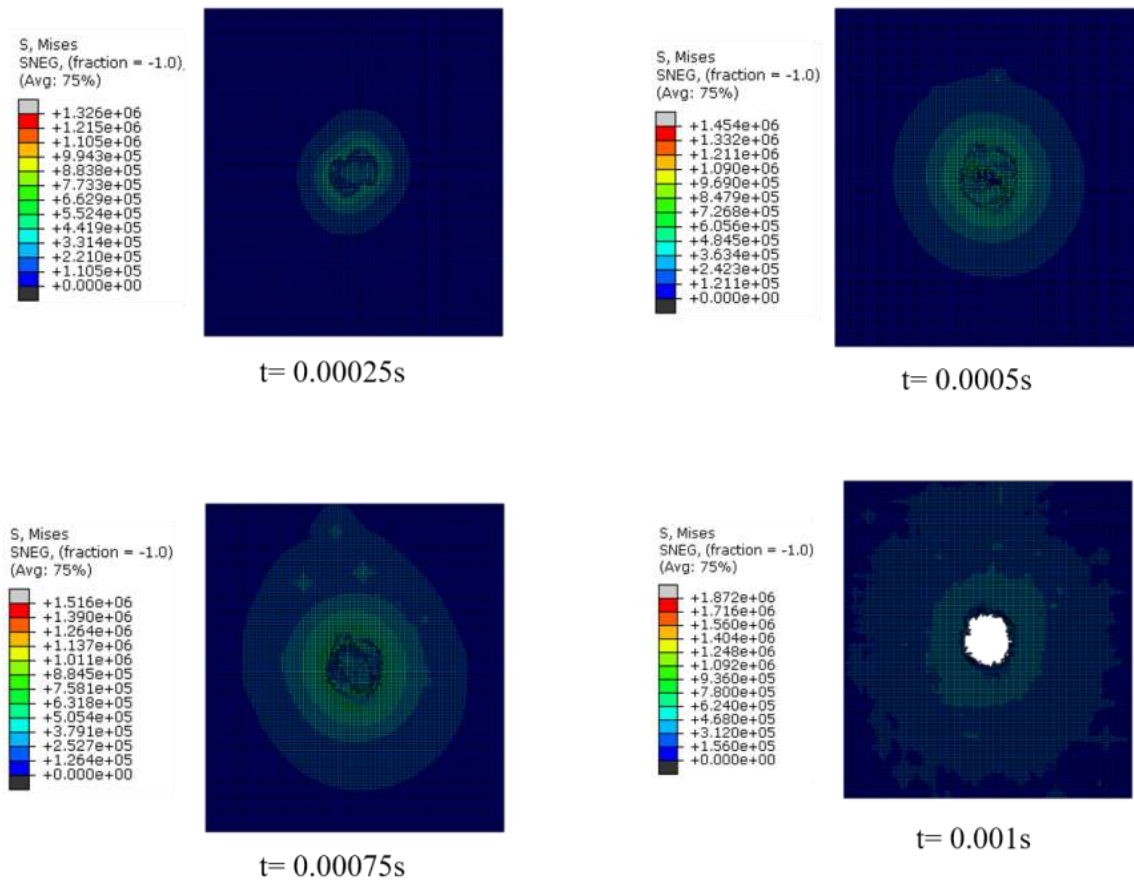


Figure 4.2: Von Mises stress distribution on workpiece material with varying time at speed 60 krpm and feed 0.3 mm/s

4.2.2 Thrust Force Analysis

As per the FE simulation, variation of thrust forces with varying speed at a constant feed of 0.3 mm/s for ultrasonic vibration assistance micro-drilling is shown in Table 4.2. The thrust forces with respect to time at constant feed 0.3 mm/s and varying speed are mentioned in Figure 4.3. The simulation results for CMD and UVAMD are compared at speed of 60 krpm

with 0.3 mm/s in Figure 4.4. The results revealed that the maximum peak thrust forces are high in CMD during drilling of copper foil as compared to the UVAMD. One of the nearest reference for experimental verification of the evolved FE simulation results of UVAMD is shown in Figure 4.5 (b) (Zhang et al., 2011). Though the cutting conditions and parameters vary slightly for the chosen reference for experimental results, but a similar trend can be seen when we compare FE simulation results for UVAMD from Figure 4.5 (a) with experimental values from Figure 4.5 (b). The graph reveals that high speeds with low feed rates has influence on reduction of forces in work piece material. It can be observed that high rotational speed not only decreases thrust force in traditional drilling, but also has a similar effect in UVAMD. This may be due to the reason that at higher rotational speed, the drill feed into the work piece per revolution reduces and this further reduces the chip load and the resistance of the work piece effectively. However, this trend may vary with different vibrational frequencies. On comparing CMD (Figure 3.10) and UVAMD (Figure 4.3), it is observed that the thrust forces obtained in CMD (-10 to 60 N) is relatively high as compared with UVAMD (-15 to 40 N). Hence, the evolved FE simulation results for the prediction of thrust forces is partially verified. In future, further experimentations need to be performed to verify the effects of resonance.

Table 4.2: Processes parameters and simulation results of UVA micro-drilling

Speed (RPM)	Feed (mm/sec)	Thrust force (N)	Von mises stress (Pa)
60,000	0.3	3.77	8.584e6
70,000	0.3	3.39	9.004e6
80,000	0.3	1.53	1.062e6
90,000	0.3	1.45	1.257e6

The variation of cutting speed with respect to feed from low to high shows a vast difference in generation of thrust forces in micro drilling. The thrust forces generated in UVAMD are low as compared to micro drilling at high speed with low feed rate. This shows that feed rate is crucial in generation of thrust forces while drilling.

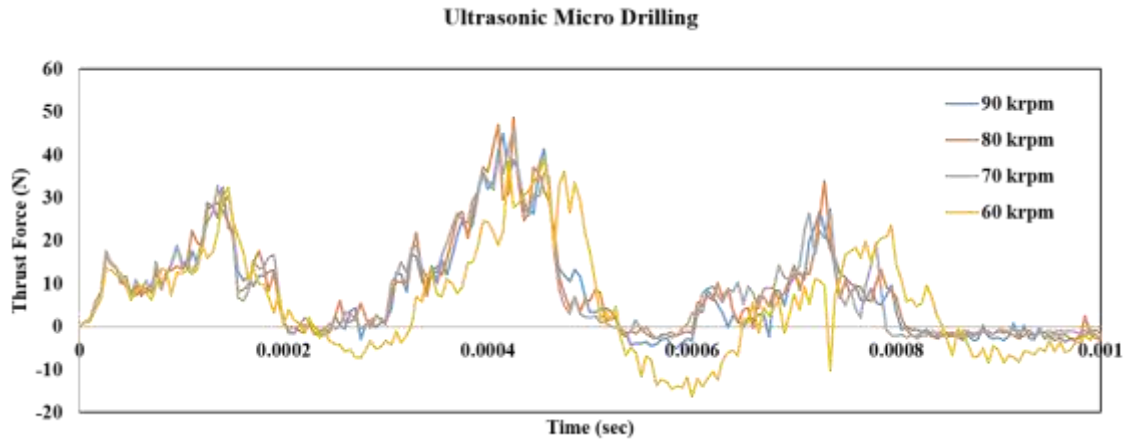


Figure 4.3: Variation of thrust forces with respect to time of step size 0.001 s at constant feed 0.3 mm/s and varying speed for UVAMD

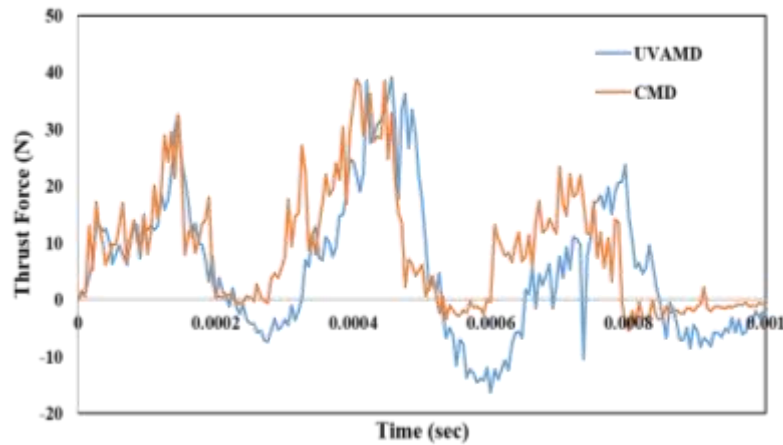


Figure 4.4: Variation of thrust forces at 60 krpm with feed of 0.3 mm/s with respect to time for CMD and UVAMD

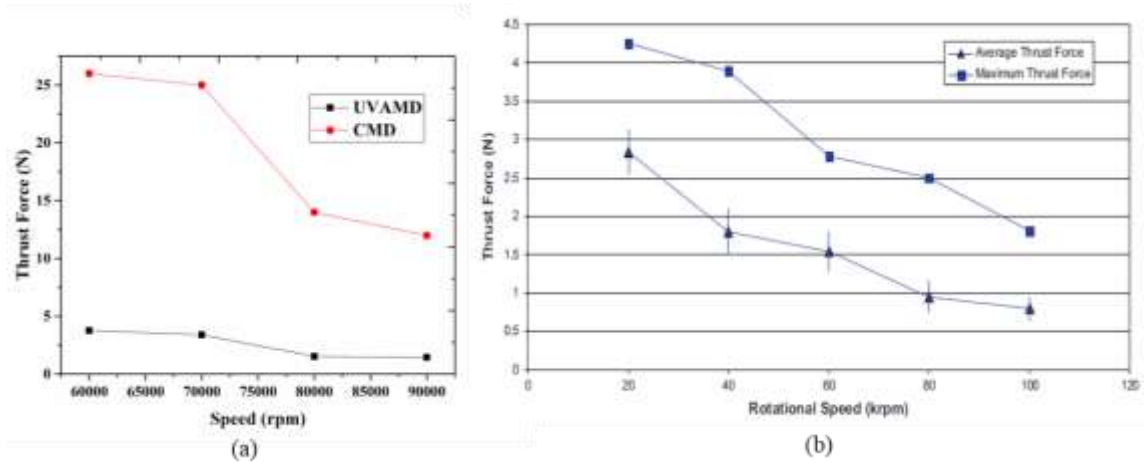


Figure 4.5: Variation of thrust forces for CMD and UVAMD with varying speed (a) at constant feed of 0.3 mm/s (FE results) (b) at 19.1 kHz resonance and constant feed of 0.202 m/min with micro drill bit of size $\Phi 1$ mm (experimental results) (Zhang et al. 2010)

In addition to this, the simulation results of ultrasonic assisted micro drilling were compared with the analytical model of ultrasonic assisted drilling (UAD) process presented by Astashev et al. (2007). Here, the mathematical calculations for the analytical model are counted by considering the cutting parameters with constant speed 60,000 rpm with varying feed rate at ultrasonic vibration circular frequency of 20 kHz. The comparison of thrust forces obtained in analytical solution and simulated results for UVAMD are shown in Table 4.3.

Analytical Force Model

The analytical non-linear force model for the process of cutting tool vibration and material deformation under ultrasonic vibration loading has been discussed by Astashev et al. (2007). The relative displacement between cutting tool and work piece is mathematically expressed as,

$$u(t) = vt + \dot{u}(t) = vt + a \sin \omega t, \quad (4.1)$$

where, $u(t)$ is the relative displacement of cutting tool, v is the feed rate, $\dot{u}(t)$ is the speed of the cutting tool, a is the amplitude and ω is the angular frequency of the cutting tool. The characteristics of nonlinear interaction force between tool and work piece is calculated by the displacement and the dynamic characteristics as defined below.

$$f = f(u, \dot{u}) = \left. \begin{array}{l} 0 \\ k_0(u - \Delta) \\ D \\ D + k_0(u - u_m) \\ 0 \end{array} \right\} \left. \begin{array}{l} u \leq \Delta, \dot{u} > 0 \\ \Delta \leq u \leq \Delta + \frac{D}{K_0}, \dot{u} > 0 \\ + \frac{D}{K_0} \leq u \leq u_m, \dot{u} > 0 \\ u_m - \frac{D}{K_0} \leq u \leq u_m, \dot{u} < 0 \\ u \leq u_m - \frac{D}{K_0}, \dot{u} < 0 \end{array} \right\} \quad (4.2)$$

$$u_m = a \left[\sqrt{1 - \left(\frac{v}{a\omega}\right)^2} + \frac{v}{a\omega} \arccos\left(-\frac{v}{a\omega}\right) \right], \quad (4.3)$$

where, f is force, u is displacement, \dot{u} is speed of the tool and Δ represents the constant shift between tool and work piece, D is the elastic limit of the work piece material, k_0 is the stiffness of the work piece prior to plastic deformation.

Figure 4.6 shows the graphical representation of thrust forces generated as per the analytical model and FE simulation results for UVAMD. The relative error occurs due to the assumptions considered in the FE model for simulating the actual machining conditions.

Table 4.3: Comparative result of thrust forces in UVAMD as per analytical and FE simulation approach

Feed (mm/s)	Analytical model (thrust forces) (N)	Simulation result (thrust forces) (N)	Relative Error (%)
0.3	35.4	37.0	6.49
0.4	51.0	52.0	1.96
0.6	55.6	59.8	7.55
0.8	59.0	61.2	3.72

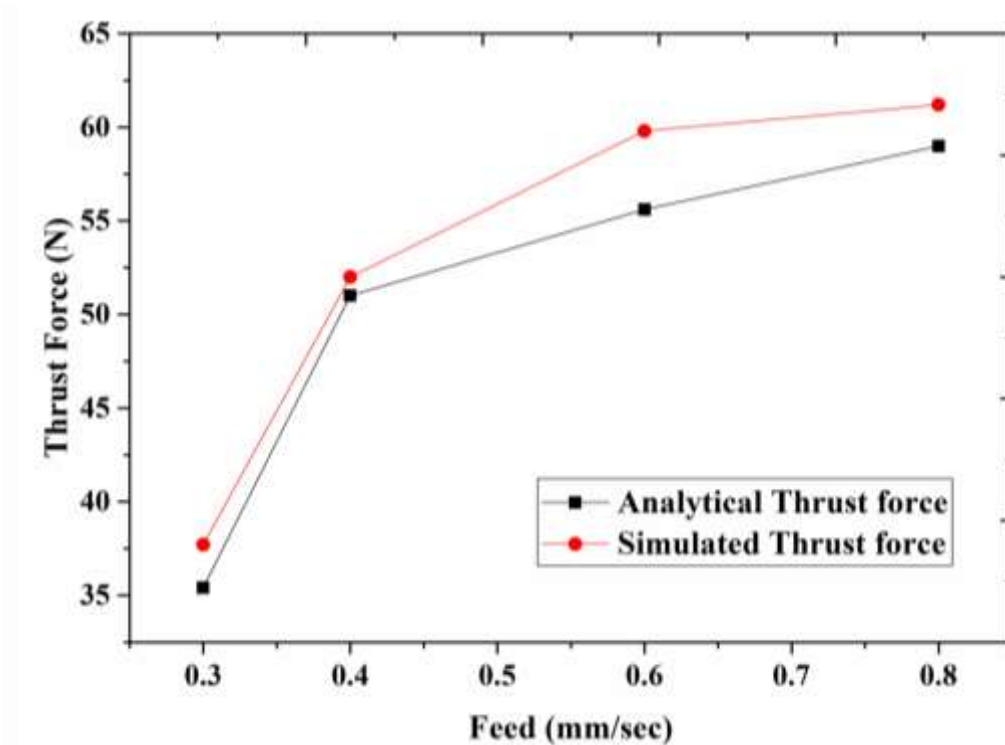


Figure 4.6: Comparison of simulation vs. analytical thrust forces for UVAMD at constant speed 60,000 rpm with varying feed rate.

4.3 Conclusion

The present work develops a 3D FE model for ultrasonic assisted micro-drilling. A 0.3 mm diameter drill bit was used for performing the simulation at four different cutting speeds with 0.3 mm/s feed rate. The simulation was carried out at an ultrasonic frequency of 20

kHz at an amplitude of 20 μm for a time period of 0.001 s. The results were compared to those of the analytical model. In addition to this, an attempt has been made to contrast the difference between micro-drilling and application of ultrasonic vibration in micro-drilling. The effect of proposed drilling parameters, such as cutting speed and feed rate on ultrasonic vibration assisted micro-drilling have been presented. The results show that the cutting parameters have a significant effect on thrust forces and stresses in micro-drilling. Ultrasonic assisted micro drilling has a good scope in reduction of forces generated with the considered machining parameters. Study justifies that the finite element simulation technique is viable and accurate for various methods in drilling process. Having better models for prediction of ultrasonic vibration assistance regime to interface with the tool and the work piece would have better results. Hybrid and solid models (Zhang et al., 2011) and accurate parametric model (Tandon et al., 2010) of micro drill bit can be generated to achieve more precise results. The FE simulation of UVA micro machining can further be enhanced and extended to various materials like plastics, sheet metal, other PCBs, etc. to predict the performance with varying machining and geometric parameters.

Chapter 5

FE MODAL AND HARMONIC ANALYSIS OF ULTRASONIC HORN

The present chapter aims to perform and explore the three-dimensional FE analysis of micro-drill bit and horn assembly under ultrasonic vibration resonance frequency range. Modal analysis has been performed to illustrate the influence of natural frequency and various mode shapes of stepped and conical horns assembled with micro-drill bit with varying arrangement of horn and drill-bit materials. Besides, harmonic analysis has also been evaluated to identify the displacement loads on horns along with micro-drill bit at varying amplitudes.

5.1 Wave Equation for Horn Profile

An ultrasonic horn works on the principle that the vibrational energy transmitted to the cutting tool via transducer is amplified at an operational range of ultrasonic resonance frequency to achieve efficient machining performance (Nad, 2010). Horns with varying profiles such as cylindrical, stepped, conical and exponential are employed for various ultrasonic applications. Presently, stepped and conical shaped horns have been used to match the desired ultrasonic frequency. For a horn with varying circular cross-sectional profile, the governing equation along longitudinal vibration in one-dimensional (1D) continuum is numerically defined by Nad, 2010 as,

$$\frac{\partial^2 u(x,t)}{\partial t^2} = c_p^2 \left[\frac{1}{S(x)} \frac{\partial S(x)}{\partial x} \frac{\partial u(x,t)}{\partial x} + \frac{\partial^2 u(x,t)}{\partial x^2} \right], \quad (5.1)$$

where, x is the position coordinate of any point along the cross-sectional profile of the horn, $u(x,t)$ is the longitudinal displacement of cross-section from its position within the undeformed horn. $c_p = \sqrt{E/\rho}$ is the velocity of longitudinal waves in 1D continuum, $S(x) = \pi(r(x))^2$ is the cross-sectional area of horn, $r(x)$ is the radius of its circular cross-

section and E and ρ are the Young's modulus and the density of the horn materials respectively.

5.1.1 Stepped Horn

The resonant length of the stepped shaped horn is defined as Seah et al. (1993),

$$L = k_1(c_p / 4f) + k_2(c_p / 4f), \quad (5.2)$$

Where, L is the resonant length, c_p is velocity of sound in the horn material. Here, the correction factors k_1 and k_2 are assumed to be unity. Hence, $L = c_p / 2f$. The amplitude ratio for the stepped horn is given as $(D_1 / D_2)^2$, where, D_1 and D_2 are the diameters of the larger and smaller ends of the horn respectively.

5.1.2 Conical Horn

The resonant length of the conical shaped horn is derived from the exponential horn length mentioned in Babitsky, 2007 and is expressed as,

$$\tan \alpha l_2 = \frac{\alpha l_1 (\sqrt{S_1 / S_2} - 1)^2 - [\sqrt{S_1 / S_2} (\alpha l_1)^2 + (\sqrt{S_1 / S_2} - 1)^2] \tan \alpha l_1}{\alpha l_1 [\sqrt{S_1 / S_2} \cdot \alpha l_1 - (\sqrt{S_1 / S_2} - 1) \tan \alpha l_1]} \quad (5.3)$$

where, l_1 and l_2 are the lengths of the conical horn and cylindrical cross-section of the horn respectively, α is the wave length constant, and S_1 and S_2 are the cross-sections of the input and output end of the conical bar.

5.2 Geometry of Micro-Drill Bit and Ultrasonic Horn

Geometric design required for any analysis should be precise in order to achieve an accurate results. An accurate CAD model which meets the quality standards is important to meet the task precisely. For modeling, there are numerous CAD packages existing in the market to represent the models in desired format for downstream applications. Here, the three-dimensional solid models of micro-drill bit and horn assembly have been rendered in CATIA V6 environment. A micro-drill bit of 0.3 mm diameter having a point angle 118° and helix angle 35° with two step shank design is considered in the analysis. The other dimensional parameters of micro-drill bit are depicted in Figure 5.1.

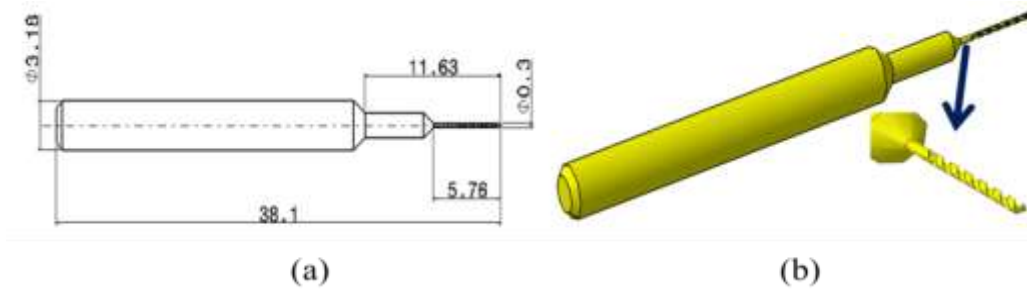


Figure 5.1: Micro-drill bit (a) 2D pictorial view (all dimensions in mm), (b) 3D CAD model with expanded view of flute

Considering the above mathematical equations (5.2 and 5.3), stepped and conical horns are geometrically designed to match the ultrasonic resonance frequency of 20 kHz. The CAD designs of stepped and conical horns assembled with micro-drill bit are shown in Figures 5.2 and 5.3. The micro-drill bit is inserted centrally into the horn at lower diameter end along the axial direction. Two slotted cheese head screws (Figure 5.2) have been used to hold the micro-drill bit in stepped horn.

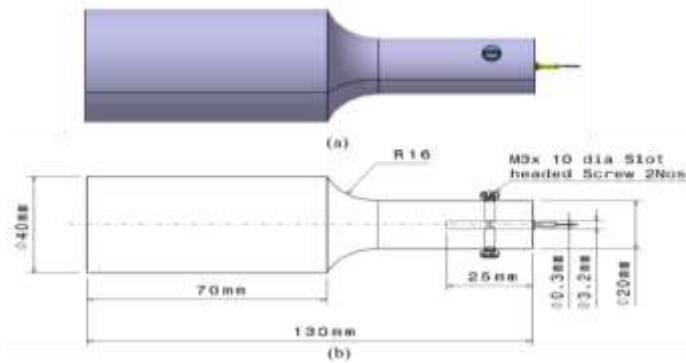


Figure 5.2: CAD design of stepped horn assembled with micro-drill bit (a) 3D model, (b) 2D orthographic view

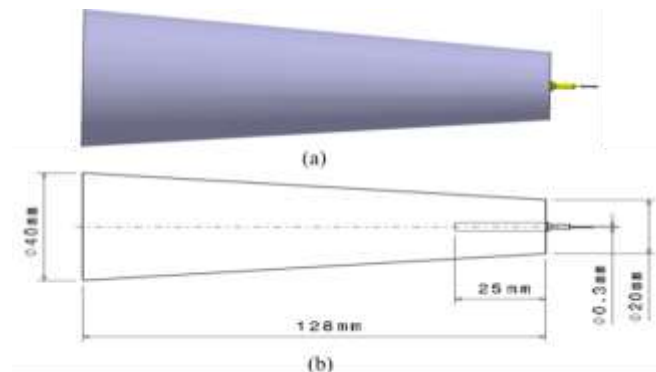


Figure 5.3: CAD design of conical horn assembled with micro-drill bit (a) 3D model, (b) 2D orthographic view

5.3 FE Modal Analysis

Modal analysis is the basic platform to study the dynamic properties of any materials to determine the natural frequencies and mode shapes of a structure under vibrational excitation. In the present work, FE modal analysis have been performed to examine the behaviour of micro-drill bit during ultrasonic frequency excitation. Here, the frequency characteristics of stepped and conical shaped horn assembled with micro-drill bit have been explored using Block Lanczos solver method.

5.3.1 Material Selection

In our analysis, Tungsten carbide (WC) and High speed steel (HSS) are chosen as micro-drill bit materials which posses good strength and resistance against various workpiece materials. For horn, Aluminum 6061-T6, Titanium (Ti-6Al-4V) and Mild steel materials are considered. These materials are light in weight and possesses good characteristics under the influence of vibration. The mechanical properties of horn and micro-drill bit materials are mentioned in Table 5.1.

Table 5.1: Material properties of horn and micro-drill bit

Mechanical properties	Materials				
	Micro-drill bit		Horn		
	WC	HSS	Aluminium	Titanium	Mild steel
Density (kg/m ³)	15,600	8160	2700	4510	7870
Young's Modulus (GPa)	690	210	69	120	205
Poisson's Ratio (ν)	0.31	0.30	0.33	0.34	0.3
Speed of sound (c_p) (m/sec)	6220	5141	5091	5158	5103

5.3.2 Meshing and Boundary Conditions

A fine Hex dominant mesh with all quad elements has been considered in all the assemblies of horns. The element size for both the horns and the micro-drill are taken as 4 mm and 0.1 mm respectively. Bonded contact has been set apart to the assembly of the horn with drill bit. Only linear properties are considered in Modal analysis and Free- support is assumed for calculating the natural frequencies. Table 5.2 provides the mesh details of both the horns

assembled with micro-drill bit. Figures 5.4 and 5.5 shows the meshing of stepped and conical horns assembly respectively.

Table 5.2: Mesh details of horn and drill bit assembly

Mesh type	Body	No. of elements	No. of nodes
Hex dominant (all quad)	Stepped Horn and micro drill assembly	19,329	59,051
	Conical Horn and micro drill assembly	11,851	39,373

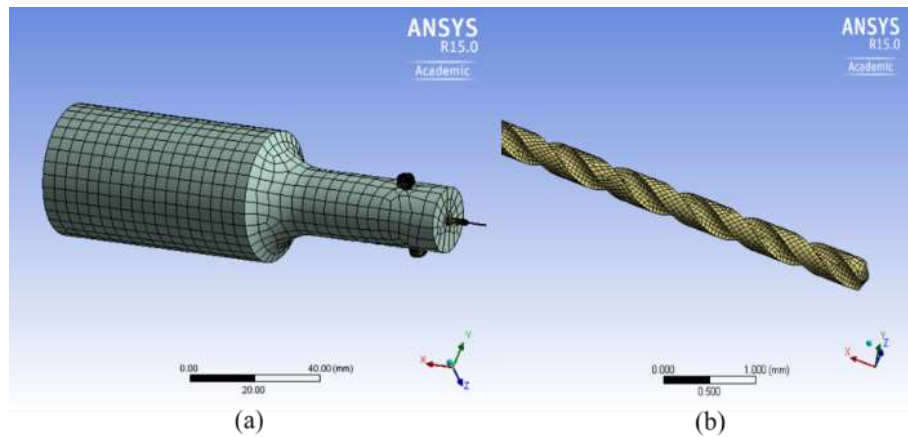


Figure 5.4 Meshing of (a) stepped horn and micro-drill assembly, (b) flute portion (closer view)

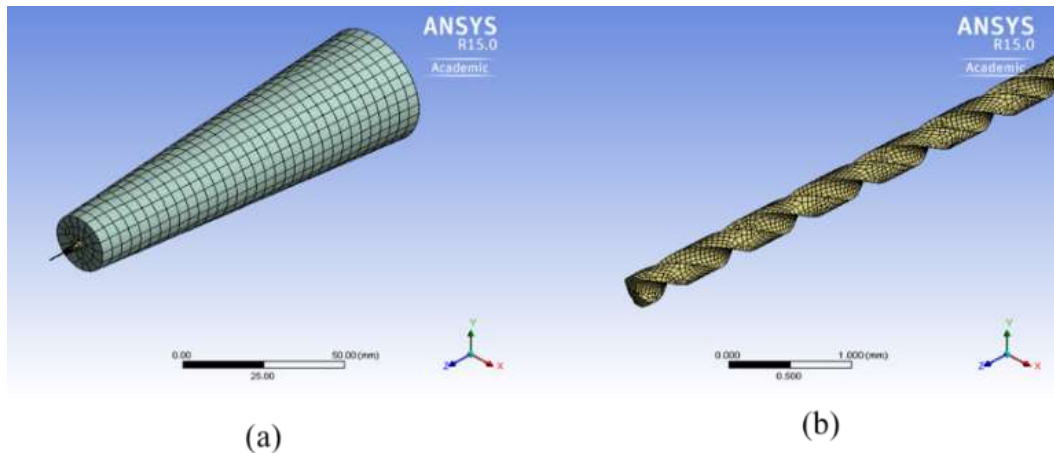


Figure 5.5: Meshing of (a) conical horn and micro-drill assembly, (b) flute portion (closer view)

A frequency range of 15-30 kHz has been preferred to identify the natural frequencies and mode shapes behavior of both the horns and drill bit assembly. Material combinations of these assemblies were selected from Table 5.1. The observed natural frequencies and mode shapes along transverse (T), longitudinal (L) and twisting (Tw) directions measured for

stepped horn of Aluminum 6061-T6, Titanium and Mild Steel materials assembled with micro-drill bit of Tungsten Carbide and High Speed Steel materials respectively are recorded in Tables 5.3 and 5.4 respectively. Figure 5.6 shows the different mode shapes obtained for Aluminum 6061-T6 stepped horn with tungsten carbide drill bit. The natural frequencies and mode shapes obtained for conical horn of Aluminum 6061-T6, Titanium and Mild Steel materials along with micro drill bit of Tungsten Carbide and High Speed Steel materials respectively are listed in Tables 5.5 and 5.6. Mode shapes observed in Aluminum 6061-T6 conical shaped horn assembled with tungsten carbide drill bit is depicted in Figure 5.7.

Table 5.3: Natural frequencies recorded for stepped horn assembled with tungsten carbide micro-drill bit

Mode No & Mode Shape	Frequency in horn materials (Hz)		
	Aluminum 6061- T6	Titanium	Mild steel
1 (T)	17308	17386	17639
2 (T)	17452	17470	17689
3 (L)	20008	20431	20845
4 (Tw)	22087	21729	22199
5 (T)	25619	25785	26182
6 (T)	25813	25905	26261

Table 5.4: Natural frequencies recorded for stepped horn assembled with high speed steel micro-drill bit

Mode No. & Mode Shape	Frequency in horn materials (Hz)		
	Aluminium 6061- T6	Titanium	Mild steel
1 (T)	17437	17462	17676
2 (T)	17586	17549	17721
3 (L)	20326	20625	20956
4 (Tw)	22086	21728	22196
5 (T)	25736	25858	26220
6 (T)	25937	25982	26298

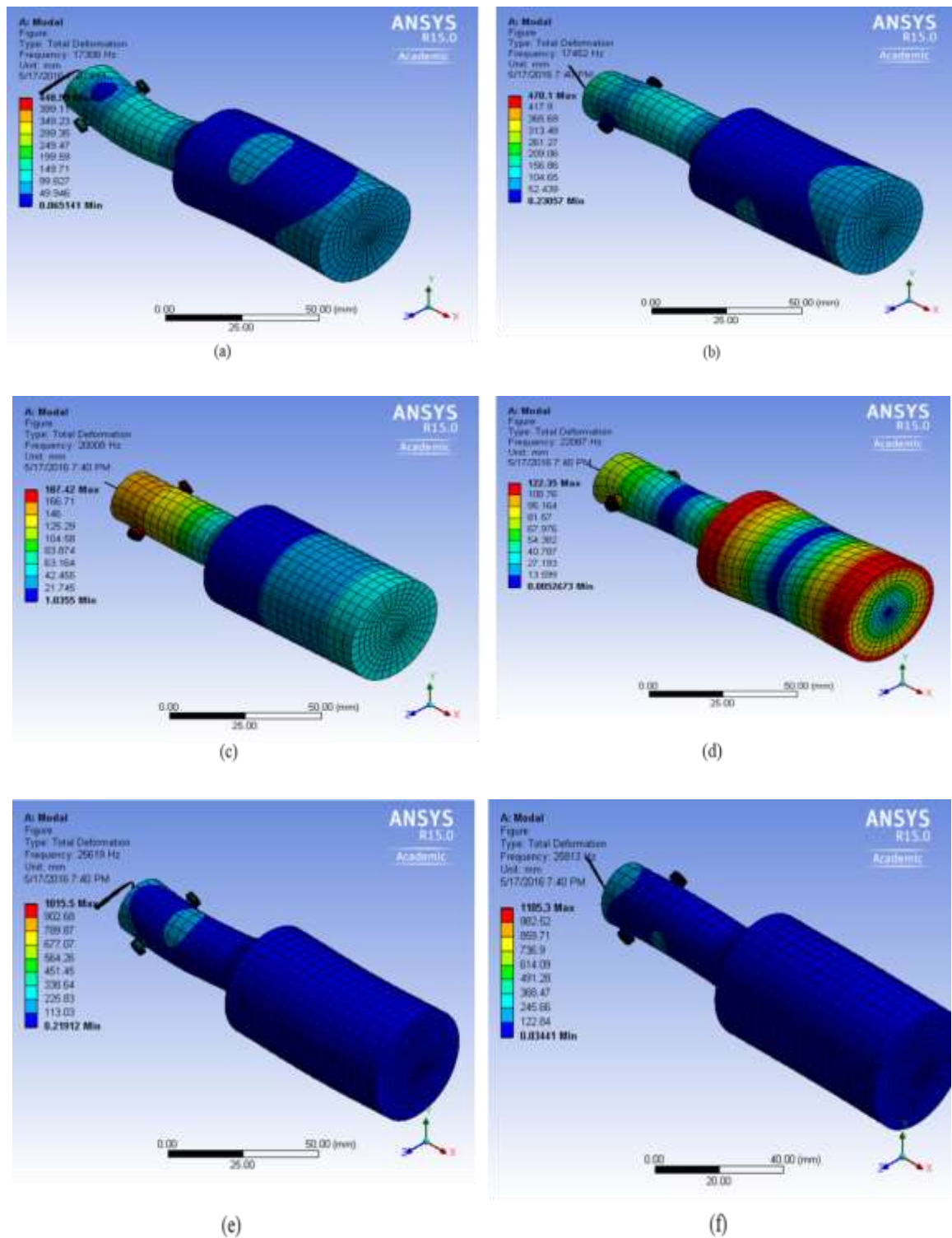


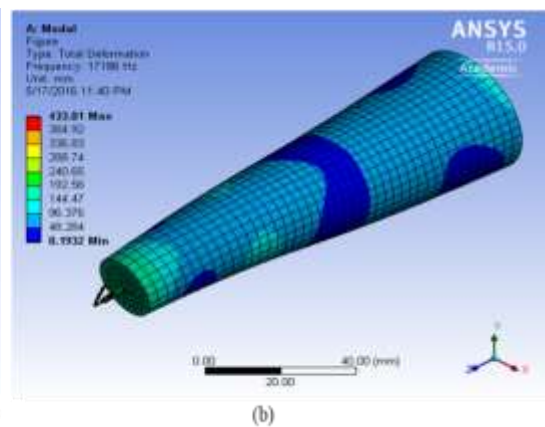
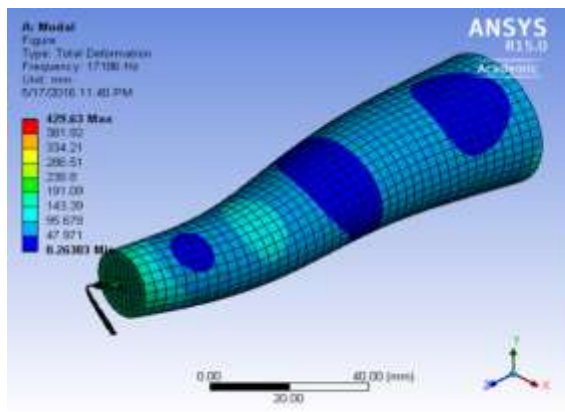
Figure 5.6: Mode shapes recorded for stepped horn (Al 6061-T6) assembled with micro-drill bit (WC) at various natural frequencies (a) 17308 Hz, (b) 17452 Hz, (c) 20008 Hz, (d) 22087 Hz, (e) 25619 Hz and (f) 28813 Hz

Table 5.5: Natural frequencies recorded for conical horn assembled with micro drill bit
(WC)

Mode No. & Mode Shape	Frequency in horn materials (Hz)		
	Aluminum 6061- T6	Titanium	Mild steel
1 (T)	16975	17001	17208
2 (T)	16976	17001	17208
3 (L)	20298	20404	20646
4 (Tw)	25517	25064	25581
5 (T)	28101	28136	28537
6 (T)	28102	28137	28537

Table 5.6: Natural frequencies recorded for conical horn assembled with HSS micro-drill bit

Mode No. & Mode Shape	Frequency in horn materials (Hz)		
	Aluminum 6061- T6	Titanium	Mild steel
1 (T)	17106	17291	17465
2 (T)	17106	17291	17465
3 (L)	20506	20685	20715
4 (Tw)	25518	25261	25782
5 (T)	27556	27720	27892
6 (T)	27761	28034	28306



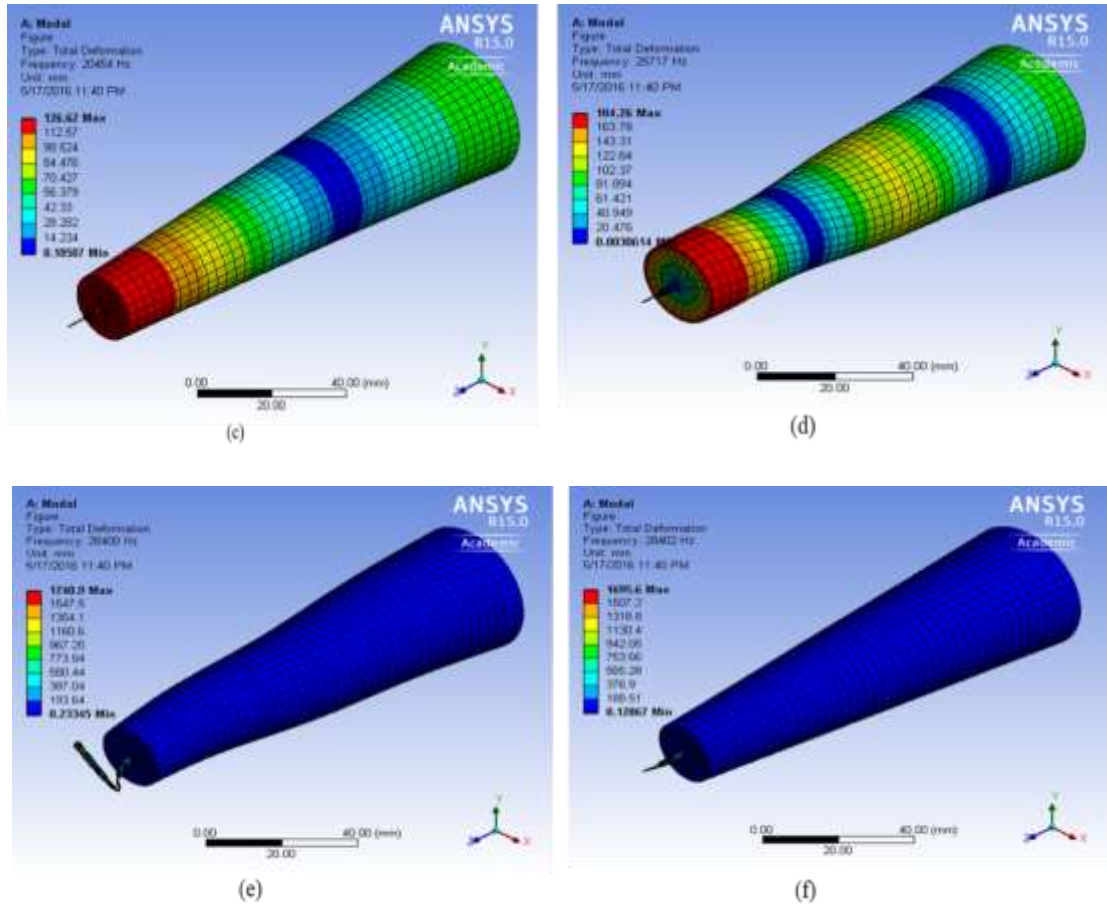


Figure 5.7: Mode shapes recorded for conical horn (Al 6061-T6) assembled with micro-drill bit (WC) at different natural frequencies (a) 16975 Hz, (b) 16976 Hz, (c) 20298 Hz, (d) 25517 Hz, (e) 28101 Hz and (f) 28102 Hz

As per the observed results, it is concluded that both the horns assembled with micro-drill bit are well set for the given ultrasonic frequency range. For both the chosen horn and micro drill bit material combinations, initially transverse bending modes have been seen at frequencies below ultrasonic range (<20 kHz). The longitudinal mode was observed within the desirable ultrasonic range above 20 kHz (<100 kHz). Later the twisting and transverse mode shapes have been recorded beyond the desirable frequency range (> 20 kHz) as depicted in Figures 5.6 and 5.7 respectively. The stepped and conical shaped horns of Aluminum 6061-T6 with Tungsten carbide micro-drill bit assembly illustrates closeness to ultrasonic frequency response longitudinally as compared to others. Further, the results recorded during modal analysis with longitudinal modes are utilized to perform the harmonic analysis and to verify the dynamic frequency responses with respect to various material combination considered for stepped and conical shaped horn assembled with micro-drill bit.

5.4 FE Harmonic Analysis

Harmonic analysis is used to determine the steady-state response of a linear structure to loads that vary sinusoidally with time. For the ultrasonic vibration assistance systems, the transmission of vibration energy may vary for different cross-sectional structures. In the present section, Full method analysis is applied to predict the response of vibrating bodies i.e. horn with micro-drill bit assembly for stepped and conical shaped horns under desirable ultrasonic frequency range. Here, frequency responses are considered for longitudinal modes only. For the present work, the displacement loading boundary conditions are assumed to verify the frequency response and amplification factors of the Aluminum 6061-T6 horn material with tungsten carbide micro-drill bit for both the horn shapes. The displacement loads of 15 and 30 μm are applied on horn larger end diameter in axial direction. As the horn is connected to the transducer, the boundary conditions are given to the input end of the stepped and conical horn as shown in Figure 5.8.

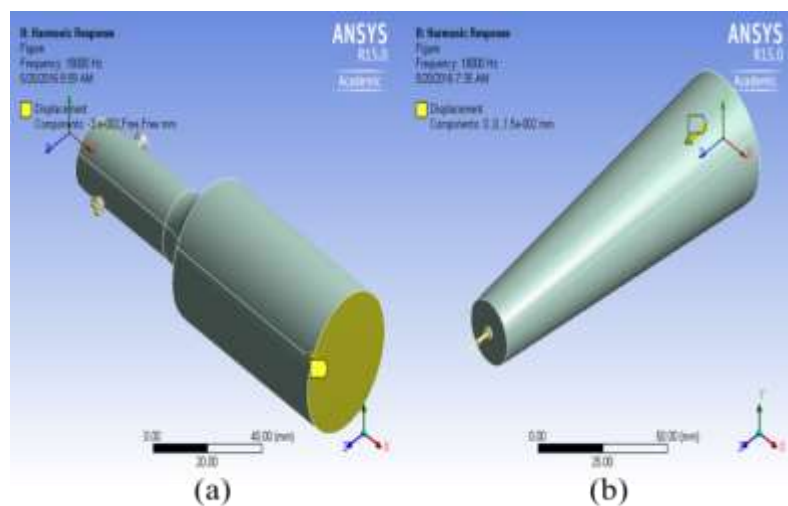


Figure 5.8: Displacement boundary applied on back end (a) stepped horn, (b) conical horn

Frequency response is considered in terms of stress and total deformation from the face of the micro-drill bit chisel edge. Figure 5.9 depicts the stress distribution and total deformation formed on Al 6061-T6 stepped shaped horn and WC micro-drill bit assembly at a frequency of 20008 Hz. Figure 5.10 displays the stress distribution and total deformation formed on Al 6061-T6 conical shaped horn and WC micro-drill bit assembly at a frequency of 20298 Hz. The frequency responses in terms of stresses and total deformation at longitudinal modes of 30 μm amplitude for Al 6061T6 stepped and conical shaped horn along with tungsten carbide micro drill bit are graphically shown (Figures 5.11 and 5.12).

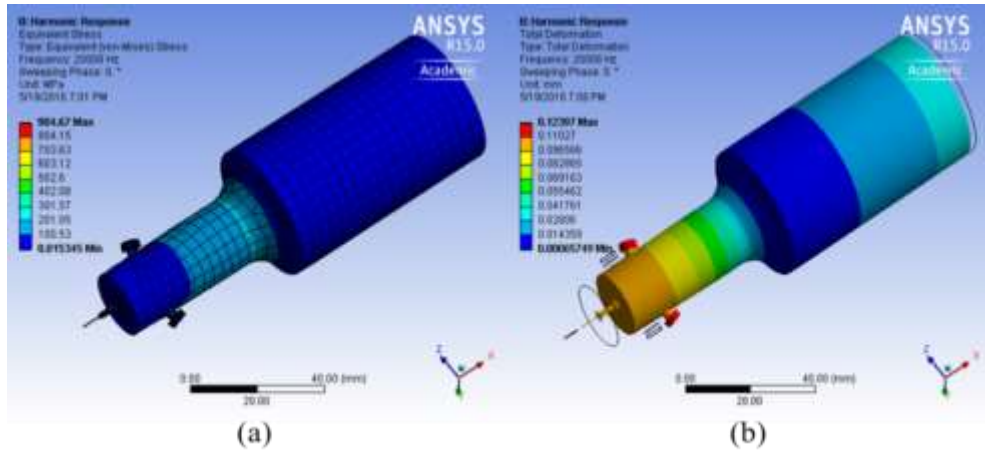


Figure 5.9: Frequency response at 20008 Hz for Al 6061-T6 stepped horn and WC micro drill bit assembly (a) equivalent stress, (b) total deformation

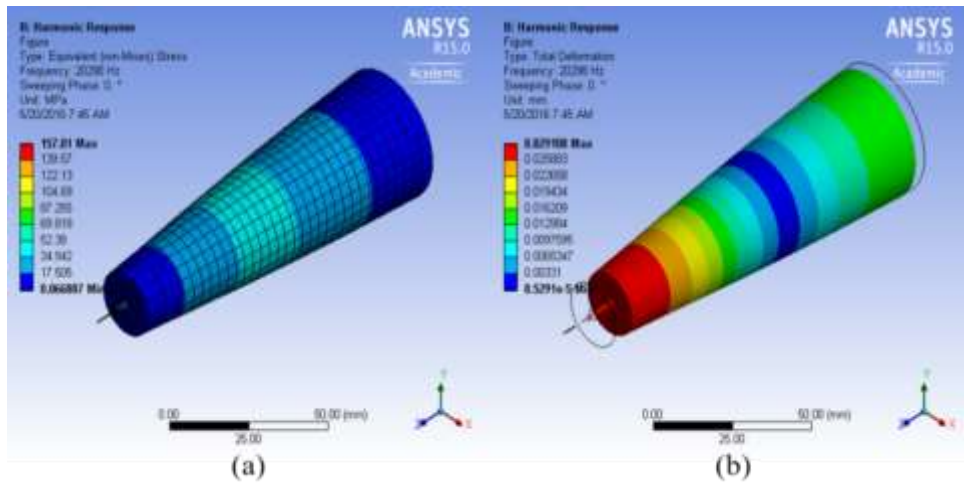


Figure 5.10: Frequency response at 20298 Hz for Al 6061-T6 conical horn and WC micro drill bit assembly (a) equivalent stress, (b) total deformation

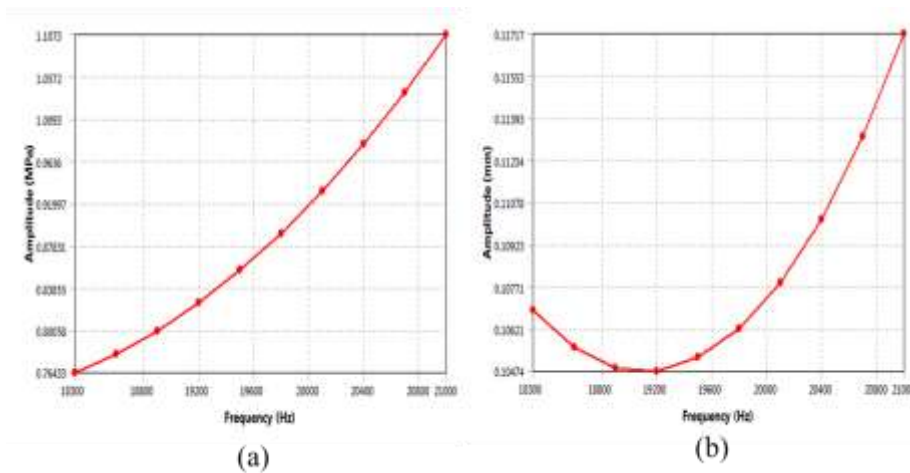


Figure 5.11: Frequency vs. Amplitude of stepped horn (Al 6061-T6) assembled with micro-drill bit (WC) at 30 μm (a) equivalent stress, (b) total deformation

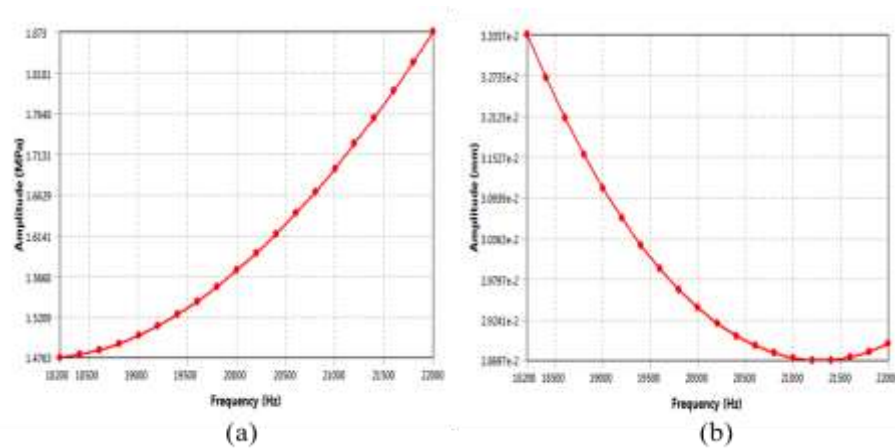


Figure 5.12: Frequency vs Amplitude of conical horn (Al 6061-T6) assembled with micro-drill bit (WC) at 30 μm (a) equivalent stress, (b) total deformation

5.5 Discussion

For the modal analysis, the natural frequencies obtained for stepped and conical shaped horn with varying material combinations have matched well with the specified frequency range 15-30 kHz. The initial frequencies for all the material combinations have shown transverse mode shapes below the ultrasonic frequency. The most essential longitudinal mode shape has been formed above the ultrasonic vibration frequency range and later followed by twisting and transverse modes. Aluminum 6061-T6 material with combination of tungsten carbide drill bit for stepped shaped horn attained mode shape very close to ultrasonic tuning frequency (20008 Hz). Titanium and Mild steel materials with combination of WC and HSS drill bit materials for stepped horn have also shown the similarities with varying frequencies closer to Al 6061-T6. In case of Conical shaped horn, the Al 6061 T6 material with combination of WC drill bit showed 20298Hz frequency which is less than the other materials such as titanium and mild steel. In usual practice there will be vibration energy losses in between the assembly of transducer with horn and drill bit due to material internal structures and boundary conditions.

Harmonic analysis have also been performed for the stepped and conical horn (Al 6061-T6) with micro-drill bit (WC) to verify the frequency responses. The equivalent stress distribution and total deformation for both the horns at desirable longitudinal modes of 20008 Hz for stepped horn and 20298 Hz for conical horn have been observed (Figures 5.9 and 5.10). The equivalent stress acting on Al 6061-T6 materials for stepped horn and conical horn are well set with in the elastic limit range without exceeding the material property limits. The maximum stress concentration observed in the conical horn (157 MPa) is less as

compared in the case of stepped horn (904 MPa) (Figures 5.9 (a) and 5.10 (a)). The equivalent stress of stepped and conical shaped horns shows steadily rise with the increasing frequencies (Figures 5.11(a) and 5.12 (a)) which is due to the cross section of the horns. The total deformation occurred in stepped and conical horns are 0.096 mm and 0.022 mm respectively as depicted in Figures 5.9 (b) and 5.10 (b). It is seen that the amplitude gradually increases with respect to the frequencies for the stepped shaped horn and the amplitude decreases in conical shaped horn (Figures 5.11 (b) and 5.12 (b)). This is due to the smaller edge curvature of the stepped horn. As compared to stepped shaped horn, the conical shaped horn is showing lower deformation of material. This is due to the variation in material properties, speed of sound, horn length, etc. The amplification factors for stepped and conical shaped horn from the input end to output end satisfies with the amplification ratio i.e. greater than 1.

As per the results, the Al6061-T6 stepped horn with WC micro-drill bit can be recommended for ease of manufacturing and can be suitable for matching the ultrasonic frequency of 20 ± 500 kHz tuning generator. The present horns are designed after several repeated modal analysis conducted to match the resonance frequency with different material combinations while varying the horn length from 2 mm above the theoretical calculations.

5.6 Conclusion

The FE analysis eases the evaluation of various shapes of ultrasonic horns prior to manufacture and experimentation. Also, it allows the proper selection of the different horn shape for assisting specific machining process. The important point to be considered for designing ultrasonic micro-drilling tool setup is that the horn should have at least one natural frequency within the allowable ultrasonic frequency. The designed dimensions of both the horns satisfied the longitudinal modes with the ultrasonic vibrational frequency 20008 Hz and 20298 Hz (< 20000 Hz). The equivalent stresses and total deformation has been examined for both the horns at longitudinal modes. It can be concluded that the geometrical dimension and material properties used in the analysis of horn with micro drill can deliver the essential frequency. The present simulation results will be beneficial to select desired horn shape and materials combination to conduct proper experimentation for achieving effective machining and surface quality. In future, more number of material combinations for horns or newer materials which are light in weight need to be analyzed to define the ultrasonic vibration frequency range for improved machining.

Chapter 6

CONCLUSIONS AND FUTURE DIRECTIONS

The work described in the thesis consists of the description of a finite element model that enables finite element analysis of complex micro-drilling process and machining parameters to compute the hole formation behaviour of a multi-layered printed circuit board material. The analysis of the problems in three-dimensional models involves huge complexity that requires attention on adopting the actual machining environment conditions. Emphasis is placed on the simulation of the effect of high speed and feed rates since substantial hole surfaces are generally required for accurate prediction. FE analysis for the present research approach is relatively new and no general three-dimensional models exist in the literature review. The FE analysis for this dissertation is based on the Lagrangian description for conventional and ultrasonic vibration assisted micro-drilling. Block Lanczos and Full solver method are adopted for simulating the ultrasonic horn model in order to satisfy the objectives. This chapter concludes the comprehensive research focused on the FE simulation analysis of micro-drilling on multi-layered PCB material.

6.1 Conclusions

Specific conclusions were drawn for corresponding subject at the end of the appropriate chapter. The present chapter summarise the main conclusions on the use of FE simulation for generalised machining conditions.

1. Three-dimensional FE simulation method is a valuable tool for investigating the stress, thrust forces generated in multi-layered PCB materials. The cutting parameters like speed and feed rates can be rapidly and economically quantified. In addition, the FE results can be calibrated against the experimental results for particular process parameters in terms of geometric, material properties and boundary conditions to generate additional results which can be used in development of database for design guidance.

2. FE results show that the drilling force changes when the drill tool make contacts with different layered materials. The highest drilling force is generated while drilling copper foil. The peak values of the thrust force in micro-drilling increases with an increase in feed rate and decreases with high rotational speeds in traditional micro-drilling. The exit burr was observed in all conventional machining parameters. The higher feed rates are most important factor that influences the exit burr.
3. The mathematical calculations for the analytical model have been adopted by considering the cutting parameters with constant speed and varying feed rate at ultrasonic vibration circular frequency of 20 kHz. FE simulation was performed to verify the thrust forces and compared with the analytical model as well as with the previous experiment related to UVAMD. Results show that the ultrasonic assisted micro-drilling has a good potential in reduction of forces at operating parameters with improved surface finish.
4. The high rotational speed not only reduces thrust force in conventional drilling, but also has a similar effect in UVAMD. However, this trend may vary with different vibrational frequencies.
5. Further, to develop a proper ultrasonic vibration assisted machining using high speed spindle, FE analysis has been performed for stepped and conical shaped horns assembled with micro-drill bit. FE modal and harmonic analysis were conducted by utilizing various material combinations, which are basically used in present industrial applications. The equivalent stresses and total deformation have been examined for both the horn shapes at longitudinal mode. Results showed good agreement for both the horns and stresses observed are within the material elastic limits for horn materials.
6. The predicted FE simulation data could be beneficial to manufacturers of micro-machining centers / ultrasonic horns like, Fuji ultrasonic engineering, DMG MORI, Roop telesonic, Oscar electronic private ltd., etc. This may also benefit to the shop floor technicians in industries working with the machining of micro components in printed circuit boards, polymers, micro/nano electronic devices, semiconductors, etc. to achieve good surface integrity, tool wear reduction, etc. The optimized machining parameters required in conventional and ultrasonic assisted micro-machining centers could be provided in the user guide manual of particular machining centers by its manufacturers.

6.2 Scope for Future Work

The present work focus on the influence of ultrasonic frequency on the work piece material in terms of reduction of thrust forces and micro-burrs during micro-drilling using FE simulation. Design of ultrasonic horn along with micro drill bit has been proposed for multiple material combinations applied for UVAMD. Application of ultrasonic vibration in micromachining thus reduces thrust forces, burr height, tool wear and increases high dimensional accuracy, acceptable material removal rate, etc. This may indirectly reduce the costs related to energy consumption (cutting energy consumption) and increases tool life. Further, there is a clear need for carrying out the work on printed circuit board materials to cover the factors that has not been included in this thesis as below.

- Brief overview in chapter 3 suggests that comprehensive material property data including prepreg for multi-layered PCB materials can be considered to compute an accurate three-dimensional machining simulation.
- The present FE simulation includes only two constitutive material damage models like Johnson-Cook for metal plasticity and Hashin criteria for composite material. More constitutive models need to be verified for predicting actual damage on the work piece material.
- The frictional coefficient value is further required to verify the master-slave relationship between the layers associated with PCB materials to examine the damage initiation and delamination between the consequent layers that has impact on the actual drill-work piece model.
- Mesh convergence study is further required to verify with various mesh elements on multi-layered PCB materials that are not included in the present work.
- In chapter 4, the FE simulation results are compared with the limited experimental data and requires more combination of frequency and amplitude data for developing accurate three-dimensional model to simulate the ultrasonic vibration of micro drilling on various work piece materials. In future, further experimentations need to be performed to verify the effects of resonances.
- Having better models for prediction of ultrasonic vibration assistance regime to interface with the tool and the work piece would have better results. Hybrid and solid models and accurate parametric model of micro drill bit can be generated to achieve

more precise results. The FE simulation for UVA micro machining can further be enhanced and extended to various materials like plastics, sheet metal, other PCBs, etc. to predict the performance with varying machining and geometric parameters.

- The FE analysis for ultrasonic horn developed for micro-drilling process can be further extended to more number of material combinations which are light in weight to determine the ultrasonic vibration frequency range.

Bibliography

- [1] Afazov, S. M., Ratchev, S. M., & Segal, J. (2010). Modelling and simulation of micro-milling cutting forces. *Journal of Materials Processing Technology*, 210(15), 2154-2162.
- [2] Alam, K., Hassan, E., & Bahadur, I. (2015). Experimental measurements of temperatures in ultrasonically assisted drilling of cortical bone. *Biotechnology & biotechnological equipment*, 29(4), 753-757.
- [3] Alam, K., Mitrofanov, A. V., & Silberschmidt, V. V. (2011). Experimental investigations of forces and torque in conventional and ultrasonically-assisted drilling of cortical bone. *Medical Engineering and Physics*, 33(2), 234-239.
- [4] Al-Budairi, H. D. (2012). *Design and analysis of ultrasonic horns operating in longitudinal and torsional vibration* (Doctoral dissertation, University of Glasgow).
- [5] Ali, M. Y., Mohamed, A. R., & Hannah, N. (2013). Investigation of Burr in High Speed Microdrilling. In *Applied Mechanics and Materials* (Vol. 278, pp. 389-392). Trans Tech Publications.
- [6] Ali, M. Y., Mohamed, A. R., Khan, A. A., Asfana, B., Lutfi, M., & Fahmi, M. I. (2013). Empirical modelling of vibration in micro end milling of PMMA. *World Applied Sciences Journal (Mathematical Applications in Engineering)*, 21, 73-78.
- [7] Alrabii, S. A. (2009). An experimental study of burr formation in drilling and slot-end milling operations. *Journal of Engineering*, 15(4), 4219-4240.
- [8] Amaya, P. (2012). *Progressive Damage and Failure Model for Composite Laminates under Multiaxial Loading Conditions* (Doctoral dissertation, The Ohio State University).
- [9] Amini, S., Paktinat, H., Barani, A., & Tehran, A. F. (2013). Vibration drilling of Al2024-T6. *Materials and Manufacturing Processes*, 28(4), 476-480.
- [10] Amini, S., Soleimanimehr, H., Nategh, M. J., Abudollah, A., & Sadeghi, M. H. (2008). FEM analysis of ultrasonic-vibration-assisted turning and the vibratory tool. *Journal of materials processing technology*, 201(1-3), 43-47.
- [11] Aoyama, E., Nobe, H., & Hirogaki, T. (2001). Drilled hole damage of small diameter drilling in printed wiring board. *Journal of Materials Processing Technology*, 118(1-3), 436-441.
- [12] Aramcharoen, A., & Mativenga, P. T. (2009). Size effect and tool geometry in micromilling of tool steel. *Precision Engineering*, 33(4), 402-407.
- [13] Armarego, E. J. A., & Zhao, H. (1996). Predictive force models for point-thinned and circular centre edge twist drill designs. *CIRP Annals-Manufacturing Technology*, 45(1), 65-70.
- [14] Arul, S., Vijayaraghavan, L., Malhotra, S. K., & Krishnamurthy, R. (2006). The effect of vibratory drilling on hole quality in polymeric composites. *International Journal of Machine Tools and Manufacture*, 46(3-4), 252-259.
- [15] Arvajah, T., & Ismail, F. (2006). Machining stability in high-speed drilling—part 1: modeling vibration stability in bending. *International Journal of Machine Tools and Manufacture*, 46(12-13), 1563-1572.
- [16] Audy, J. (2008). A study of computer-assisted analysis of effects of drill geometry and surface coating on forces and power in drilling. *Journal of Materials Processing Technology*, 204(1-3), 130-138.

-
- [17] Azarhoushang, B., & Akbari, J. (2007). Ultrasonic-assisted drilling of Inconel 738-LC. *International Journal of Machine Tools and Manufacture*, 47(7-8), 1027-1033.
- [18] Aziz, M., Ohnishi, O., & Onikura, H. (2012). Innovative micro hole machining with minimum burr formation by the use of newly developed micro compound tool. *Journal of Manufacturing Processes*, 14(3), 224-232.
- [19] Aziz, M., Ohnishi, O., & Onikura, H. (2012). Novel micro deep drilling using micro long flat drill with ultrasonic vibration. *Precision Engineering*, 36(1), 168-174.
- [20] Babitsky, V. I., Astashev, V. K., & Meadows, A. (2007). Vibration excitation and energy transfer during ultrasonically assisted drilling. *Journal of Sound and Vibration*, 308(3-5), 805-814.
- [21] Baghlani, V., Mehbudi, P., Akbari, J., & Sohrabi, M. (2013). Ultrasonic assisted deep drilling of Inconel 738LC superalloy. *Procedia CIRP*, 6, 571-576.
- [22] Bannan, T., Gerrard, C., & Wellstead, M. (2006). Process capability factors in micro-hole drilling of BGA board materials. In *The EIPC Winter Conference, Budapest*.
- [23] Bao, W. Y., & Tansel, I. N. (2000). Modeling micro-end-milling operations. Part I: analytical cutting force model. *International Journal of Machine Tools and Manufacture*, 40(15), 2155-2173.
- [24] Bao, W. Y., & Tansel, I. N. (2000). Modeling micro-end-milling operations. Part II: tool run-out. *International Journal of Machine Tools and Manufacture*, 40(15), 2175-2192.
- [25] Batzer, S. A., Gousskov, A. M., & Voronov, S. A. (2001). Modeling vibratory drilling dynamics. *Journal of vibration and acoustics*, 123(4), 435-443.
- [26] Bayly, P. V., Metzler, S. A., Schaut, A. J., & Young, K. A. (2001). Theory of torsional chatter in twist drills: model, stability analysis and composition to test. *Journal of manufacturing science and engineering*, 123(4), 552-561.
- [27] Behera, B. K. (2011). *Parametric optimization of microdrilling in aerospace material* (Doctoral dissertation).
- [28] Benzeggagh, M. L., & Kenane, M. (1996). Measurement of mixed-mode delamination fracture toughness of unidirectional glass/epoxy composites with mixed-mode bending apparatus. *Composites science and technology*, 56(4), 439-449.
- [29] Bergstrom, A. J., Filipovic, A. J., Olson, W. W., & Sutherland, J. W. (2000). Mechanistic prediction of drilling forces incorporating a minimum cutting energy model for chip flow angle. *Transactions-North American Manufacturing Research Institution of SME*, 143-148.
- [30] Bertsche, E., Ehmann, K., & Malukhin, K. (2013). An analytical model of rotary ultrasonic milling. *The International Journal of Advanced Manufacturing Technology*, 65(9-12), 1705-1720.
- [31] Bhandari, B., Hong, Y. S., Yoon, H. S., Moon, J. S., Pham, M. Q., Lee, G. B., ... & Ahn, S. H. (2014). Development of a micro-drilling burr-control chart for PCB drilling. *Precision Engineering*, 38(1), 221-229.
- [32] Biermann, D., & Heilmann, M. (2010). Improvement of workpiece quality in face milling of aluminum alloys. *Journal of Materials Processing Technology*, 210(14), 1968-1975.

- [33] Brehl, D. E., & Dow, T. A. (2008). Review of vibration-assisted machining. *Precision engineering*, 32(3), 153-172.
- [34] Brown, S. W. (2004). *Time-and Temperature-Dependence of Fracture Energies Attributed to Copper/Epoxy Bonds* (Doctoral dissertation, Virginia Tech).
- [35] Cai, L. J., & Cai, C. T. (2012). Analysis of Z-axis rigid of PCB CNC drilling machines. *Indonesian Journal of Electrical Engineering and Computer Science*, 10(6), 1409-1414.
- [36] Camanho, P. P., & Matthews, F. L. (1997). Stress analysis and strength prediction of mechanically fastened joints in FRP: a review. *Composites Part A: Applied Science and Manufacturing*, 28(6), 529-547.
- [37] Chakladar, N. D., Pal, S. K., & Mandal, P. (2012). Drilling of woven glass fiber-reinforced plastic—an experimental and finite element study. *The International Journal of Advanced Manufacturing Technology*, 58(1-4), 267-278.
- [38] Chandrasekharan, V., Kapoor, S. G., & DeVor, R. E. (1998). A mechanistic model to predict the cutting force system for arbitrary drill point geometry. *Journal of Manufacturing Science and Engineering*, 120(3), 563-570.
- [39] Chang, S. S., & Bone, G. M. (2005). Burr size reduction in drilling by ultrasonic assistance. *Robotics and computer-integrated manufacturing*, 21(4-5), 442-450.
- [40] Chang, S. S., & Bone, G. M. (2009). Thrust force model for vibration-assisted drilling of aluminum 6061-T6. *International Journal of Machine Tools and Manufacture*, 49(14), 1070-1076.
- [41] Chang, S. S., & Bone, G. M. (2010). Burr height model for vibration assisted drilling of aluminum 6061-T6. *Precision Engineering*, 34(3), 369-375.
- [42] Chen, M. J., Ni, H. B., Wang, Z. J., & Jiang, Y. (2012). Research on the modeling of burr formation process in micro-ball end milling operation on Ti-6Al-4V. *The International Journal of Advanced Manufacturing Technology*, 62(9-12), 901-912.
- [43] Chen, W. C. (1997). Some experimental investigations in the drilling of carbon fiber-reinforced plastic (CFRP) composite laminates. *International Journal of Machine Tools and Manufacture*, 37(8), 1097-1108.
- [44] Chen, W. R. (2007). Parametric studies on buckling loads and critical speeds of microdrill bits. *International journal of mechanical sciences*, 49(8), 935-949.
- [45] Chen, W. S., & Ehmann, K. F. (1994). Experimental investigation on the wear and performance of micro-drills. In *Proceedings of the 1994 International Mechanical Engineering Congress and Exposition*. ASME.
- [46] Chen, Y. R., & Ni, J. (1999). *Analysis and optimization of drill cross-sectional geometry* (pp. 1-6). Dearborn, MI: Society of Manufacturing Engineers.
- [47] Cheong, M. S., Cho, D. W., & Ehmann, K. F. (1999). Identification and control for micro-drilling productivity enhancement. *International Journal of Machine Tools and Manufacture*, 39(10), 1539-1561.
- [48] Chern, G. L., & Chang, Y. C. (2006). Using two-dimensional vibration cutting for micro-milling. *International Journal of Machine Tools and Manufacture*, 46(6), 659-666.
- [49] Chern, G. L., & Lee, H. J. (2006). Using workpiece vibration cutting for micro-drilling. *The International Journal of Advanced Manufacturing Technology*, 27(7-8), 688-692.
- [50] Chern, G. L., & Liang, J. M. (2007). Study on boring and drilling with vibration cutting. *International Journal of Machine Tools and Manufacture*, 47(1), 133-140.

-
- [51] Chyan, H. C., & Ehmann, K. F. (1998). Development of curved helical micro-drill point technology for micro-hole drilling. *Mechatronics*, 8(4), 337-358.
- [52] Dandekar, C. R., & Shin, Y. C. (2008). Multiphase finite element modeling of machining unidirectional composites: prediction of debonding and fiber damage. *Journal of Manufacturing Science and Engineering*, 130(5), 051016.
- [53] Davim, J. P., Reis, P., & Antonio, C. C. (2004). Experimental study of drilling glass fiber reinforced plastics (GFRP) manufactured by hand lay-up. *Composites Science and Technology*, 64(2), 289-297.
- [54] De Lacalle, L. N. L., Rivero, A., & Lamikiz, A. (2009). Mechanistic model for drills with double point-angle edges. *The International Journal of Advanced Manufacturing Technology*, 40(5-6), 447-457.
- [55] Debnath, K., Singh, I., & Dvivedi, A. (2015). Rotary mode ultrasonic drilling of glass fiber-reinforced epoxy laminates. *Journal of Composite Materials*, 49(8), 949-963.
- [56] Doomra, V. K., Debnath, K., & Singh, I. (2015). Drilling of metal matrix composites: Experimental and finite element analysis. *Proceedings of the Institution of Mechanical Engineers, Part B: Journal of Engineering Manufacture*, 229(5), 886-890.
- [57] Dornfeld, D. A., Kim, J. S., Dechow, H., Hewson, J., & Chen, L. J. (1999). Drilling burr formation in titanium alloy, Ti-6Al-4V. *CIRP Annals-Manufacturing Technology*, 48(1), 73-76.
- [58] Duhamel, D., Mace, B. R., & Brennan, M. J. (2006). Finite element analysis of the vibrations of waveguides and periodic structures. *Journal of sound and vibration*, 294(1-2), 205-220.
- [59] Egashira, K., & Mizutani, K. (2002). Micro-drilling of monocrystalline silicon using a cutting tool. *Precision Engineering*, 26(3), 263-268.
- [60] Ehmann, K., Kang, S. K., & Lin, C. (1993). Comparative analysis of planar and helical micro-drill points. *Transactions of the North American Manufacturing Research Institution of SME*, 21, 189-196.
- [61] Elhachimi, M., Torbaty, S., & Joyot, P. (1999). Mechanical modelling of high speed drilling. 1: predicting torque and thrust. *International Journal of Machine Tools and Manufacture*, 39(4), 553-568.
- [62] Elhachimi, M., Torbaty, S., & Joyot, P. (1999). Mechanical modelling of high speed drilling. 2: predicted and experimental results. *International Journal of Machine Tools and Manufacture*, 39(4), 569-581.
- [63] El-Hofy, H. A. G. (2013). *Fundamentals of machining processes: conventional and nonconventional processes*. CRC press.
- [64] Ema, S., & Marui, E. (2003). Theoretical analysis on chatter vibration in drilling and its suppression. *Journal of Materials Processing Technology*, 138(1-3), 572-578.
- [65] Engin, S., & Altintas, Y. (2001). Mechanics and dynamics of general milling cutters: Part I: helical end mills. *International journal of machine tools and manufacture*, 41(15), 2195-2212.
- [66] Ensminger, D., & Stulen, F. B. (Eds.). (2008). *Ultrasonics: data, equations and their practical uses*. CRC press.
- [67] Eski, İ. (2012). Vibration analysis of drilling machine using proposed artificial neural network predictors. *Journal of mechanical science and technology*, 26(10), 3037-3046.

- [68] Feito, N., López-Puente, J., Santiuste, C., & Miguélez, M. H. (2014). Numerical prediction of delamination in CFRP drilling. *Composite Structures*, *108*, 677-683.
- [69] Filipp Fuchs, P., Fellner, K., & Pinter, G. (2013). Local damage simulations of printed circuit boards based on in-plane cohesive zone parameters. *Circuit World*, *39*(2), 60-66.
- [70] Filiz, S., & Ozdoganlar, O. B. (2010). A Model for Bending, Torsional, and Axial Vibrations of Micro-and Macro-Drills Including Actual Drill Geometry—Part I: Model Development and Numerical Solution. *Journal of manufacturing science and engineering*, *132*(4), 041017.
- [71] Filiz, S., & Ozdoganlar, O. B. (2010). A model for bending, torsional, and axial vibrations of micro-and macro-drills including actual drill geometry—part II: model validation and application. *Journal of manufacturing science and engineering*, *132*(4), 041018.
- [72] Filiz, S., & Ozdoganlar, O. B. (2011). A three-dimensional model for the dynamics of micro-endmills including bending, torsional and axial vibrations. *Precision Engineering*, *35*(1), 24-37.
- [73] Flachs, J. R. (2011). *Force modeling in drilling with application to burr minimization* (Doctoral dissertation, Georgia Institute of Technology).
- [74] Flachs, J. R., Salahshoor, M., & Melkote, S. N. (2014). Mechanistic models of thrust force and torque in step-drilling of Al7075-T651. *Production Engineering*, *8*(3), 319-333.
- [75] Fleischer, J., Deuchert, M., Ruhs, C., Kühlewein, C., Halvadjisky, G., & Schmidt, C. (2008). Design and manufacturing of micro milling tools. *Microsystem Technologies*, *14*(9-11), 1771-1775.
- [76] Fu, L., & Guo, Q. (2010). Development of an ultra-small micro drill bit for packaging substrates. *Circuit World*, *36*(3), 23-27.
- [77] Fu, L., & Yang, F. (2008). A solution for PCB drilling with strict requirement on hole wall quality. *Circuit World*, *34*(2), 8-11.
- [78] Garg, A., Tai, K., Vijayaraghavan, V., & Singru, P. M. (2014). Mathematical modelling of burr height of the drilling process using a statistical-based multi-gene genetic programming approach. *The International Journal of Advanced Manufacturing Technology*, *73*(1-4), 113-126.
- [79] Ghahremaninezhad, A., & Ravi-Chandar, K. (2011). Ductile failure in polycrystalline OFHC copper. *International Journal of Solids and Structures*, *48*(24), 3299-3311.
- [80] Gillespie, L. K. (1976). *Effects of drilling variables on burr properties* (No. BDX-613-1502). Bendix Corp., Kansas City, Mo.(USA).
- [81] Gong, Y., Ehmann, K. F., & Lin, C. (2003). Analysis of dynamic characteristics of micro-drills. *Journal of Materials Processing Technology*, *141*(1), 16-28.
- [82] Gong, Y., Lin, C., & Ehmann, K. F. (2005). Dynamics of initial penetration in drilling: part 1—mechanistic model for dynamic forces. *Journal of manufacturing science and engineering*, *127*(2), 280-288.
- [83] Gong, Y., Lin, C., & Ehmann, K. F. (2005). Dynamics of Initial Penetration in Drilling: Part 2—Motion Models for Drill Skidding and Wandering With Experimental Verification. *Journal of manufacturing science and engineering*, *127*(2), 289-297.

- [84] Gopinath, G. (2011). *Progressive damage and failure of unidirectional fiber reinforced laminates under impact loading with composite properties derived from a micro-mechanics approach* (Doctoral dissertation, Virginia Tech).
- [85] Hashin, Z. (1981). Fatigue failure criteria for unidirectional fiber composites. *Journal of Applied Mechanics*, 48(4), 846-852.
- [86] Heisel, U., & Pfeifroth, T. (2012). Influence of point angle on drill hole quality and machining forces when drilling CFRP. *Procedia CIRP*, 1, 471-476.
- [87] Hellstern, C. (2009). *Investigation of interlayer burr formation in the drilling of stacked aluminum sheets* (Doctoral dissertation, Georgia Institute of Technology).
- [88] Hinds, B. K., & Treanor, G. M. (2000). Analysis of stresses in micro-drills using the finite element method. *International Journal of Machine Tools and Manufacture*, 40(10), 1443-1456.
- [89] Hocheng, H., & Tsao, C. C. (2005). The path towards delamination-free drilling of composite materials. *Journal of materials processing technology*, 167(2-3), 251-264.
- [90] Huo, D. (2013). *Micro-cutting: fundamentals and applications*. John Wiley & Sons.
- [91] Imran, M., Mativenga, P. T., & Withers, P. J. (2012). Assessment of machining performance using the wear map approach in micro-drilling. *The International Journal of Advanced Manufacturing Technology*, 59(1-4), 119-126.
- [92] Isbilir, O., & Ghassemieh, E. (2011). Finite element analysis of drilling of titanium alloy. *Procedia Engineering*, 10, 1877-1882.
- [93] Isbilir, O., & Ghassemieh, E. (2012). Finite element analysis of drilling of carbon fibre reinforced composites. *Applied Composite Materials*, 19(3-4), 637-656.
- [94] Isbilir, O., & Ghassemieh, E. (2013). Comparative study of tool life and hole quality in drilling of CFRP/titanium stack using coated carbide drill. *Machining Science and Technology*, 17(3), 380-409.
- [95] Isbilir, O., & Ghassemieh, E. (2014). Three-dimensional numerical modelling of drilling of carbon fiber-reinforced plastic composites. *Journal of Composite Materials*, 48(10), 1209-1219.
- [96] Jantunen, E. (2002). A summary of methods applied to tool condition monitoring in drilling. *International Journal of Machine Tools and Manufacture*, 42(9), 997-1010.
- [97] Jun, M. B., DeVor, R. E., & Kapoor, S. G. (2006). Investigation of the dynamics of microend milling-part II: model validation and interpretation. *Journal of manufacturing science and engineering*, 128(4), 901-912.
- [98] Jun, M. B., Goo, C., Malekian, M., & Park, S. (2012). A new mechanistic approach for micro end milling force modeling. *Journal of Manufacturing Science and Engineering*, 134(1), 011006.
- [99] Jun, M.B., Liu, X., Devor, R.E. and Kapoor, S.G. (2006), Investigation of the dynamics of micro-end milling-Part I: model development, *Journal of Manufacturing Science and Engineering*, 128(4),894-900.
- [100] Kang, I. S., Kim, J. S., & Seo, Y. W. (2008). Cutting force model considering tool edge geometry for micro end milling process. *Journal of Mechanical Science and Technology*, 22(2), 293-299.
- [101] Kang, I. S., Kim, J. S., Kim, J. H., Kang, M. C., & Seo, Y. W. (2007). A mechanistic model of cutting force in the micro end milling process. *Journal of Materials Processing Technology*, 187, 250-255.

- [102] Kao, W. H., Su, Y. L., Yao, S. H., Huang, H. C., & Chen, M. S. (2012). The study of high speed micro-drilling performance and machining quality of coated micro-drills with Zr-C: H coatings. In *Advanced Materials Research* (Vol. 591, pp. 342-346). Trans Tech Publications.
- [103] Kapoor, S. G., DeVor, R. E., Zhu, R., Gajjala, R., Parakkal, G., & Smithey, D. (1998). Development of mechanistic models for the prediction of machining performance: model building methodology. *Machining Science and Technology*, 2(2), 213-238.
- [104] Karim, M. R. (2005). *Constitutive modeling and failure criteria of carbon-fiber reinforced polymers under high strain rates*(Doctoral dissertation, University of Akron).
- [105] Kavadi, B. V., Pandey, A. B., Tadavi, M. V., & Jakharia, H. C. (2014). A review paper on effects of drilling on glass fiber reinforced plastic. *Procedia Technology*, 14, 457-464.
- [106] Khoran, M., Ghabezi, P., Frahani, M., & Besharati, M. K. (2015). Investigation of drilling composite sandwich structures. *The International Journal of Advanced Manufacturing Technology*, 76(9-12), 1927-1936.
- [107] Kim, C. J., Mayor, J. R., & Ni, J. (2004). A static model of chip formation in microscale milling. *Journal of manufacturing science and engineering*, 126(4), 710-718.
- [108] Kim, D. W., Cho, M. W., Seo, T. I., & Lee, E. S. (2008). Application of design of experiment method for thrust force minimization in step-feed micro drilling. *Sensors*, 8(1), 211-221.
- [109] Kim, D. W., Lee, Y. S., Chu, C. N., & Oh, Y. T. (2006). Prevention of exit burr in microdrilling of metal foils by using a cyanoacrylate adhesive. *The International Journal of Advanced Manufacturing Technology*, 27(11-12), 1071-1076.
- [110] Kim, D. W., Lee, Y. S., Park, M. S., & Chu, C. N. (2009). Tool life improvement by peck drilling and thrust force monitoring during deep-micro-hole drilling of steel. *International Journal of Machine Tools and Manufacture*, 49(3-4), 246-255.
- [111] Kim, H. H., Chung, S., Kim, S. C., Jee, W. H., & Chung, S. C. (2006). Condition monitoring of micro-drilling processes on glass by using machine vision. *Proceedings of the ASPE Challenges at the Intersection of Precision Engineering and Vacuum Technology, Pittsburgh, PA, USA*, 1-2.
- [112] Kim, J. O., & Kwon, O. S. (2003). Vibration characteristics of piezoelectric torsional transducers. *Journal of sound and vibration*, 264(2), 453-473.
- [113] Ko, S. L., Chang, J. E., & Kaipakjian, S. (2003). Development of drill geometry for burr minimization in drilling. *CIRP Annals-Manufacturing Technology*, 52(1), 45-48.
- [114] Kondo, E., & Shimana, K. (2012). Monitoring of prefailure phase and detection of tool breakage in micro-drilling operations. *Procedia CIRP*, 1, 581-586.
- [115] Kondo, E., Kamo, R., & Murakami, H. (2012). Monitoring of burr and prefailure phase caused by tool wear in micro-drilling operations using thrust force signals. *Journal of Advanced Mechanical Design, Systems, and Manufacturing*, 6(6), 885-897.
- [116] Kudla, L. (2001). Influence of feed motion features on small holes drilling process. *Journal of Materials Processing Technology*, 109(3), 236-241.

- [117] Kulkarni, P. R., & Gaikwad, M. U. (2013). Static and dynamic analysis of end mill tool for stability, *Advanced Materials Manufacturing & Characterization*, Vol. 3 (1), 341-344.
- [118] Kumar, S., & Dornfeld, D. (2003). Basic approach to a prediction system for burr formation in face milling. *Journal of manufacturing processes*, 5(2), 127-142.
- [119] Kuo, K. L. (2008). Design of rotary ultrasonic milling tool using FEM simulation. *Journal of Materials Processing Technology*, 201(1-3), 48-52.
- [120] Kuo, K. L., & TSAO, C. C. (2012). Rotary ultrasonic-assisted milling of brittle materials. *Transactions of Nonferrous Metals Society of China*, 22, s793-s800.
- [121] Kyratsis, P., Tapoglou, N., Bilalis, N., & Antoniadis, A. (2011). Thrust force prediction of twist drill tools using a 3D CAD system application programming interface. *International Journal of Machining and Machinability of Materials*, 10(1-2), 18-33.
- [122] Lai, X., Li, H., Li, C., Lin, Z., & Ni, J. (2008). Modelling and analysis of micro scale milling considering size effect, micro cutter edge radius and minimum chip thickness. *International Journal of Machine Tools and Manufacture*, 48(1), 1-14.
- [123] Lee, C. S., Kim, J. H., Kim, S. K., Ryu, D. M., & Lee, J. M. (2015). Initial and progressive failure analyses for composite laminates using Puck failure criterion and damage-coupled finite element method. *Composite Structures*, 121, 406-419.
- [124] Lee, D. G., Lee, H. G., Kim, P. J., & Bang, K. G. (2003). Micro-drilling of alumina green bodies with diamond grit abrasive micro-drills. *International Journal of Machine Tools and Manufacture*, 43(6), 551-558.
- [125] Lee, H. G. (2004). Tool life model for abrasive wet micro-drilling of ceramic green bodies. *International Journal of Machine Tools and Manufacture*, 44(7-8), 839-846.
- [126] Lee, K., & Dornfeld, D. A. (2005). Micro-burr formation and minimization through process control. *Precision Engineering*, 29(2), 246-252.
- [127] Lekkala, R., Bajpai, V., Singh, R. K., & Joshi, S. S. (2011). Characterization and modeling of burr formation in micro-end milling. *Precision Engineering*, 35(4), 625-637.
- [128] Li, C., Lai, X., Li, H., & Ni, J. (2007). Modeling of three-dimensional cutting forces in micro-end-milling. *Journal of Micromechanics and Microengineering*, 17(4), 671-678.
- [129] Li, K. M., & Wang, S. L. (2014). Effect of tool wear in ultrasonic vibration-assisted micro-milling. *Proceedings of the Institution of Mechanical Engineers, Part B: Journal of Engineering Manufacture*, 228(6), 847-855.
- [130] Li, P., Oosterling, J. A. J., Hoogstrate, A. M., Langen, H. H., & Schmidt, R. M. (2011). Design of micro square endmills for hard milling applications. *The International Journal of Advanced Manufacturing Technology*, 57(9-12), 859-870.
- [131] Li, X., Meadows, A., Babitsky, V., & Parkin, R. (2015). Experimental analysis on autoresonant control of ultrasonically assisted drilling. *Mechatronics*, 29, 57-66.
- [132] Lian, H., Guo, Z., Huang, Z., Tang, Y., & Song, J. (2013). Experimental research of Al6061 on ultrasonic vibration assisted micro-milling. *Procedia CIRP*, 6, 561-564.
- [133] Liang, Y. C., Yang, K., Bai, Q. S., Chen, J. X., & Wang, B. (2009). Modeling and experimental analysis of micro burr formation considering tool edge radius and tool-tip breakage in microend milling. *Journal of Vacuum Science & Technology B: Microelectronics and Nanometer Structures Processing, Measurement, and Phenomena*, 27(3), 1531-1535.

- [134] Liao, Y. S., Chen, Y. C., & Lin, H. M. (2007). Feasibility study of the ultrasonic vibration assisted drilling of Inconel superalloy. *International Journal of Machine Tools and Manufacture*, 47(12-13), 1988-1996.
- [135] Lin, C., Kang, S. M., & Ehmann, K. F. (1992). Planar micro-drill point design and grinding methods. *Trans. North Am. Manuf. Res. Inst. SME*, 20, 173-179.
- [136] Lin, T. R., & Shyu, R. F. (2000). Improvement of tool life and exit burr using variable feeds when drilling stainless steel with coated drills. *The International Journal of Advanced Manufacturing Technology*, 16(5), 308-313.
- [137] Liu, D., Cong, W. L., Pei, Z. J., & Tang, Y. (2012). A cutting force model for rotary ultrasonic machining of brittle materials. *International Journal of Machine Tools and Manufacture*, 52(1), 77-84.
- [138] Liu, X., DeVor, R. E., & Kapoor, S. G. (2007). Model-based analysis of the surface generation in microendmilling—part I: model development. *Journal of manufacturing science and engineering*, 129(3), 453-460.
- [139] Liu, X., DeVor, R. E., & Kapoor, S. G. (2007). Model-based analysis of the surface generation in microendmilling—part II: experimental validation and analysis. *Journal of manufacturing science and engineering*, 129(3), 461-469.
- [140] López-Puente, J., Zaera, R., & Navarro, C. (2008). Experimental and numerical analysis of normal and oblique ballistic impacts on thin carbon/epoxy woven laminates. *Composites Part A: applied science and manufacturing*, 39(2), 374-387.
- [141] Majzoobi, G. H., & Dehghan, F. R. (2011). Determination of the constants of damage models. *Procedia Engineering*, 10, 764-773.
- [142] Makhdum, F., Jennings, L. T., Roy, A., & Silberschmidt, V. V. (2012). Cutting forces in ultrasonically assisted drilling of carbon fibre-reinforced plastics. In *Journal of Physics: Conference Series* (Vol. 382, No. 1, p. 012019). IOP Publishing.
- [143] Makhdum, F., Phadnis, V. A., Roy, A., & Silberschmidt, V. V. (2014). Effect of ultrasonically-assisted drilling on carbon-fibre-reinforced plastics. *Journal of Sound and Vibration*, 333(23), 5939-5952.
- [144] Malekian, M., Park, S. S., & Jun, M. B. (2009). Modeling of dynamic micro-milling cutting forces. *International Journal of Machine Tools and Manufacture*, 49(7-8), 586-598.
- [145] Mamedov, A., & Lazoglu, I. (2013). Machining forces and tool deflections in micro milling. *Procedia Cirp*, 8, 147-151.
- [146] Mativenga, P. T., & Hon, K. K. B. (2005). An experimental study of cutting forces in high-speed end milling and implications for dynamic force modeling. *Journal of manufacturing science and engineering*, 127(2), 251-261.
- [147] Matsumura, T., & Tamura, S. (2013). Cutting force model in drilling of multi-layered materials. *Procedia CIRP*, 8, 182-187.
- [148] Mehbudi, P., Baghlani, V., Akbari, J., Bushroa, A. R., & Mardi, N. A. (2013). Applying ultrasonic vibration to decrease drilling-induced delamination in GFRP laminates. *Procedia Cirp*, 6, 577-582.
- [149] Michigami, N., Yamaga, M., Kawamura, M., Kuze, O., & Nakamura, S. (2011). High-performance printed circuit board production equipment for ultra-high density multi-layer wiring. *Hitachi Review*, 60(5), 217.
- [150] Mijušković, G., Krajnik, P., & Kopač, J. (2015). Analysis of tool deflection in micro milling of graphite electrodes. *The International Journal of Advanced Manufacturing Technology*, 76(1-4), 209-217.

- [151] Minukhin, I. (2013). *An improved method of cutting forces prediction for the primary cutting edges of twist drills* (Doctoral dissertation, Concordia University).
- [152] Mohan, N. S., Ramachandra, A., & Kulkarni, S. M. (2005). Influence of process parameters on cutting force and torque during drilling of glass–fiber polyester reinforced composites. *Composite structures*, 71(3-4), 407-413.
- [153] Monaghan, J., & O'reilly, P. (1992). The drilling of an Al/SiC metal-matrix composite. *Journal of materials processing technology*, 33(4), 469-480.
- [154] Mondal, N., Sardar, B. S., Halder, R. N., & Das, S. (2014). Observation of drilling burr and finding out the condition for minimum burr formation. *International Journal of Manufacturing Engineering*, 2014.
- [155] Moser, F., Jacobs, L. J., & Qu, J. (1999). Modeling elastic wave propagation in waveguides with the finite element method. *Ndt & E International*, 32(4), 225-234.
- [156] Mustapha, K. B., & Zhong, Z. W. (2013). A hybrid analytical model for the transverse vibration response of a micro-end mill. *Mechanical Systems and Signal Processing*, 34(1-2), 321-339.
- [157] Nad', M. (2010). Ultrasonic horn design for ultrasonic machining technologies. *Applied and Computational Mechanics*, 4, 79–88.
- [158] Nakagawa, H., Ogawa, K., Kihara, A., & Hirogaki, T. (2007). Improvement of micro-drilled hole quality for printed wiring boards. *Journal of Materials Processing Technology*, 191(1-3), 293-296.
- [159] Nam, J. S., Lee, P. H., & Lee, S. W. (2011). Experimental characterization of micro-drilling process using nanofluid minimum quantity lubrication. *International Journal of Machine Tools and Manufacture*, 51(7-8), 649-652.
- [160] Nanu, A. S., Marinescu, N. I., & Ghiculescu, D. (2011). Study on ultrasonic stepped horn geometry design and FEM simulation. *Revista de Tehnologii Neconventionale*, 15(4), 25.
- [161] Nategh, M. J., Razavi, H., & Abdullah, A. (2012). Analytical modeling and experimental investigation of ultrasonic-vibration assisted oblique turning, part I: Kinematics analysis. *International Journal of Mechanical Sciences*, 63(1), 1-11.
- [162] Nath, C. (2009). *A study on ultrasonic vibration cutting of difficult-to-cut materials* (Doctoral dissertation).
- [163] Nath, C., & Rahman, M. (2008). Effect of machining parameters in ultrasonic vibration cutting. *International Journal of Machine Tools and Manufacture*, 48(9), 965-974.
- [164] Newby, G., Venkatachalam, S., & Liang, S. Y. (2007). Empirical analysis of cutting force constants in micro-end-milling operations. *Journal of Materials Processing Technology*, 192, 41-47.
- [165] Nie, Z. (2014). *Advanced mesomechanical modeling of triaxially braided composites for dynamic impact analysis with failure*. The University of Akron.
- [166] Ning, F., Wang, H., Cong, W., & Fernando, P. K. S. C. (2017). A mechanistic ultrasonic vibration amplitude model during rotary ultrasonic machining of CFRP composites. *Ultrasonics*, 76, 44-51.
- [167] Novakov, T., & Jackson, M. J. (2010). Chatter problems in micro-and macrocutting operations, existing models, and influential parameters—a review. *The International Journal of Advanced Manufacturing Technology*, 47(5-8), 597-620.
- [168] Okasha, M. M., Driver, N., Mativenga, P. T., & Li, L. (2012). Mechanical microdrilling of negative-tapered laser-predrilled holes: a new approach for burr

- minimization. *The International Journal of Advanced Manufacturing Technology*, 61(1-4), 213-225.
- [169] Okutan, B. (2002). The effects of geometric parameters on the failure strength for pin-loaded multi-directional fiber-glass reinforced epoxy laminate. *Composites Part B: Engineering*, 33(8), 567-578.
- [170] Park, I. W., & Dornfeld, D. A. (2000). A study of burr formation processes using the finite element method: part I. *Journal of Engineering Materials and Technology*, 122(2), 221-228.
- [171] Park, I. W., & Dornfeld, D. A. (2000). A study of burr formation processes using the finite element method: part II—the influences of exit angle, rake angle, and backup material on burr formation processes. *Journal of engineering materials and technology*, 122(2), 229-237.
- [172] Park, S. S., & Malekian, M. (2009). Mechanistic modeling and accurate measurement of micro end milling forces. *CIRP annals*, 58(1), 49-52.
- [173] Patra, K., Anand, R. S., Steiner, M., & Biermann, D. (2015). Experimental analysis of cutting forces in microdrilling of austenitic stainless steel (X5CrNi18-10). *Materials and Manufacturing Processes*, 30(2), 248-255.
- [174] Paul, A., Kapoor, S. G., & Devor, R. E. (2005). A chisel edge model for arbitrary drill point geometry. *Journal of Manufacturing Science and Engineering*, 127(1), 23-32.
- [175] Paul, A., Kapoor, S. G., & DeVor, R. E. (2005). Chisel edge and cutting lip shape optimization for improved twist drill point design. *International Journal of Machine Tools and Manufacture*, 45(4-5), 421-431.
- [176] Phadnis, V. A., Makhdum, F., Roy, A., & Silberschmidt, V. V. (2012). Experimental and numerical investigations in conventional and ultrasonically assisted drilling of CFRP laminate. *Procedia Cirp*, 1, 455-459.
- [177] Phadnis, V. A., Makhdum, F., Roy, A., & Silberschmidt, V. V. (2013). Drilling in carbon/epoxy composites: experimental investigations and finite element implementation. *Composites Part A: Applied Science and Manufacturing*, 47, 41-51.
- [178] Phadnis, V. A., Roy, A., & Silberschmidt, V. V. (2013). A finite element model of ultrasonically assisted drilling in carbon/epoxy composites. *Procedia Cirp*, 8, 141-146.
- [179] Piljek, P., Keran, Z., & Math, M. (2014). Micromachining—Review of Literature from 1980 to 2010. *Interdisciplinary Description of Complex Systems: INDECS*, 12(1), 1-27.
- [180] Pirtini, M., & Lazoglu, I. (2005). Forces and hole quality in drilling. *International journal of machine tools and Manufacture*, 45(11), 1271-1281.
- [181] Pujana, J., Rivero, A., Celaya, A., & De Lacalle, L. L. (2009). Analysis of ultrasonic-assisted drilling of Ti6Al4V. *International Journal of Machine Tools and Manufacture*, 49(6), 500-508.
- [182] Qin, N. (2011). *Modeling and experimental investigation on ultrasonic-vibration-assisted grinding* (Doctoral dissertation, Kansas State University).
- [183] Rahamathullah, I., & Shunmugam, M. S. (2014). Mechanistic approach for prediction of forces in micro-drilling of plain and glass-reinforced epoxy sheets. *The International Journal of Advanced Manufacturing Technology*, 75(5-8), 1177-1187.

- [184] Rahman, A. A., Mamat, A., &Wagiman, A. (2009). Effect of machining parameters on hole quality of micro drilling for brass. *Modern applied science*, 3(5), 221.
- [185] Rahme, P., Landon, Y., Lachaud, F., Piquet, R., &Lagarrigue, P. (2015). Drilling of thick composite material with a small-diameter twist drill. *The International Journal of Advanced Manufacturing Technology*, 76(9-12), 1543-1553.
- [186] Rahmé, P., Landon, Y., Lachaud, F., Piquet, R., &Lagarrigue, P. (2011). Analytical models of composite material drilling. *The International Journal of Advanced Manufacturing Technology*, 52(5-8), 609-617.
- [187] Ramkumar, J., Malhotra, S. K., & Krishnamurthy, R. (2004). Effect of workpiece vibration on drilling of GFRP laminates. *Journal of Materials Processing Technology*, 152(3), 329-332.
- [188] Ravisubramanian, S., &Shunmugam, M. S. (2015). On reliable measurement of micro drilling forces and identification of different phases. *Measurement*, 73, 335-340.
- [189] Rawat, S., &Attia, H. (2009). Characterization of the dry high speed drilling process of woven composites using Machinability Maps approach. *CIRP annals*, 58(1), 105-108.
- [190] Razavi, H., Nategh, M. J., & Abdullah, A. (2012). Analytical modeling and experimental investigation of ultrasonic-vibration assisted oblique turning, part II: dynamics analysis. *International Journal of Mechanical Sciences*, 63(1), 12-25.
- [191] Rincon, D. M., &Ulsoy, A. G. (1995). Complex geometry, rotary inertia and gyroscopic moment effects on drill vibrations. *Journal of Sound and Vibration*, 188(5), 701-715.
- [192] Rincon, D. M., Ulsoy, A. G., &Kaftanoğlu, B. (1994). Effects of drill vibrations on cutting forces and torque. *CIRP Annals-Manufacturing Technology*, 43(1), 59-62.
- [193] Roukema, J. C., &Altintas, Y. (2007). Generalized modeling of drilling vibrations. Part I: Time domain model of drilling kinematics, dynamics and hole formation. *International Journal of Machine Tools and Manufacture*, 47(9), 1455-1473.
- [194] Roy, S. (2017). Design of a circular hollow ultrasonic horn for USM using finite element analysis. *The International Journal of Advanced Manufacturing Technology*, 93(1-4), 319-328.
- [195] Rzepka, S., Kramer, F., Grassmé, O., &Lienig, J. (2008, April). A multilayer PCB material modeling approach based on laminate theory. In *Thermal, Mechanical and Multi-Physics Simulation and Experiments in Microelectronics and Micro-Systems, 2008. EuroSimE 2008. International Conference on*(pp. 1-10). IEEE.
- [196] Sadek, A., Attia, M. H., Meshreki, M., & Shi, B. (2013). Characterization and optimization of vibration-assisted drilling of fibre reinforced epoxy laminates. *CIRP Annals-Manufacturing Technology*, 62(1), 91-94.
- [197] Sahoo, S., Thakur, A., &Gangopadhyay, S. (2016). Application of analytical simulation on various characteristics of hole quality during micro-drilling of printed circuit board. *Materials and Manufacturing Processes*, 31(14), 1927-1934.
- [198] Sambhav, K., Tandon, P., & Dhande, S. G. (2012). Geometric modeling and validation of twist drills with a generic point profile. *Applied Mathematical Modelling*, 36(6), 2384-2403.

- [199] Sambhav, K., Tandon, P., Kapoor, S. G., & Dhande, S. G. (2013). Mathematical modeling of cutting forces in micro drilling. *Journal of Manufacturing Science and Engineering*, 135(1), 014501.
- [200] Saptaji, K., Subbiah, S., & Dhupia, J. S. (2012). Effect of side edge angle and effective rake angle on top burrs in micro-milling. *Precision Engineering*, 36(3), 444-450.
- [201] Saunders, L. K. L. (2003). A finite element model of exit burrs for drilling of metals. *Finite elements in analysis and design*, 40(2), 139-158.
- [202] Saunders, L. K. L., & Mauch, C. A. (2001). An exit burr model for drilling of metals. *Journal of manufacturing science and engineering*, 123(4), 562-566.
- [203] Seah, K. H. W., Wong, Y. S., & Lee, L. C. (1993). Design of tool holders for ultrasonic machining using FEM. *Journal of Materials Processing Technology*, 37(1-4), 801-816.
- [204] Sedláček, J., & Humár, A. (2008). Analysis of fracture mechanisms and surface quality in drilling of composite materials. *Strength of Materials*, 40(1), 40-43.
- [205] Segonds, S., Masounave, J., Songmene, V., & Bès, C. (2013). A simple analytical model for burr type prediction in drilling of ductile materials. *Journal of Materials Processing Technology*, 213(6), 971-977.
- [206] Sen, M., & Shan, H. S. (2005). A review of electrochemical macro-to micro-hole drilling processes. *International Journal of Machine Tools and Manufacture*, 45(2), 137-152.
- [207] Shatla, M., & Altan, T. (2000). Analytical modeling of drilling and ball end milling. *Journal of Materials Processing Technology*, 98(1), 125-133.
- [208] Shen, X. H., Zhang, J. H., Li, H., Wang, J. J., & Wang, X. C. (2012). Ultrasonic vibration-assisted milling of aluminum alloy. *The International Journal of Advanced Manufacturing Technology*, 63(1-4), 41-49.
- [209] Shen, X. H., Zhang, J., Xing, D. X., & Zhao, Y. (2012). A study of surface roughness variation in ultrasonic vibration-assisted milling. *The International Journal of Advanced Manufacturing Technology*, 58(5-8), 553-561.
- [210] Shi, H., & Li, H. (2013). Challenges and developments of micro drill bit for printed circuit board: a review. *Circuit World*, 39(2), 75-81.
- [211] Shi, H., Song, F., & Fu, L. (2011). Experimental study on drilling force in printed circuit board micro drilling process. *Circuit World*, 37(1), 24-29.
- [212] Shu, K. M., Hsieh, W. H., & Chi, C. W. (2012). On the Design and Analysis of Acoustic Horns for Ultrasonic Welding. In *Advanced Materials Research* (Vol. 472, pp. 1555-1558). Trans Tech Publications.
- [213] Singh, R., & Khamba, J. S. (2009). Mathematical modeling of tool wear rate in ultrasonic machining of titanium. *The International Journal of Advanced Manufacturing Technology*, 43(5-6), 573-580.
- [214] Srinivasa, Y. V., & Shunmugam, M. S. (2013). Mechanistic model for prediction of cutting forces in micro end-milling and experimental comparison. *International Journal of Machine Tools and Manufacture*, 67, 18-27.
- [215] Stein, J. M., & Dornfeld, D. A. (1997). Burr formation in drilling miniature holes. *Cirp Annals*, 46(1), 63-66.

- [216] Stirn, B., Lee, K., & Dornfeld, D. A. (2001). Burr formation in micro-drilling. In *Proceedings of the sixteenth annual meeting of the American Society for Precision Engineering* (pp. 473-476).
- [217] Strenkowski, J. S., Hsieh, C. C., & Shih, A. J. (2004). An analytical finite element technique for predicting thrust force and torque in drilling. *International Journal of Machine Tools and Manufacture*, 44(12-13), 1413-1421.
- [218] Suganthi, X. H., Natarajan, U., & Ramasubbu, N. (2015). A review of accuracy enhancement in microdrilling operations. *The International Journal of Advanced Manufacturing Technology*, 81(1-4), 199-217.
- [219] Sugawara, A., & Inagaki, K. (1982). Effect of workpiece structure on burr formation in micro-drilling. *Precision Engineering*, 4(1), 9-14.
- [220] Tandon, P., & Khan, M. R. (2009). Three dimensional modeling and finite element simulation of a generic end mill. *Computer-Aided Design*, 41(2), 106-114.
- [221] Tang, H. Q., Wen, J., Wang, C. Y., Wu, L. S., & Song, Y. X. (2011). Simulation of drilling on the copper of PCB with ultra-high-speed. In *Advanced Materials Research*, Trans Tech Publications.188,739-742.
- [222] Tao, G., Zhang, J., Shen, X., Bai, L., Ma, C., & Wang, J. (2016). Feasibility Study on Ultrasonic Vibration Assisted Milling for Squamous Surface. *Procedia CIRP*, 42, 847-852.
- [223] Tapoglou, N., & Antoniadis, A. (2012). 3-Dimensional kinematics simulation of face milling. *Measurement*, 45(6), 1396-1405.
- [224] Tawakoli, T., & Azarhoushang, B. (2008). Influence of ultrasonic vibrations on dry grinding of soft steel. *International Journal of Machine Tools and Manufacture*, 48(14), 1585-1591.
- [225] Thomas, P. (2008). *Modelling of an ultrasonically assisted drill bit* (Doctoral dissertation, © PNH Thomas).
- [226] Thomas, P. N. H., & Babitsky, V. I. (2007). Experiments and simulations on ultrasonically assisted drilling. *Journal of Sound and Vibration*, 308(3-5), 815-830.
- [227] Tsai, W. D., & Wu, S. M. (1979). Computer analysis of drill point geometry. *International Journal of Machine Tool Design and Research*, 19(2), 95-108.
- [228] Uhlmann, E., & Schauer, K. (2005). Dynamic load and strain analysis for the optimization of micro end mills. *CIRP Annals-Manufacturing Technology*, 54(1), 75-78.
- [229] Vijayaraghavan, A. (2005). Drilling of fiber-reinforced plastics—tool modeling and defect prediction. *Masters report, University of California, Berkeley*.
- [230] Vijayaraghavan, A., & Dornfeld, D. A. (2005). Challenges in modeling machining in multilayer materials.
- [231] Vogler, M. P., DeVor, R. E., & Kapoor, S. G. (2004). On the modeling and analysis of machining performance in micro-endmilling, Part I: Surface generation. *Journal of Manufacturing Science and Engineering*, 126(4), 685-694.
- [232] Vogler, M. P., Kapoor, S. G., & DeVor, R. E. (2004). On the modeling and analysis of machining performance in micro-endmilling, Part II: Cutting force prediction. *Journal of manufacturing science and engineering*, 126(4), 695-705.
- [233] Wang, L., Zheng, L., yong Wang, C., Li, S., Song, Y., Zhang, L., & Sun, P. (2014). Experimental study on micro-drills wear during high speed of drilling IC substrate. *Circuit World*, 40(2), 61-70.

- [234] Wang, X., Wang, L. J., & Tao, J. P. (2004). Investigation on thrust in vibration drilling of fiber-reinforced plastics. *Journal of Materials Processing Technology*, 148(2), 239-244.
- [235] Wang, X., Zhou, M., Gan, J. K., & Ngoi, B. (2002). Theoretical and experimental studies of ultraprecision machining of brittle materials with ultrasonic vibration. *The International Journal of Advanced Manufacturing Technology*, 20(2), 99-102.
- [236] Wang, Z. G., Wong, Y. S., & Rahman, M. (2005). High-speed milling of titanium alloys using binderless CBN tools. *International Journal of Machine Tools and Manufacture*, 45(1), 105-114.
- [237] Watanabe, H., Tsuzaka, H., & Masuda, M. (2008). Microdrilling for printed circuit boards (PCBs)—influence of radial run-out of microdrills on hole quality. *Precision Engineering*, 32(4), 329-335.
- [238] Weule, H., Hüntrup, V., & Tritschler, H. (2001). Micro-cutting of steel to meet new requirements in miniaturization. *CIRP Annals-Manufacturing Technology*, 50(1), 61-64.
- [239] Wu, T., Cheng, K., & Rakowski, R. (2012). Investigation on tooling geometrical effects of micro tools and the associated micro milling performance. *Proceedings of the Institution of Mechanical Engineers, Part B: Journal of Engineering Manufacture*, 226(9), 1442-1453.
- [240] Xiao, M., Sato, K., Karube, S., & Soutome, T. (2003). The effect of tool nose radius in ultrasonic vibration cutting of hard metal. *International Journal of Machine Tools and Manufacture*, 43(13), 1375-1382.
- [241] Xiao, X., Zheng, K., & Liao, W. (2014). Theoretical model for cutting force in rotary ultrasonic milling of dental zirconia ceramics. *The International Journal of Advanced Manufacturing Technology*, 75(9-12), 1263-1277.
- [242] Xing, D., Zhang, J., Shen, X., Zhao, Y., & Wang, T. (2013). Tribological properties of ultrasonic vibration assisted milling aluminium alloy surfaces. *Procedia CIRP*, 6, 539-544.
- [243] Ya, G., Qin, H. W., Yang, S. C., & Xu, Y. W. (2002). Analysis of the rotary ultrasonic machining mechanism. *Journal of materials processing technology*, 129(1-3), 182-185.
- [244] Yadava, V., & Deoghare, A. (2008). Design of horn for rotary ultrasonic machining using the finite element method. *The International Journal of Advanced Manufacturing Technology*, 39(1-2), 9-20.
- [245] Yan, L., & Jiang, F. (2013). A practical optimization design of helical geometry drill point and its grinding process. *The International Journal of Advanced Manufacturing Technology*, 64(9-12), 1387-1394.
- [246] Yongchen, P., Qingchang, T., & Zhaojun, Y. (2006). A study of dynamic stresses in micro-drills under high-speed machining. *International Journal of Machine Tools and Manufacture*, 46(14), 1892-1900.
- [247] Yoon, H. S., Wu, R., Lee, T. M., & Ahn, S. H. (2011). Geometric optimization of micro drills using Taguchi methods and response surface methodology. *International Journal of Precision Engineering and Manufacturing*, 12(5), 871-875.
- [248] Zhang, C., Zhang, J., & Feng, P. (2013). Mathematical model for cutting force in rotary ultrasonic face milling of brittle materials. *The International Journal of Advanced Manufacturing Technology*, 69(1-4), 161-170.

- [249] Zhang, D. Y., Feng, X. J., Wang, L. J., & Chen, D. C. (1994). Study on the drill skidding motion in ultrasonic vibration microdrilling. *International journal of machine tools and manufacture*, 34(6), 847-857.
- [250] Zhang, H., Wang, X., & Pang, S. (2014). A mathematical modeling to predict the cutting forces in microdrilling. *Mathematical Problems in Engineering*, 2014.
- [251] Zhang, L. B., Wang, L. J., Liu, X. Y., Zhao, H. W., Wang, X., & Luo, H. Y. (2001). Mechanical model for predicting thrust and torque in vibration drilling fibre-reinforced composite materials. *International Journal of Machine Tools and Manufacture*, 41(5), 641-657.
- [252] Zhang, T., Liu, Z., & Xu, C. (2013). Influence of size effect on burr formation in micro cutting. *The International Journal of Advanced Manufacturing Technology*, 68(9-12), 1911-1917.
- [253] Zhang, Z. (2010). *Modelling of ultrasonically assisted micro drilling* (Doctoral dissertation, © Zhiwei Zhang).
- [254] Zhang, Z., & Babitsky, V. I. (2011). Finite element modeling of a micro-drill and experiments on high speed ultrasonically assisted micro-drilling. *Journal of Sound and Vibration*, 330(10), 2124-2137.
- [255] Zhaojun, Y., Wei, L., Yanhong, C., & Lijiang, W. (1998). Study for increasing micro-drill reliability by vibrating drilling. *Reliability engineering & system safety*, 61(3), 229-233.
- [256] Zheng, L. J., Wang, C. Y., Fu, L. Y., Yang, L. P., Qu, Y. P., & Song, Y. X. (2012). Wear mechanisms of micro-drills during dry high speed drilling of PCB. *Journal of Materials Processing Technology*, 212(10), 1989-1997.
- [257] Zheng, L. J., Wang, C. Y., Qu, Y. P., Song, Y. X., & Fu, L. Y. (2015). Interaction of cemented carbide micro-drills and printed circuit boards during micro-drilling. *The International Journal of Advanced Manufacturing Technology*, 77(5-8), 1305-1314.
- [258] Zheng, L. J., Wang, C. Y., Song, Y. X., Yang, L. P., Qu, Y. P., Ma, P., & Fu, L. Y. (2011). A review on drilling printed circuit boards. In *Advanced Materials Research* (Vol. 188, pp. 441-449). Trans Tech Publications.
- [259] Zheng, L. J., Zhang, X., Wang, C. Y., Wang, L. F., Li, S., Song, Y. X., & Zhang, L. Q. (2013). Experimental Study of Micro-holes Position Accuracy on Drilling Flexible Printed Circuit Board. *10.14279/depositonce-3753*.
- [260] Zheng, L., Wang, C., Yang, L., Song, Y., & Fu, L. (2012). Characteristics of chip formation in the micro-drilling of multi-material sheets. *International Journal of Machine Tools and Manufacture*, 52(1), 40-49.
- [261] Zheng, X., Dong, D., Huang, L., An, Q., Wang, X., & Chen, M. (2013). Research on fixture hole drilling quality of printed circuit board. *International Journal of Precision Engineering and Manufacturing*, 14(4), 525-534.
- [262] Zheng, X., Liu, Z., An, Q., Wang, X., Xu, Z., & Chen, M. (2013). Experimental investigation of microdrilling of printed circuit board. *Circuit World*, 39(2), 82-94.
- [263] Zitoune, R., & Collombet, F. (2007). Numerical prediction of the thrust force responsible of delamination during the drilling of the long-fibre composite structures. *Composites Part A: Applied Science and Manufacturing*, 38(3), 858-866.

Websites

- [264] <https://www.amazon.ca/Vktech-10Pcs-Print-Circuit-Carbide/dp/B00IMXHGG>

- [265] <http://www.indentnow.com/cutting-tools/drills/solid-carbide-drills/guhring-solid-carbide-parallel-shank-twist-drill-5515>
- [266] <https://www.twistedtraces.com/>
- [267] <http://www.directindustry.com/prod/dmg-mori/product-5973-1101289.html>

Dissemination

Publications

1. *Allaparthi Muddu*, Khan Mohammed Rajik & Brahma Teja, “Three-Dimensional Finite element dynamic analysis for micro drilling of multi-layer printed circuit board material”, **Materials Today: Proceedings, 2018**, Vol. 5, Issue 2, Part 2, pp. 7019–7028. DOI: [org/10.1016/j.matpr.2017.11.365](https://doi.org/10.1016/j.matpr.2017.11.365)
2. *Allaparthi Muddu*, Khan Mohammed Rajik & A. Shyamnarayan, “FE Modal and Harmonic Analysis of Micro Drill with Ultrasonic Horn”, **The 1st International Conference on Materials Design and Applications (MDA 2016), Porto, Portugal, 30 June - 1 July 2016**, DOI [10.1007/978-3-319-50784-2_21](https://doi.org/10.1007/978-3-319-50784-2_21).
3. *Allaparthi Muddu* and Khan Mohammed Rajik, “Recent Advances in Burr Height Minimization in Micro-Machining”, **Proceedings of the 5th International and 26th All India Manufacturing Technology, Design & Research Conference – 26thAIMTDR, IIT Guwahati, India, December 12-14, 2014**, pp.386-1-6. (ISBN: 978-8-19274-612-8).

Book Chapters

1. *Allaparthi Muddu*, Khan Mohammed Rajik & A. Shyamnarayan, “**FE Modal and Harmonic Analysis of Micro Drill with Ultrasonic Horn**”, In: Silva L. (eds) *Materials Design and Applications. Advanced Structured Materials*, vol 65, pp. 281-293, **Springer**, Cham 2017, DOI [10.1007/978-3-319-50784-2_21](https://doi.org/10.1007/978-3-319-50784-2_21)

Awards received

1. Received **best technical paper award** for the research paper “**Three-Dimensional Finite element dynamic analysis for micro drilling of multi-layer printed circuit board material**” presented in International Conference on Emerging Trends in Materials & Manufacturing Engineering (iMME17), **NIT Tiruchirappalli, TN, India, March 10- 12, 2017**.